

3D SEISMIC ATTRIBUTES ANALYSIS TO OUTLINE CHANNEL FACIES AND REVEAL
HETEROGENEOUS RESERVOIR STRATIGRAPHY; WEIRMAN FIELD, NESS COUNTY,
KANSAS, USA

by

CHARLOTTE CONWELL PHILIP

B.S., Kansas State University, 2009

A THESIS

submitted in partial fulfillment of the requirements for the degree

MASTER OF SCIENCE

Department of Geology
College of Arts and Sciences

KANSAS STATE UNIVERSITY
Manhattan, Kansas

2011

Approved by:

Major Professor
Dr. Abdelmoneam Raef

Copyright

CHARLOTTE CONWELL PHILIP

2011

Abstract

This research presents a workflow integrating several post-stack seismic attributes to assist in understanding the development history of Weirman Field, Ness County, KS. This study contributes to shaping future drilling plans by establishing a workflow combining analysis of seismic attributes and well cuttings to locate a channel fill zone of better reservoir quality, and to highlight reservoir boundaries due to compartmentalization. In this study, I have successfully outlined a fluvial channel, which is expected to be significantly different in terms of petrophysical properties. The Pennsylvanian aged Cherokee sandstones that potentially comprise channel fill lithofacies, in this study, have been linked to oil production throughout the state of Kansas. It is important to understand channel sandstones when evaluating drilling prospects, because of their potential as an oil reservoir and unpredictable shapes and locations. Since their introduction in the 1970s, seismic attributes have become an essential part of lithological and petrophysical characterization of hydrocarbon reservoirs. Seismic attributes can correlate to and help reveal certain subsurface characteristics and specific geobodies that cannot be distinguished otherwise. Extracting and analyzing acoustic impedance, root-mean-square amplitude and amplitude attenuation, guided by a time window focused on the top of the Mississippian formation, resulted in an understanding of the key seismic channel-facies framework and helped to explain some of the disappointing drilling results at Weirman Field. To form a better understanding of these seismic attributes, this study combined certain attributes and overlaid them in partially transparent states in order to summarize and better visualize the resulting data. A preliminary study of spectral decomposition, which was introduced in the late 1990s, was performed, and a more in-depth study of this multi-resolution attribute is recommended for future study of this particular field. This study also recommends integrating the revealed compartmentalization boundary and the seismic channel-facies framework in future drilling plans of Weirman Field.

Table of Contents

List of Figures.....	v
List of Tables.....	viii
Acknowledgements.....	ix
Chapter 1 - Introduction.....	1
Summary.....	1
Study Area.....	1
Background and Significance of Study.....	2
Chapter 2 - Geological Setting.....	5
Upper Mississippian.....	6
Cherokee Group.....	6
Depositional Environment.....	8
Chapter 3 - Data and Methods.....	13
Data Loading.....	13
Data Collected.....	13
Methodology.....	15
Synthetic Seismograms.....	15
Formation Tops and Horizon Tracking.....	20
Spectral Decomposition and Wavelet Transform.....	24
Qualitative Seismic Attributes.....	33
Chapter 4 - Discussion and Results.....	37
Discussion.....	37
Results.....	40
Chapter 5 - Conclusions.....	47
Conclusions.....	47
References Cited.....	48
Appendix A - Appendix.....	51

List of Figures

Figure 1-1 United States map. Red star indicates state of Kansas and approximate location of the study area.	3
Figure 1-2 Kansas County map. Blue star indicates study area in Ness County.	4
Figure 1-3 Map of oil and gas fields, Ness County, KS. Includes blue square indicating study area.	4
Figure 2-1 SW-NE stratigraphic cross section, showing both the Mississippian and Cherokee formations. Area of interest is located approximately between wells 9 and 10.	7
Figure 2-2 Potential Depositional Environment for Cherokee Group: A) Overview of system B) Facies of channel.	8
Figure 2-3 Modern analog of Deep Creek, Manhattan, KS to show variability in sediment facies.	9
Figure 2-4 Exhibits the relationship between an SP/Neutron log and a stratigraphic section in study area; the box marks the channel sand facies.	10
Figure 2-5 Map of Weirman Field wells and surrounding areas (Kansas Geological Survey, 2011).	11
Figure 2-6 Kansas Stratigraphic Column showing the Cherokee Group.	12
Figure 3-1 Kingdom Suite loading screen.	14
Figure 3-2 Filtering as an example of convolution.	16
Figure 3-3 Comparison of three synthetic seismograms for a deep Yeuga well. The left-hand panels show the comparison of true sonic and density and the logs calculated using Faust, Gardner and Inverse Gardner (IG). All logs and synthetics are displayed in time and are corrected by velocity and survey (the uncorrected IG-sonic was considerably too high). The deep, porous gas sandstone depresses density but not sonic, leading to errors using IG (Ewing, 2007).	18
Figure 3-4 Steps of seismic response to the given lithologic log (Anstey, 1982).	19
Figure 3-5 Generated synthetic seismogram for well KEITH 1; Ness County, KS, r-value (0.707) indicates reasonable correlation of time depth conversion of data.	20

Figure 3-6 Inputting formation top data gathered from the Kansas Geological Survey for wells located in seismic data.....	21
Figure 3-7 Seismic section (crossline) with the top of the Mississippian formation top horizon labeled in green.....	23
Figure 3-8 Initial spectral decomposition using the wavelet transform of seismic signal from Ness County, KS. Attributes analysis will be carried out at these various levels of spectral decomposition.....	27
Figure 3-9 Spectral Decomposition 30 Hz Step 10 Hz: Mississippi Horizon.....	28
Figure 3-10 Spectral Decomposition 40 Hz Step 10 Hz: Mississippi Horizon.....	29
Figure 3-11 Spectral Decomposition 50 Hz Step 10 Hz: Mississippi Horizon.....	30
Figure 3-12 Spectral Decomposition 60 Hz Step 10 Hz: Mississippi Horizon.....	31
Figure 3-13 Spectral Decomposition 70 Hz Step 10 Hz: Mississippi Horizon.....	32
Figure 4-1 Amplitude Attenuation, RMS Amplitude, Acoustic Impedance.....	39
Figure 4-2 Coherency Map showing interpreted geologic discontinuities enhanced with gold lines.....	40
Figure 4-3 RMS amplitude on amplitude attenuation.....	41
Figure 4-4 Coherency on amplitude attenuation.....	42
Figure 4-5 Acoustic impedance in grayscale on amplitude attenuation.....	43
Figure 4-6 RMS amplitude in grayscale on acoustic impedance.....	44
Figure 4-7 Well cuttings correlate to Mississippian horizon amplitude map.....	46
Figure A-1 Spectral Decomposition 20Hz Step 20Hz: Mississippi Horizon.....	52
Figure A-2 Spectral Decomposition 40 Hz Step 20 Hz: Mississippi Horizon.....	53
Figure A-3 Spectral Decomposition 60 Hz Step 20 Hz: Mississippi Horizon.....	54
Figure A-4 Spectral Decomposition 80 Hz Step 20 Hz: Mississippi Horizon.....	55
Figure A-5 Keith #2 Geologist's Report and Drilling time Log.....	56
Figure A-6 Keith #1 Porosity Log.....	57
Figure A-7 Time slice with Mississippi Horizon at approximate inline # 902.....	58
Figure A-8 Time slice overhead view of inline # 902.....	59
Figure A-9 Spectral Decomposition at Timeslice 30 Hz Step 10 Hz.....	60
Figure A-10 Spectral Decomposition at Timeslice 40 Hz Step 10 Hz.....	61
Figure A-11 Spectral Decomposition at Timeslice 50 Hz Step 10 Hz.....	62

Figure A-12 Spectral Decomposition at Timeslice 60 Hz Step 10 Hz.....	63
Figure A-13 Spectral Decomposition at Timeslice 70 Hz Step 10 Hz.....	64
Figure A-14 OpenDtect Attribute generation homescreen.....	65
Figure A-15 RMS amplitude at Spectral Decomposition 50 Hz Step 10 Hz	66
Figure A-16 Attribute Evaluation using varying time gates.....	67
Figure A-17 RMS amplitude Spectral Decomposition 50 Hz Step 10 Hz and time gate (-9,9)....	68
Figure A-18 RMS amplitude Spectral Decomposition 40 Hz Step 10 Hz	69
Figure A-19 Attribute Evaluation using varying time gates.....	70
Figure A-20 RMS amplitude Spectral Decomposition 40 Hz Step 10 Hz time gate (-7,7)	71
Figure A-21 RMS amplitude Spectral Decomposition 30 Hz Step 10 Hz	72
Figure A-22 Attribute Evaluation using varying time gates.....	73
Figure A-23 RMS amplitude Spectral Decomposition 30 Hz Step 10 Hz time gate (-9,9)	74
Figure A-24 RMS amplitude Spectral Decomposition 60 Hz Step 10 Hz, time window of (- 15,10)	75
Figure A-25 Attribute evaluation using varying time gates	76
Figure A-26 RMS amplitude Spectral Decomposition 60 Hz Step 10 Hz time gate (-7,7)	77
Figure A-27 RMS amplitude Spectral Decomposition 70 Hz Step 10 Hz, time window of (- 15,10)	78
Figure A-28 Attribute evaluation of varying time gates.....	79
Figure A-29 RMS amplitude Spectral Decomposition 70 Hz Step 10 Hz time gate (-9,9)	80

List of Tables

Table 1 Kingdom Suite workflow	14
Table 2 Data available in each well.....	22
Table 3 3D Seismic Attribute descriptions.....	36

Acknowledgements

I would like to express my sincere gratitude and appreciation to Dr. Abdelmoneam Raef, who provided me with all the necessary guidance to carry out this research. I would also like to thank my committee members, Dr. Matthew Totten and Dr. Jack Oviatt for their input and advice, which was vital to my thesis. Coral Coast Petroleum provided the seismic data for this study, and I owe strong gratitude for the owner, Dan Reynolds who allowed me to use this data to complete my thesis research. I am also thankful to my parents, Jim and Randall Perdew, my brothers, Harrison and Nathan, and my husband, Dan Philip, for their support and unwavering encouragement in the pursuit of my Master's degree. Finally, I would not be here today without my colleagues at Kansas State University. I owe my fellow graduate students many thanks for the great memories I will take with me after graduation.

Chapter 1 - Introduction

Summary

The use of seismic attributes, such as amplitude, P-wave attenuation, curvature, and coherence, in stratigraphic characterization of hydrocarbon reservoirs have been reported by many authors, e.g. Chopra and Marfurt (2008); Lozano and Marfurt (2008); Chopra and Marfurt (2007); Russell et al. (2003). Seismic interpreters may have a difficult time in distinguishing shale-filled channels vs. sand-filled channels, without attribute-assisted interpretation (Suarez et al., 2008). According to Suarez et al. (2008), the use of different seismic attributes may assist in defining a channel fill zones in more detail. In this study, I will use key attributes; acoustic impedance, amplitude attenuation, RMS (root-mean-square) amplitude and spectral decomposition to pinpoint the location of meandering channel sands in order to further develop the Weirman field and its production. By cautiously selecting and applying independent or a combination of seismic attributes, we can discover the depositional systems of a potential reservoir (Verma et al., 2009). Integrating production and well-log data with 3D seismic attributes is always of great interest in order to calibrate seismic attributes in a quantitative sense or to classify groupings/clusters of variability in seismic attributes. In this study, production or development data of the Weirman field has been integrated with a set of post-stack seismic attributes. This set of seismic attributes, especially attenuation, has been instrumental in highlighting channel-fill lithofacies.

Study Area

Ness County is located in the western part of the state of Kansas, as shown in Figures 1-1 and 1-2. The eastern side of the county is situated along the western edge of the central Kansas uplift. Hydrocarbon fields in Ness County are shown in Figure 1-3. Coral Coast Petroleum

began drilling the well, Keith No. 1 in 2003, located in section 18, T16S, R22W as a wildcat well. The target area of production for this well was the Cherokee sandstone, which is contained in the Cherokee Group. Keith No. 1 produced 162 barrels before it was plugged as a dry well and abandoned. Since then, many other wells have been drilled in the Weirman field and have failed to produce any oil. The prospect for Keith No. 1 was based on a 3D seismic survey that potentially identified a widespread sandstone reservoir of the Cherokee sandstones. Walters et al. (1979) identifies the Cherokee Group as one, which contains channel sandstones as an oil reservoir.

Background and Significance of Study

On the western edge of the Central Kansas Uplift lies Ness County. Petroleum exploration in the county began by the drilling of its first oil well in 1922. A few years later, in 1929, Aldrich # 1 was drilled intentionally on the Beeler anticline and began producing 100 bpd at a depth of 4,422 feet on top of the Mississippi (Mazin, 2009). In 2010, according to the Kansas Geological Survey, Ness County is home to 1003 oil wells, which produced 1,602,494 bbls for that particular year with a cumulative production of 108,616,783 bbls of oil. See Figure 1-3 for a map of the distribution of oil fields located within the county. There are some structural features that influence the subsurface rocks in Ness County, and may affect oil production in the area. These structural features include the Beeler anticline (T. 17S., R. 25-26 W.), and the Bazine Anticline located near T. 21 S., R. 24W. and T. 20S., R. 23 W (Kansas Geological Survey, 2011).

The problem with channel sands is that they are very often below seismic temporal resolution; they also meander, twist, and never follow exact patterns; therefore they are unpredictable and difficult to locate. Figure 2-3 is a modern analog image of the distribution of sediments in a fluvial setting, located in Deep Creek, Manhattan, KS. Here in this modern analog it is evident the high spatial frequency variability of facies of sediments. Nevertheless integrating knowledge of depositional model influencing the area with careful selection of time-

window seismic attributes, seismic patterns related to channel deposits could be highlighted. To this end I carried out a multi-resolution 3D seismic attributes analysis in a time window guided by and including the seismic horizon of the top of the Mississippian. The preformed analysis is in conformity with the depositional model, which describes the unconformity at the top of the Mississippian at the depositional surface of the channel sands. According to my preliminary results, the area of interest is predicted to have lithofacies compartmentalization related to faults and depositional surface gradient irregularities. This is strongly evidenced by interpreted seismic attenuation patterns shown in Figure 4-1. The preliminary results supporting this compartmentalization are in close agreement with production history of the field.



Figure 1-1 United States map. Red star indicates state of Kansas and approximate location of the study area. (Adjusted from Kansas Geological Survey, 2011)



Figure 1-2 Kansas County map. Blue star indicates study area in Ness County (Adjusted from Kansas Geological Survey, 2011).



Figure 1-3 Map of oil and gas fields, Ness County, KS. Includes blue square indicating study area. Map obtained and modified from distribution of oil and gas fields of Ness County, Kansas (Kansas Geological Survey, 2011).

Chapter 2 - Geological Setting

The area of interest in this study includes the Cherokee Group, which was deposited during the Desmoinesian Stage of the Pennsylvanian System, occurring after the Mississippian unconformity. This group is comprised of mostly shale and sandstone, with minute quantities of limestone. The thickness of the Cherokee Group ranges from 5-200 feet, (Stoneburner, 1982). The Cherokee Group was transitionally deposited from a continental environment to marginally marine environment when the receding of the Hugoton Sea caused the Mississippian unconformity onto the Central Kansas uplift (Cuzella, 1991). Figure 2-1 represents the stratigraphic relationships of the Cherokee Group to the older and younger rock units in the section. The study area is roughly located between wells 9 and 10 in the cross section. The Cherokee Group appears to be thicker towards the southwest, and thinner towards the northeast, closer to the Central Kansas uplift. The Cherokee sandstones are mostly deposited along the Mississippian unconformity, which is overlain by a sequence of tilted resistive rocks and shales, along with underlying clastic sequences. The Mississippian unconformity controls the trend and distribution of sandstones, which ultimately produces a series of escarpments and valleys. Later, streams have proceeded to cut into the less resistant strata thus enabling the formation of channel sands, Stoneburner (1982).

Analysis of my study area using Gamma ray logs has shown characteristics of channel sandstones. Figure 2-4 exhibits a SP and Neutron log, where I have highlighted the zone of interest on the top of the Mississippian formation. Characteristics of channel sandstones were exhibited by analysis performed on the Gamma ray logs taken from the study area. These characteristics were due to an increase in radioactivity readings, which indicate coarse sandstone fill at the bottom of the channel and more fine sandstone fill at the top (Figure 2-4). The process of gradual grain size changes as we move up and down the channel is based on Walter's Law. These changes correspond to lateral facies changes as you move across a channel, beginning with shales and siltstones of the flood plain facies to fine-grained sandstones in the point-bar facies, then finally observed coarser grained sandstones and conglomerates within the channel facies itself (Stoneburner, 1982). Any channel effects will be compounded with the reflection event of the top of the Mississippian Formation in the 3D seismic data.

Upper Mississippian

Figure 2-6 shows a portion of a larger stratigraphic column published by the Kansas Geological Survey, which shows the classification of rocks in Kansas. The Mississippian System rocks occur in the subsurface of the state of Kansas and cover the majority of its entirety. The exclusions to this statement occur on the crests of the Central Kansas uplift, Cambridge arch and the Nemaha anticline. The Upper Mississippian series is the group in which holds most value for this study. The Upper Mississippian series in Kansas consists of mostly limestone and dolomite, with scattered beds of sandstone and shale, along with minor amounts of chert (Goebel, 1968). The Meramecian Stage rocks of the Upper Mississippian series lie on a disconformity at the top of Osagian rocks that include mostly marine limestones (oolitic and fossiliferous) and some interbedded dolomitic limestone and chert. A vast majority of these limestone formations were eroded prior to the Pennsylvanian.

Cherokee Group

The Pennsylvanian System outcrops in Kansas only in the eastern part of the state; in the western part of the state the Pennsylvanian rocks, which include the Cherokee Group, lie below the surface. The Cherokee Group rocks were deposited during the Desmoinesian Stage of the Middle Pennsylvanian series (Figure 2-6). These particular rocks are important stratigraphic indicators of widespread unconformities. The Cherokee Group includes both marine and non-marine rocks and consists mainly of sandstone and sandy shale. The sandstone portion of the Cherokee is present as elongated “shoestring” sandstones that are intercalated with Cherokee shales (Van Dyke, 1976). Based on the stratigraphy, the sandstone is of fluvial origin with coupled channel and overbank facies. Van Dyke (1976) classifies the Cherokee sandstones as litharenites, having seventy percent quartz, twenty percent metamorphic rock fragments, and ten percent accessory minerals. Not relevant to this study, but just as important, the most significant coal beds of the state reside in this group of rocks. The Middle Pennsylvanian, Desmoinesian,

rocks are described as having a cyclic nature, consisting of shales and limestones with alternating non-marine strata. The Desmoinesian Stage is the lower segment of Pennsylvanian rocks that outcrop in Kansas. This Cherokee Group within this stage varies greatly from the overlying Marmaton Group and the underlying Mississippian rocks. The formations within the Cherokee Group include; Krebs Formation, which consists of mainly shale, limestone, underclay and coal, and its members: Warner Sandstone Member, Bluejacket Sandstone Member, Seville Limestone Member. The other formation included in this group is the Cabaniss Formation, which is composed of mostly shale, some sandstone, limestone and coal; its members are: Chelsea Sandstone Member, Verdigris Limestone Member, and the Breezy Hill Limestone Member.

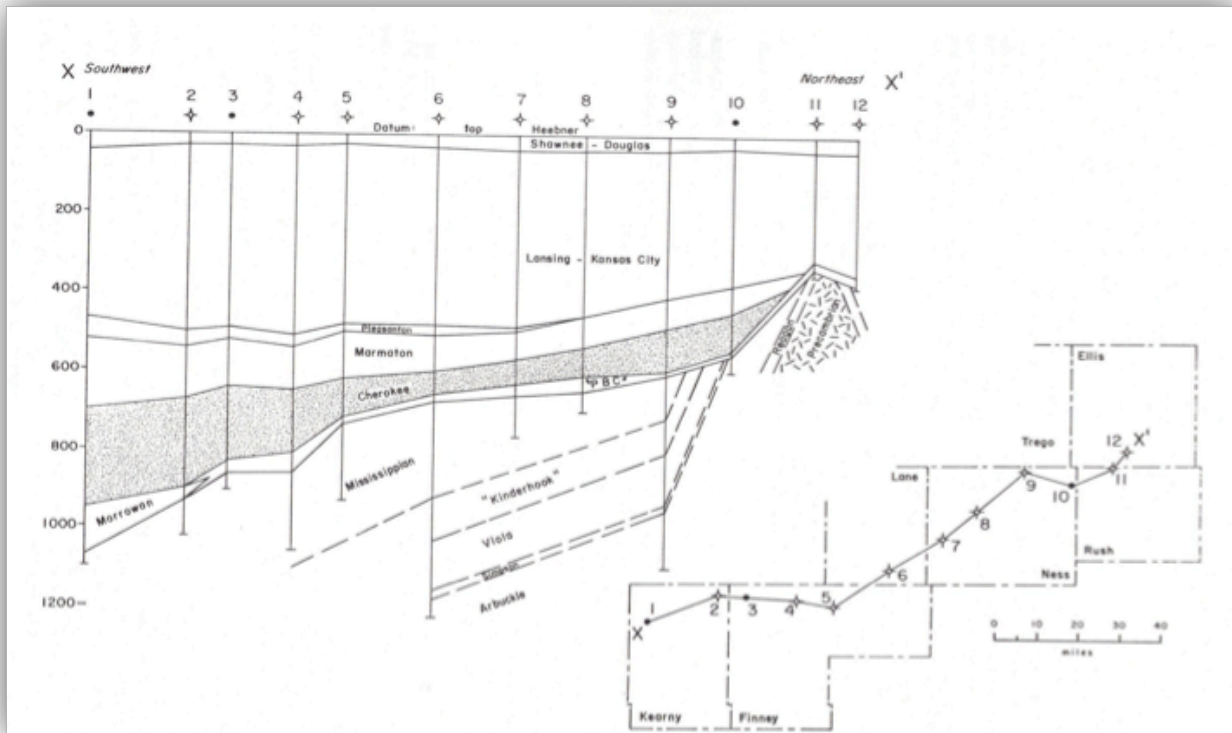


Figure 2-1 SW-NE stratigraphic cross section, showing both the Mississippian and Cherokee formations. Area of interest is located approximately between wells 9 and 10 (Adjusted from Marriam, 1963).

Depositional Environment

The Cherokee Group was deposited during a time of transgressing and regressing seas. The rock sequences observed in the Pennsylvanian rocks show certain sedimentary processes that were active during the time period. These processes help explain the deposition of sand in slender “shoestring” groups that are associated with fluvially dominated delta systems among other similar environments. These sandstone bodies seem to be where the sediment entered the seaway from a river system to the seaway margins (Brenner, 1989). Figure 2-2 shows diagrams, which represent a potential depositional system of the Cherokee group in a fluvial dominated delta lobe, including an overview of the lobe as well as a zoomed-in image of the channel itself.

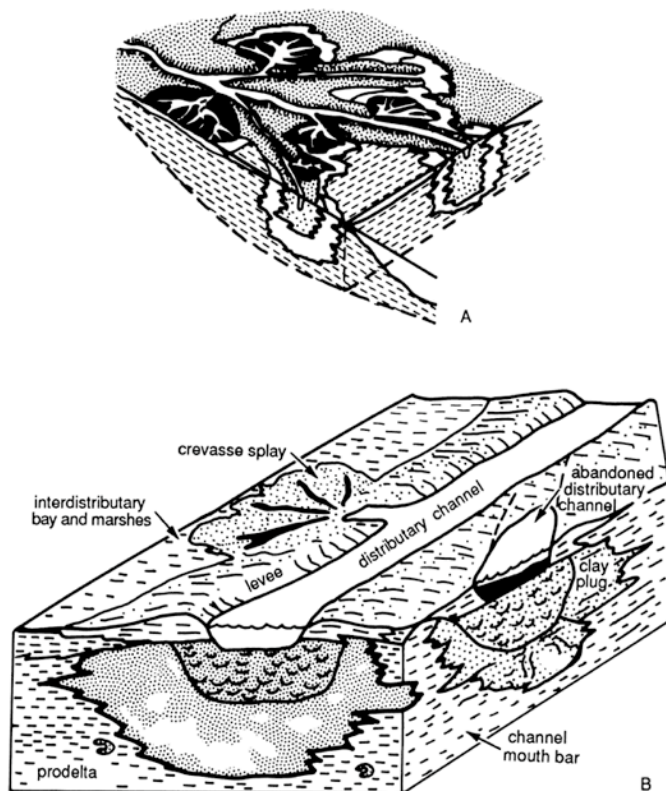


Figure 2-2 Potential Depositional Environment for Cherokee Group: A) Overview of system B) Facies of channel (Adjusted from Brenner, 1989).

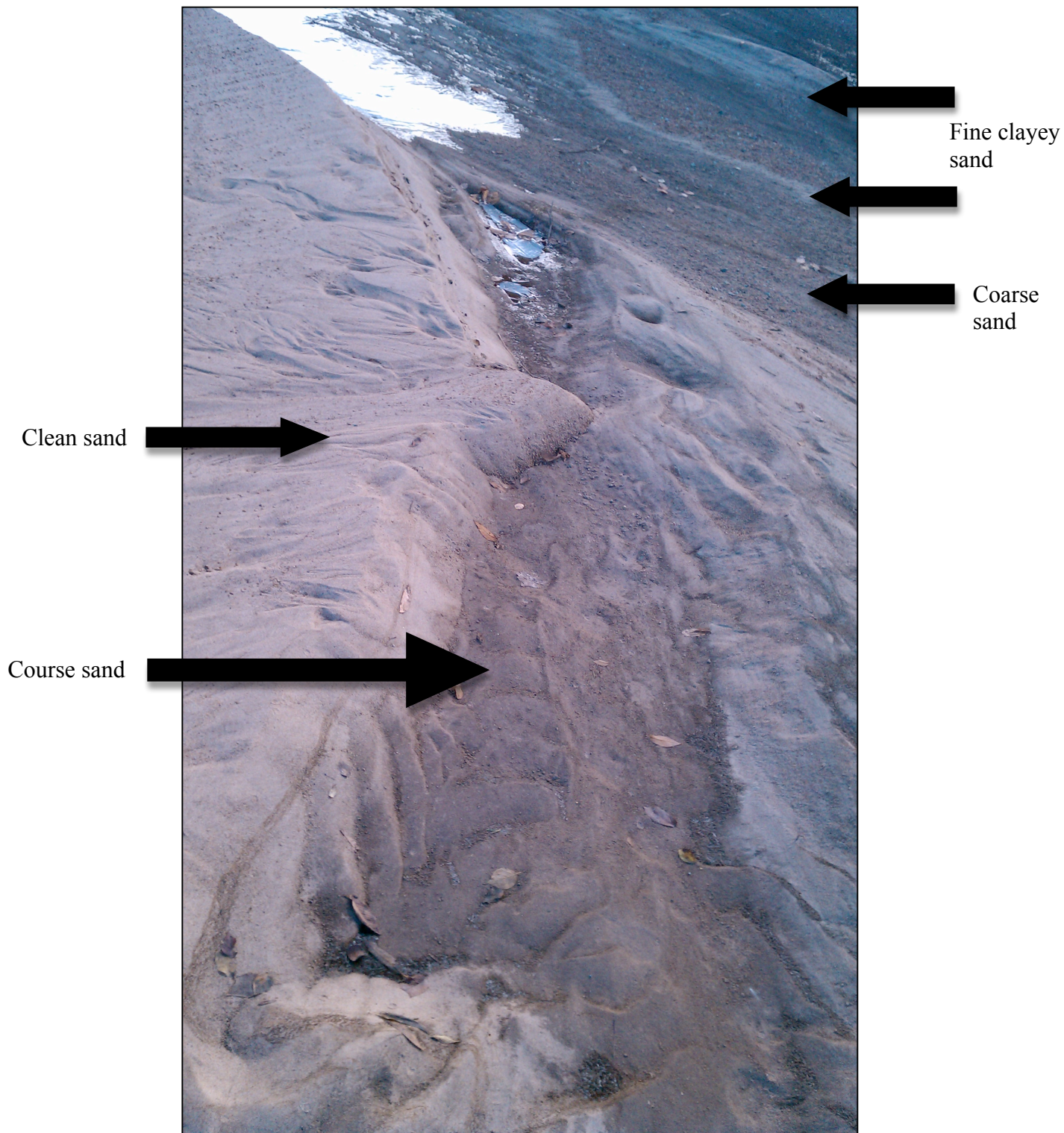


Figure 2-3 Modern analog of Deep Creek, Manhattan, KS to show variability in sediment facies.

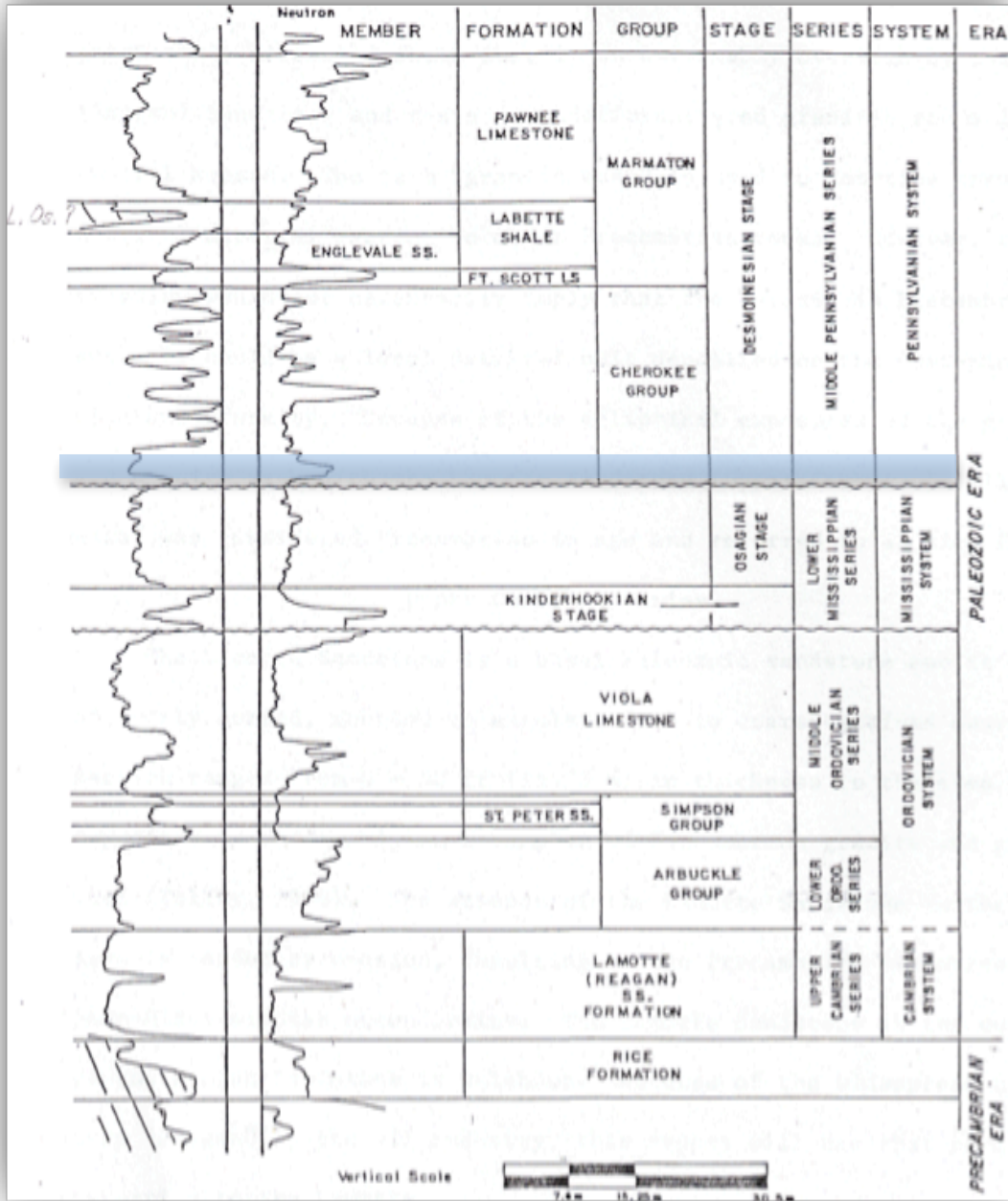


Figure 2-4 Exhibits the relationship between an SP/Neutron log and a stratigraphic section in study area; the blue box marks the channel sand facies (Adjusted from Stoneburner, 1982).

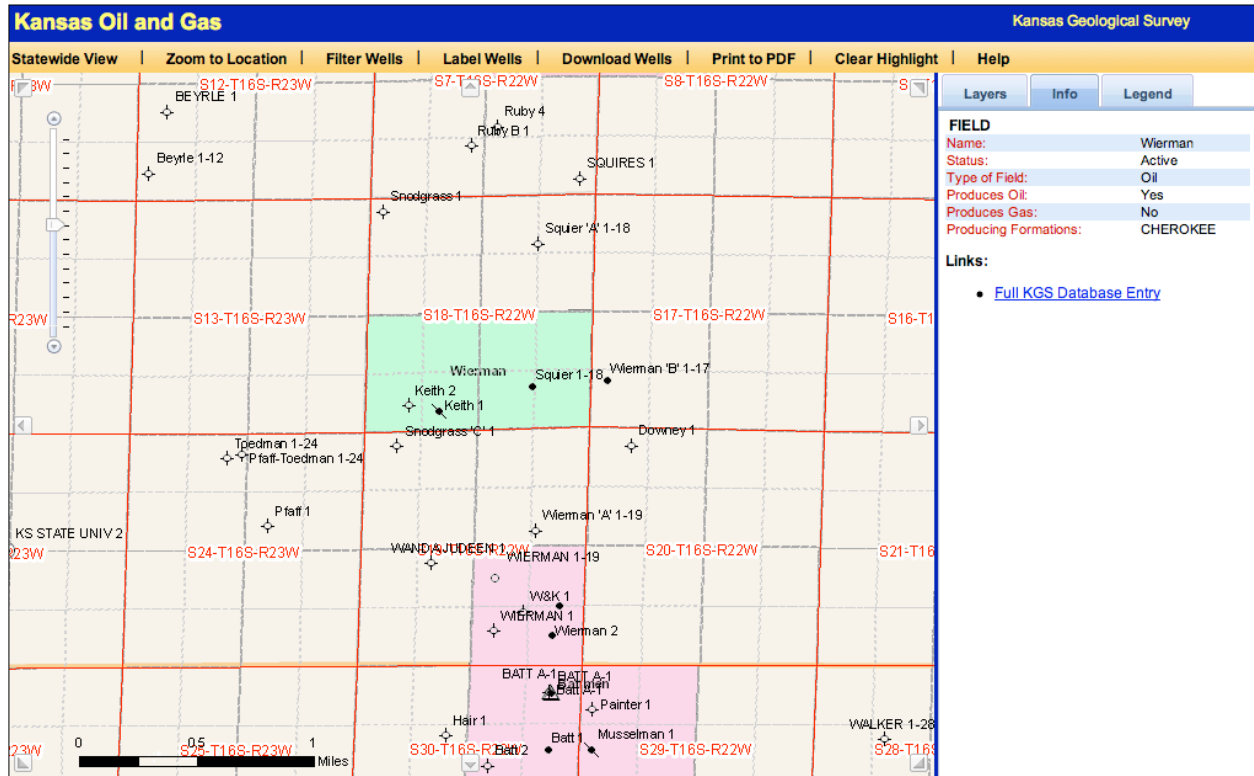


Figure 2-5 Map of Weirman Field wells and surrounding areas (Kansas Geological Survey, 2011).

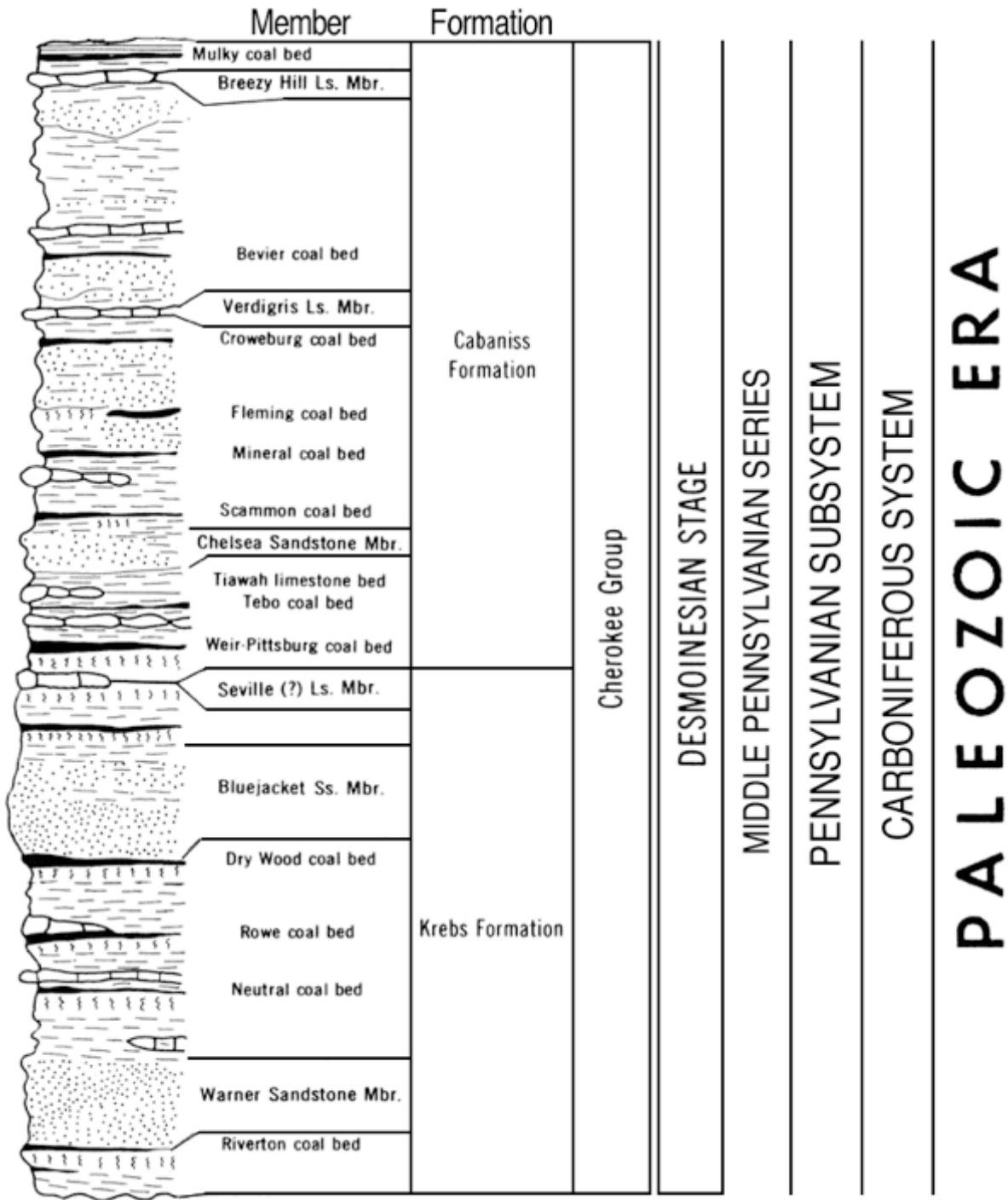


Figure 2-6 Kansas Stratigraphic Column showing the Cherokee Group (Adjusted from Kansas Geological Survey, 2011).

Chapter 3 - Data and Methods

Data Loading

Seismic data and well logs were uploaded into Kingdom Suite software (Figure 3-1) licensed by Seismic Micro-Technology, Inc., and a workflow was created. Coral Coast Petroleum executed the seismic acquisition survey in 2002, in the Weirman field, Ness County, Kansas. The survey parameters include 136 (west to east) in-lines and 61 (south to north) cross-lines. The sampling rate for this survey was approximately 2.0 milliseconds. The survey boundaries are located 0.9 mi from the west side of sec. 18 T. 16 S., R. 22 W., and about 2.1 miles from the northern edge of sec. 18 T. 16 S., R. 22 W. It was uploaded as a SEG Y file into Kingdom Suite and detailed as a Pre/Post-Stack Migrated Volume (Abbas, 2009). The data were uploaded using a Seismic Reference Datum of 2700 feet and a replacement velocity of 9000 feet per second. The survey was projected to a specific location using parameters for the projection system of NAD 27, Southern Zone, US Foot.

Data Collected

Kingdom Suite by Seismic Micro-Technology is a PC-based software that provides seismic interpretation, reservoir modeling, geo-modeling, seismic to simulation and many other workflows to the user. Companies of all sizes use Kingdom; multinational, national and regional independent companies all choose Kingdom Suite to be their seismic interpretation software of choice. To learn more about Kingdom Suite by SMT visit: www.seismicmicro.com. 3D seismic data for this study, provided by Coral Coast Petroleum, were uploaded into Kingdom Suite and a workflow was created for this study (Table 1).

Step	Description
Step 1	Upload seismic to Kingdom; create new project
Step 2	Generate synthetic seismograms
Step 3	Pick formation tops and track horizons
Step 4	Generate seismic attributes and perform spectral decomposition
Step 5	Qualitative seismic attribute interpretation
Step 6	Log and well cutting analysis

Table 1 Kingdom Suite workflow

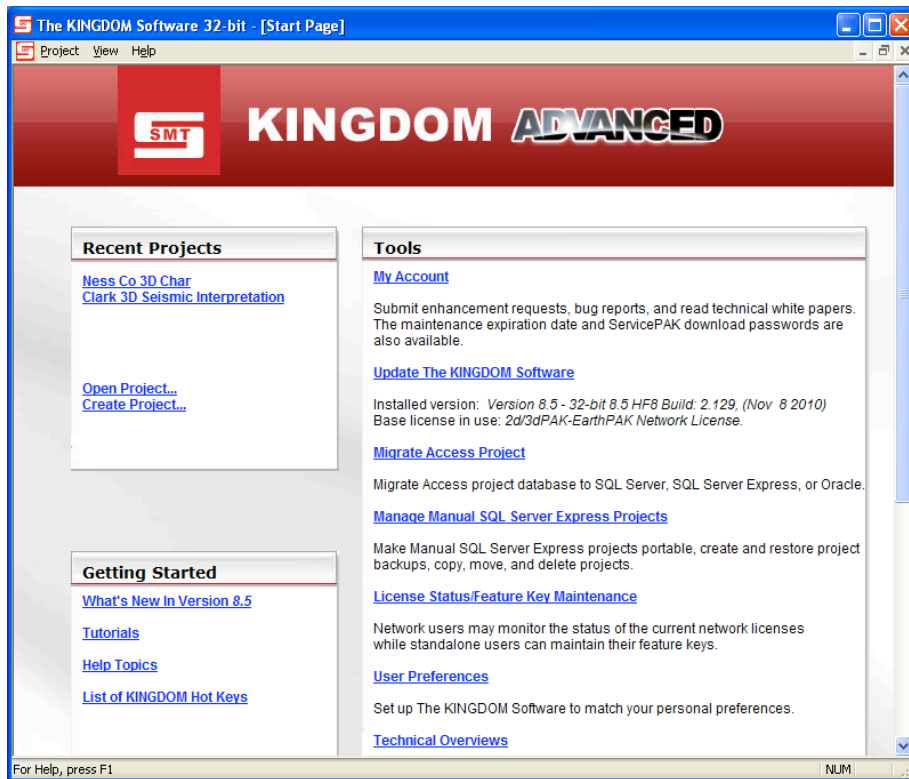


Figure 3-1 Kingdom Suite loading screen.

Methodology

Synthetic Seismograms

Synthetic seismograms were generated for each oil well in the area of interest Ness, County, KS (Figure 3-5). The seismograms are generated using density logs from each well and a wavelet derived from the seismic data. Well logs provide a smaller sampling interval than the vertical resolution within the seismic data when measurements of velocity and density of the borehole are taken. The velocity and density information from the well log are then configured to produce acoustic impedance (frequency). When the acoustic impedance is combined with the velocity information, a reflection coefficient series is produced in relation to time. This series is then convolved with the wavelet extracted from the seismic data to produce the synthetic seismogram. The purpose of creating synthetic seismograms is to see the relationship between rock properties of a borehole within an oil well, and the seismic reflection data. A synthetic seismogram produces seismic traces that we can expect to see from a specific series of layers in the earth, when one produces an actual seismic pulse. There are both advantages and disadvantages to using synthetic seismograms to predict hydrocarbon reservoirs. In petroleum exploration, synthetics are used to tie changes in rock properties in a borehole to seismic reflection data at the same location. Synthetic seismograms are commonly used to identify reflectors; in order to tie these desired reflectors to well log data. One of the main purposes of synthetic seismograms is to show what a hydrocarbon reservoir would look like using the comparison of the waveform and amplitude of the reflector, to the subsurface lithology. This is accomplished with a sonic and/or density log from a well of interest. Synthetic seismic modeling may be used to reduce different uncertainties in interpretation. Before describing the convolutional model, which is essential in obtaining synthetic seismograms, one must understand convolution as an operation. Convolution is a process that involves replacing inputs with outputs; which are scaled according to the original input. This filtering process occurs in the time-domain of a dataset. Convolution is used as a method of filtering 3D seismic data by convolving the data, then summing the inputs and outputs that occur at the same time. An example of this filtering process is shown in Figure 3-2. Using these individual, linear, elements

or reflectors we are able to superimpose them, using convolution, in order to see the effect of the filter.

A one-dimensional model in which seismic energy is transmitted and reflected along a single ray-path at normal incidence to reflecting interfaces is called the convolutional model (Henley 2004).

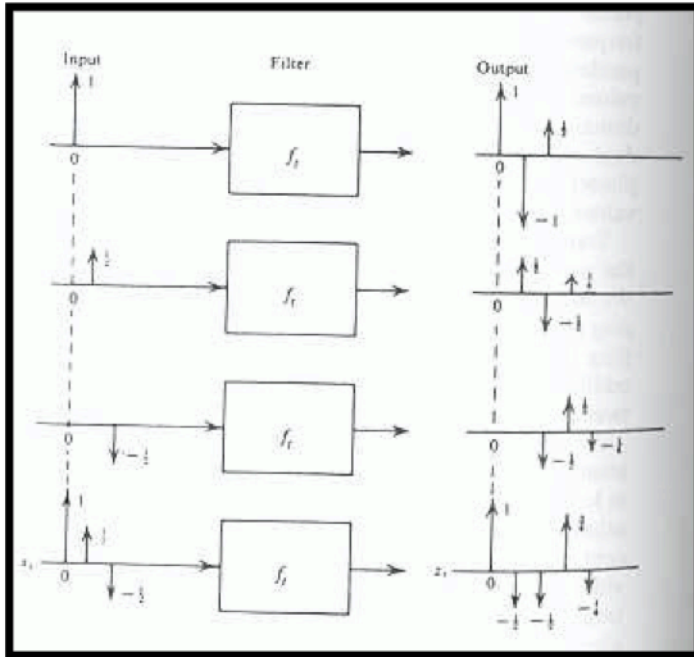


Figure 3-2 Filtering as an example of convolution (Sherriff, 1995).

One of the most common uses of synthetic seismic modeling is to identify reflections with certain interfaces, then compare these points of interest to actual seismic data. Synthetic seismic modeling is frequently used to differentiate primary reflectors from multiples and other events. Synthetic seismic modeling can also help stratigraphic interpretation of seismic data, because it assists the interpreter in obtaining an improved idea of what to look for, as well as the ability to administer necessary change. The interpretation of seismic reflection profiles is a difficult concept because individual reflections have complex behaviors, especially near geologic structures. A simple, one-dimensional synthetic seismogram is created from a convolved wavelet of reflectivity, when offset and horizontal layering, are assumed as zero. They may also

include velocity and density values which are incorporated into the seismogram from borehole logs in a well. Two-dimensional seismograms are not limited to the same restrictions that one-dimensional seismograms are. They are able to model different diffractions and the dependence on offset of arrival times, waveform, and amplitude (Yilmaz, 2001).

In order to accurately evaluate a synthetic seismogram, we must understand the steps expressed by equations that are crucial in producing a synthetic seismogram. We must first determine the seismic impedance associated with a horizontal subsurface layer.

Seismic impedance is expressed below:

$$I_k = \rho_k v_k$$

where, ρ is density and v is the velocity within the layer. The subscript k , is denoted as the variable layer in which seismic impedance is determined. From this equation, we produce the pressure amplitude reflection coefficient and therefore, with the knowledge of the reflection coefficients we can form an impulse response or a reflection coefficient log. Using a source wavelet and convolving the reflection coefficient log we can produce a synthetic seismogram. Using the convolutional model we produce the following equation:

$$x(t) = w(t) * e(t)$$

when convolving a seismic wavelet, $w(t)$ with the reflection coefficient $e(t)$ to produce the synthetic seismogram $x(t)$. The type of synthetic seismogram one produces is based on the information that you have. In order to produce a proper synthetic seismogram, both sonic and density data are used. Figure 3-3 has three different examples of how synthetic seismograms are created using a lack of data, using three different equations and their combinations. These techniques include, the Gardner equation, the Faust equation, and an inverse Gardner relationship. The Gardner equation relates density and velocity and the Faust equation relates resistivity and velocity. The inverse Gardner relationship should be used if you have density information but no sonic data. This figure is a good example of how information is taken from

density and sonic logs in order to form synthetic seismograms. One may also see the differences and similarities between the three synthetic seismograms.

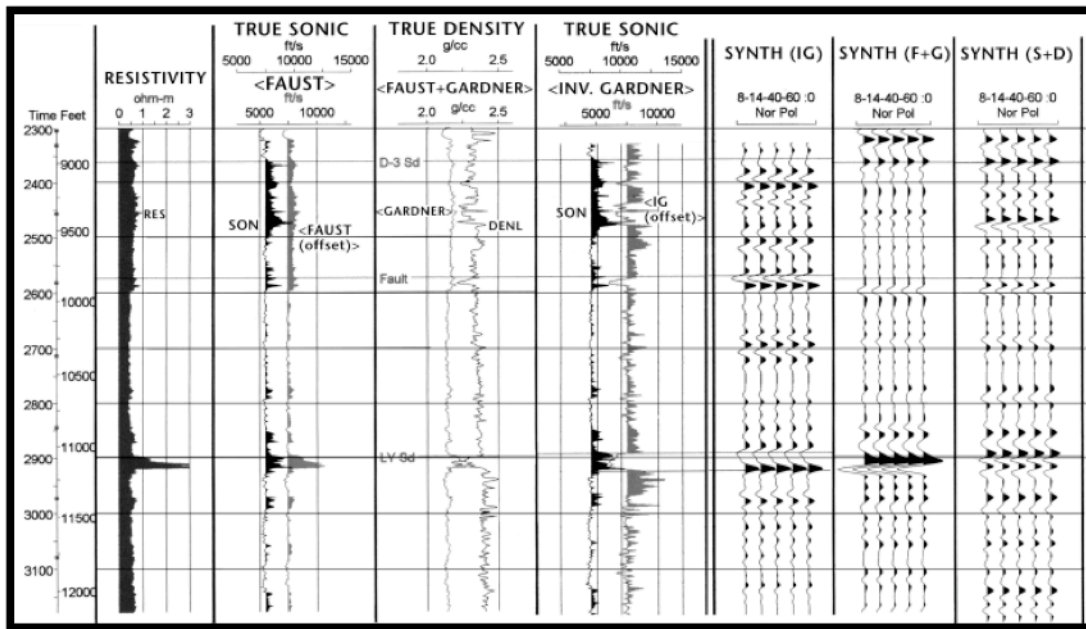


Figure 3-3 Comparison of three synthetic seismograms for a deep Yeuga well. The left-hand panels show the comparison of true sonic and density and the logs calculated using Faust, Gardner and Inverse Gardner (IG). All logs and synthetics are displayed in time and are corrected by velocity and survey (the uncorrected IG-sonic was considerably too high). The deep, porous gas sandstone depresses density but not sonic, leading to errors using IG (Ewing, 2007).

It is also important to understand how a synthetic seismogram comes together incorporating each reflector, which are represented by the reflection coefficient log. Figure 3-4 shows individual reflection pulses at the appropriate time, strength and sign denoted by the reflection coefficient log. They are furthermore added together to obtain a synthetic seismogram.

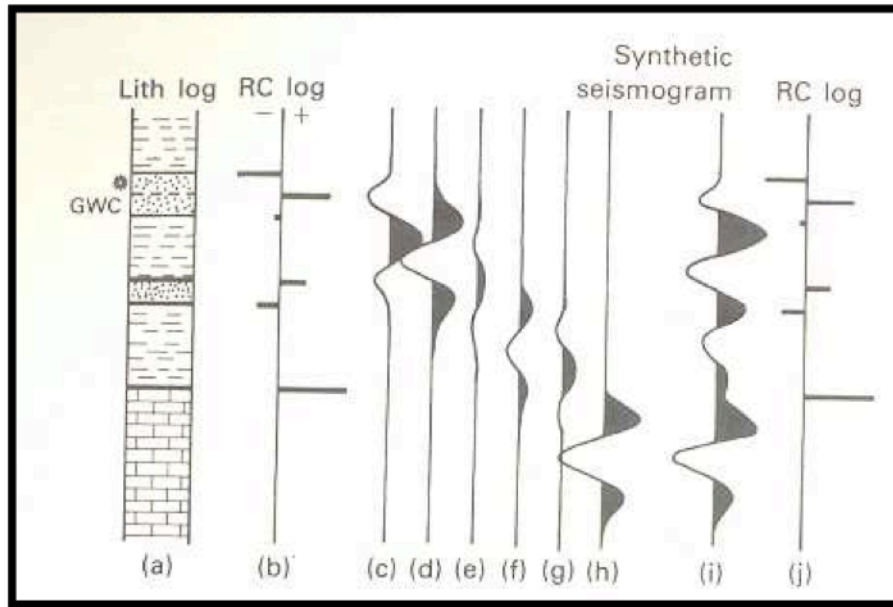


Figure 3-4 Steps of seismic response to the given lithologic log (Anstey, 1982).

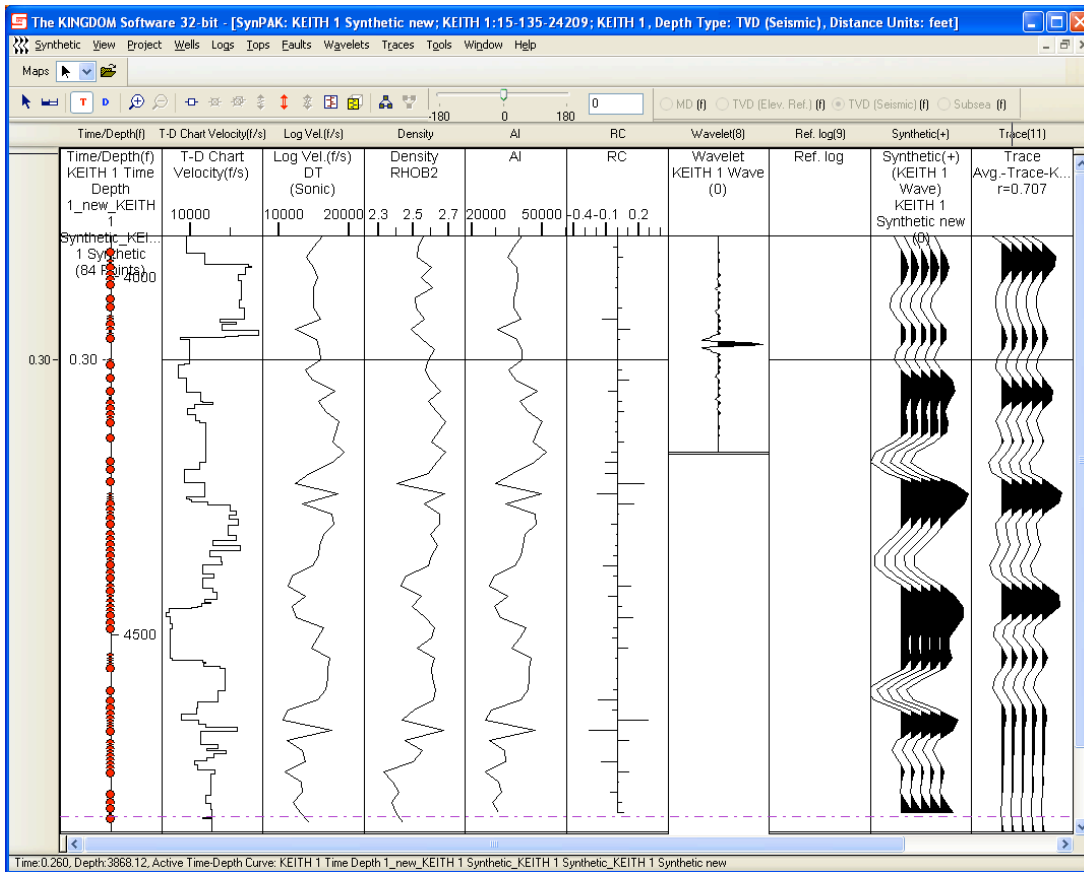


Figure 3-5 Generated synthetic seismogram for well KEITH 1; Ness County, KS, r-value (0.707) indicates reasonable correlation of time depth conversion of data.

Formation Tops and Horizon Tracking

In order to determine where the formations are present within the seismic data, one must input formation-top data into Kingdom Suite (Figure 3-6). These formation tops for each well are then mapped and picked manually, so that they are automatically tracked throughout the entire seismic section. This way, one is able to focus on a specific area of interest within the seismic data. For example, the top of the Mississippian formation is shown in Figure 3-7, as mentioned previously, the area of interest is approximately 10 milliseconds above the top of the

Mississippian into the Cherokee Group. The Mississippian formation top allows us to focus on the crucial area of study. The formation top information is vital to this study along with information about each well that is included in the seismic area. Table 2 shows information gathered from the Kansas Geological Survey website, to aid in characterizing this area.

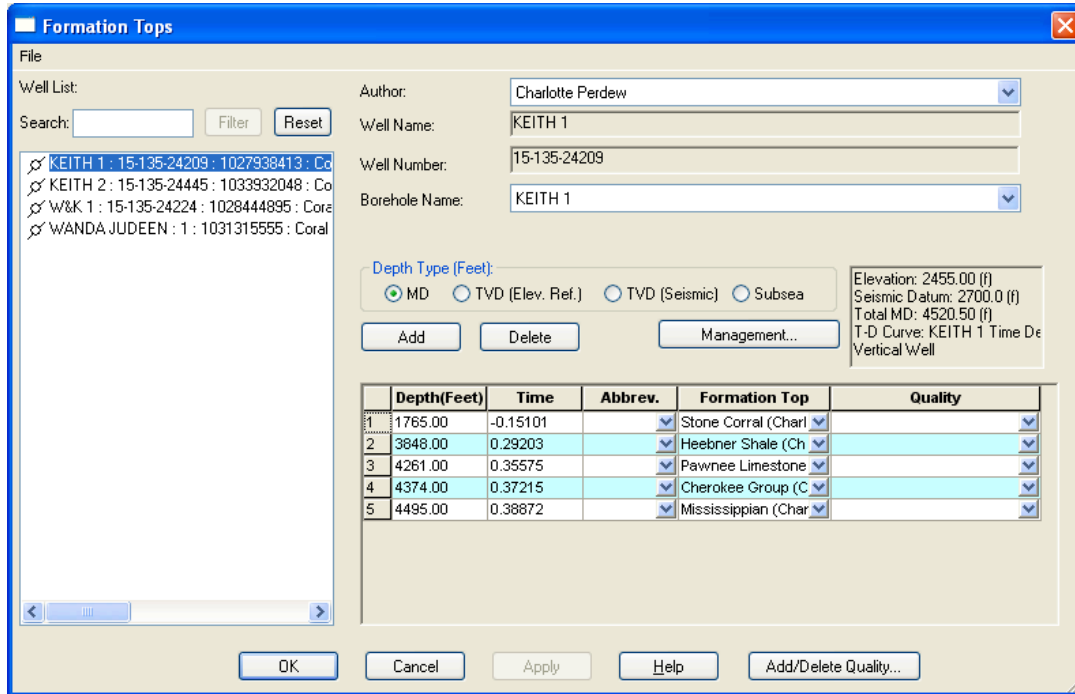


Figure 3-6 Inputting formation top data gathered from the Kansas Geological Survey (2011) for wells located in seismic data.

Well Name	Elevation	Total Depth	Well Logs	Tops	Status
Keith # 1	2455 KB	4520	Yes	Yes	Plugged & A
Keith # 2	2456 KB	4510	Yes	No	Plugged & A
Wanda Judeen	2445 KB	4530	Yes	Yes	Plugged & A
W & K # 1	2430 KB	4530	Yes	Yes	Plugged & A
Squier #1-18	2446 KB	4578	No	No	Producing
Weirman 'A' #1-19	2440 KB	4520	No	No	Plugged & A
Weirman 'B' #1-17	2444 GL	4530	No	No	Spudded
Snodgrass 'C' #1	2456 KB	4510	No	Yes	Plugged and A
Squier 'A' #1-18	2455 KB	4520	No	No	Plugged and A
Snodgrass # 1	2442 KB	4466	Yes	Yes	Plugged and A

Table 2 Data available in each well

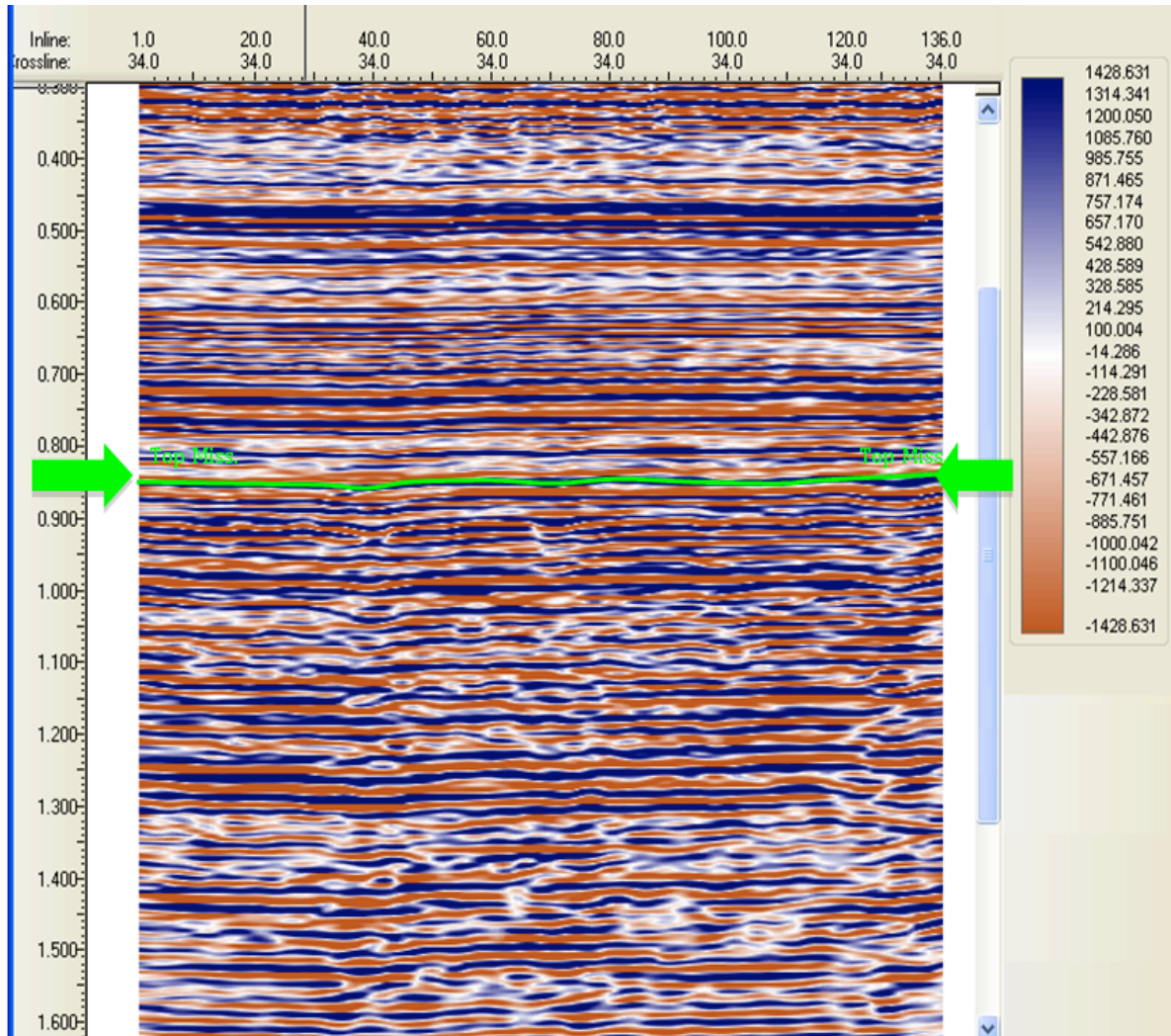


Figure 3-7 Seismic section (crossline) with the top of the Mississippian formation top horizon labeled in green.

Spectral Decomposition and Wavelet Transform

In this study, wavelet transform is utilized for spectral analysis at various levels of resolution to pursue seismic patterns that may have stratigraphic significance. Spectral decomposition, also known as time-frequency decomposition, is used to characterize the time-dependent frequency responses of reservoirs and subsurface rock formations. There are many different methods for achieving spectral decomposition. By applying different bandwidths to the seismic wavelet, one is able to adjust the time-frequency spectrum and to highlight different aspects of the seismic data. Greg Partyka introduced spectral decomposition in 1999, to allow interpreters to use frequency dependent components of the seismic bandwidth to interpret small changes in subsurface stratigraphy otherwise unseen (Chopra, 2006).

The wavelet transform allows the decomposition of a signal into various levels of scales or “resolution.” Different analyzing wavelets could be used in the decomposition process. Multi-resolution analysis has the potential to detect sub-seismic resolution channel sand bodies through some experimental attributes synthesis, which would also enhance subtle litho-facies related interpretive seismic patterns. Ojo and Sindiku (2003) used the seismic application of spectral decomposition to 3D seismic data from Southern Nigeria to map the geometry of incised channels. The spectral response of this study showed the lateral channel complex clearly and indicated fault trends. Wavelet transform is used in this study over the traditional Fourier transform function mainly because it has the ability to localize seismic information in the time-frequency domain simultaneously (Miao and Moon, 1999). The Fourier transform:

$$F(\omega) = \int_{-\infty}^{\infty} f(t)e^{-i\omega t} dt$$

extracts signals from a function $f(t)$ of infinite time which cannot be associated with the frequency information. The Fourier transform is only limited to analysis and processing of signals in either the time or the frequency domain. Fourier transform applies to many stages of

seismic data analysis and processing. A seismic trace is collected from a receiver during the acquisition of seismic data. This trace is a function of time and has a unique amplitude, frequency, and phase. The Fourier transform is a way to break down or decompose a wave field into its plane-wave components. Fourier analysis basically compares wavelets with sine waves. A wavelet is a waveform that has an average of zero and can be shaped irregularly and asymmetric. Sine waves have a limited duration from minus to plus infinity and are smooth and usual in shape. The process of analysis breaks up the wavelet into sine waves of different frequencies and cross correlates them to seismic data at predetermined frequencies.

The Short-Time Fourier Transform (STFT) is also called spectral decomposition. It can be used for the purpose of attenuating low frequency ground roll, cultural noise, and high frequency noise. STFT is an adaptation of the Fourier transform to analyze a smaller area of a selected signal. This technique is appropriately called *windowing* the signal. The STFT maps a specific signal into a 2D function of time and frequency. The size of the selected window determines the information you can receive about time and frequency of the event. The STFT is most often used when an interpreter wishes to analyze the frequency of particular events in a fixed time window across multiple frequencies. This practice provides the interpreter with a horizontal localization of frequency content. A potential disadvantage is that once the size of a time window is selected, it is the same for all frequencies. If the selected window is long, it prevents time localization of high frequency components and if the window is short, it limits the spectral resolution of the low frequency components. The fixed time window also limits the technique's temporal resolution. Many interpreters require a more accommodating method that is able to vary the window size to inspect signals more accurately.

Wavelet transform is commonly called instantaneous spectral analysis. The continuous wavelet transform (CWT) differs from the STFT when it comes to pre-determining window size. The CWT does not require a particular window size therefore it does not have a fixed time-frequency resolution over the time-frequency space. This is crucial in determining instantaneous spectral attributes from seismic data, such as frequency-dependent rock properties, because seismic data are non-stationary and have changing frequencies in time. The wavelet transform is

able to localize crucial information with a “zoom-in and zoom-out” ability, meaning that the window function is not fixed. The wavelet transform of a signal $S(t)$:

$$W_s(a,b) = \left\langle h^{(a,b)}, S(t) \right\rangle = \frac{1}{\sqrt{|a|}} \int h * \left(\frac{t-b}{a} \right) S(t) dt$$

where $h^{(a,b)} = |a|^{-\frac{1}{2}} h\left(\frac{t-b}{a}\right)$ is a group of wavelet functions that were constructed from a mother wavelet by parameters a and b which are defined as the scale which is related to frequency, and the position, respectively (Sinha et al., 2005). The goal of using wavelet transform is to be able to break down a signal into varying frequencies in order to enhance different properties. Figure 3-8 shows the seismic signal of the 3D seismic data in red, below are 7 wavelet transformations of the same signal using varying frequencies, beginning with the lowest approximate formation. This process allows the interpreter to take the 1D signal or single trace and detail the data into sub-bands, thus potentially revealing rock properties of interest.

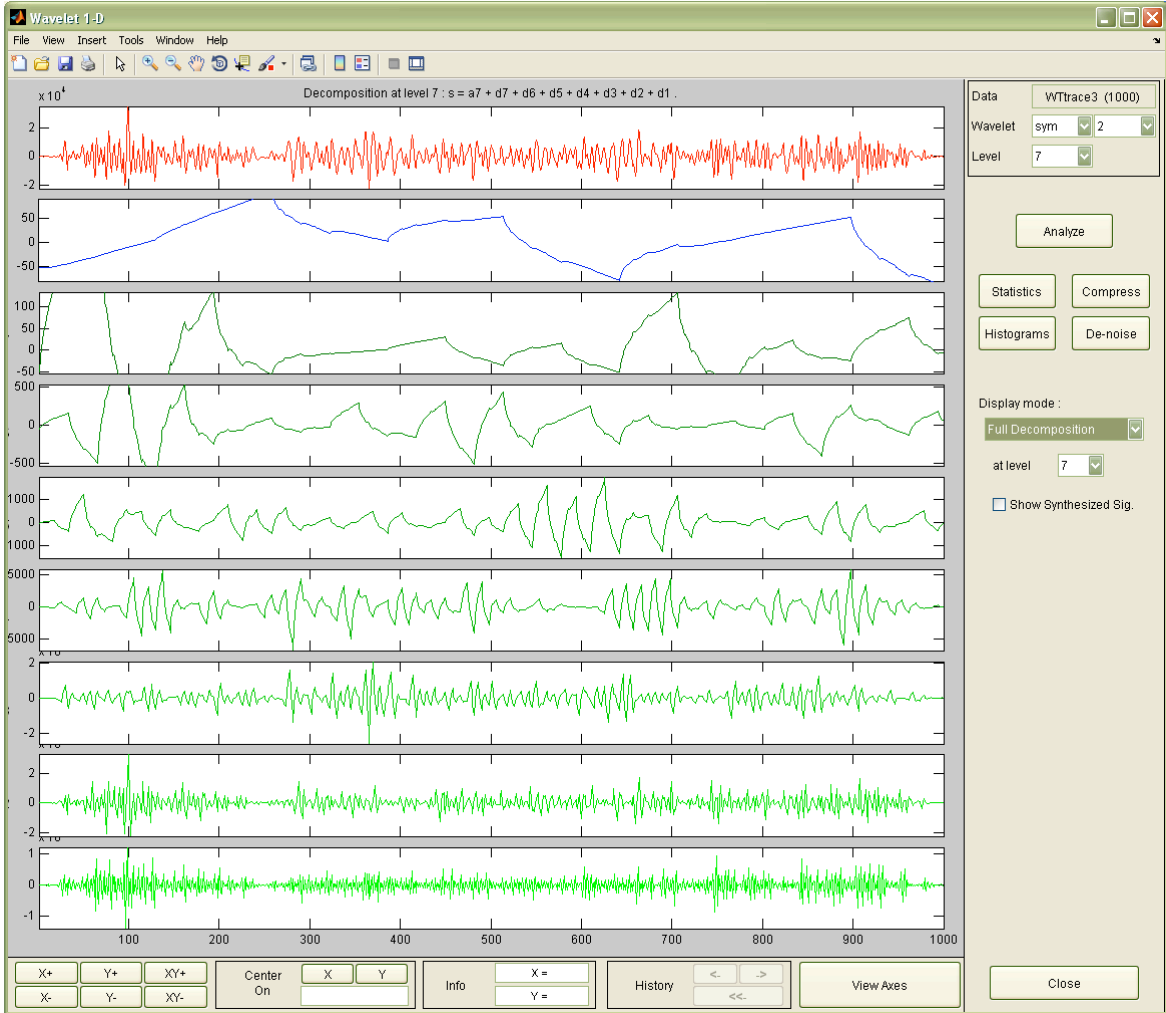


Figure 3-8 Initial spectral decomposition using the wavelet transform of seismic signal from Ness County, KS. Attributes analysis will be carried out at these various levels of spectral decomposition.

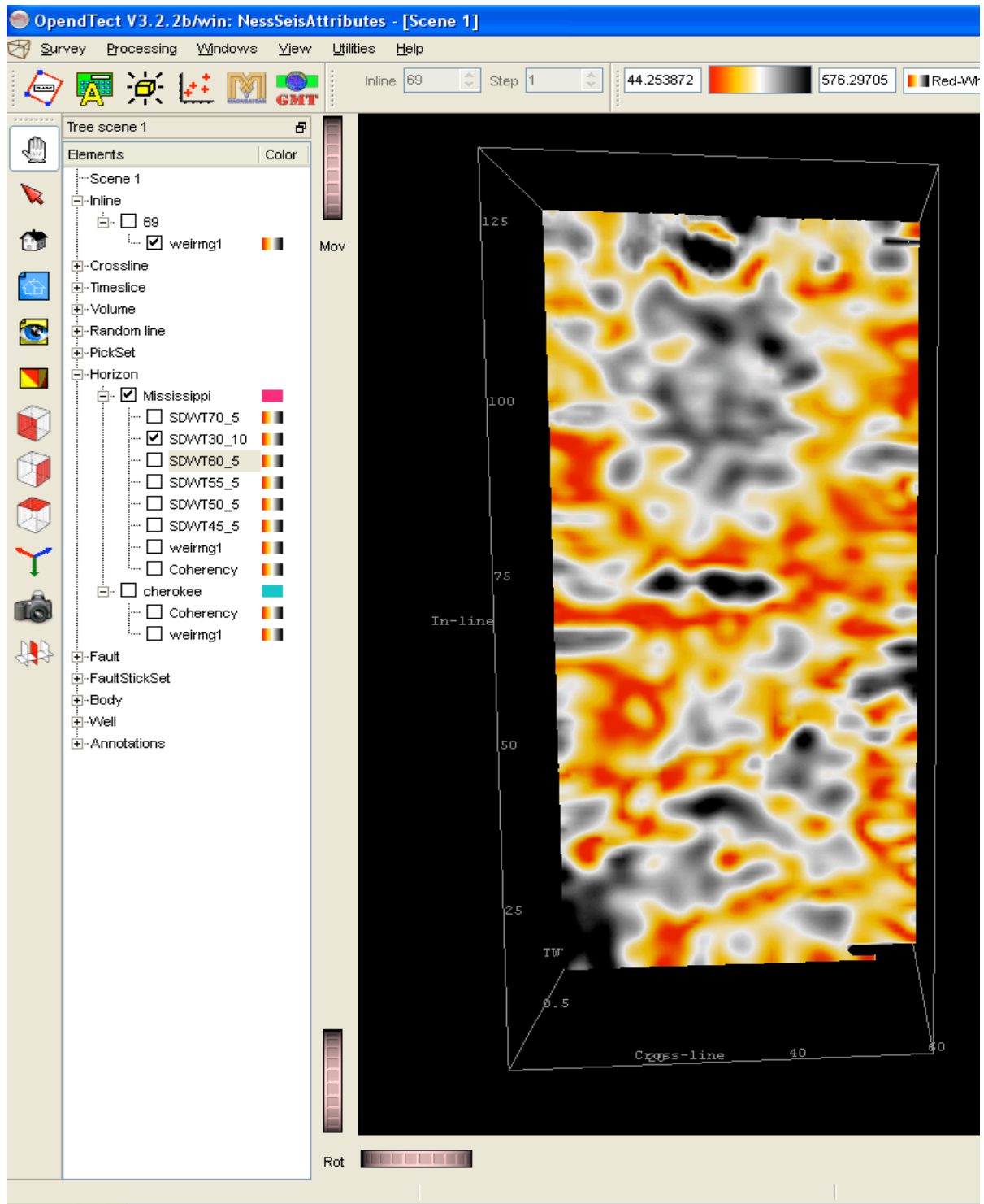


Figure 3-9 Spectral Decomposition 30 Hz Step 10 Hz: Mississippi Horizon

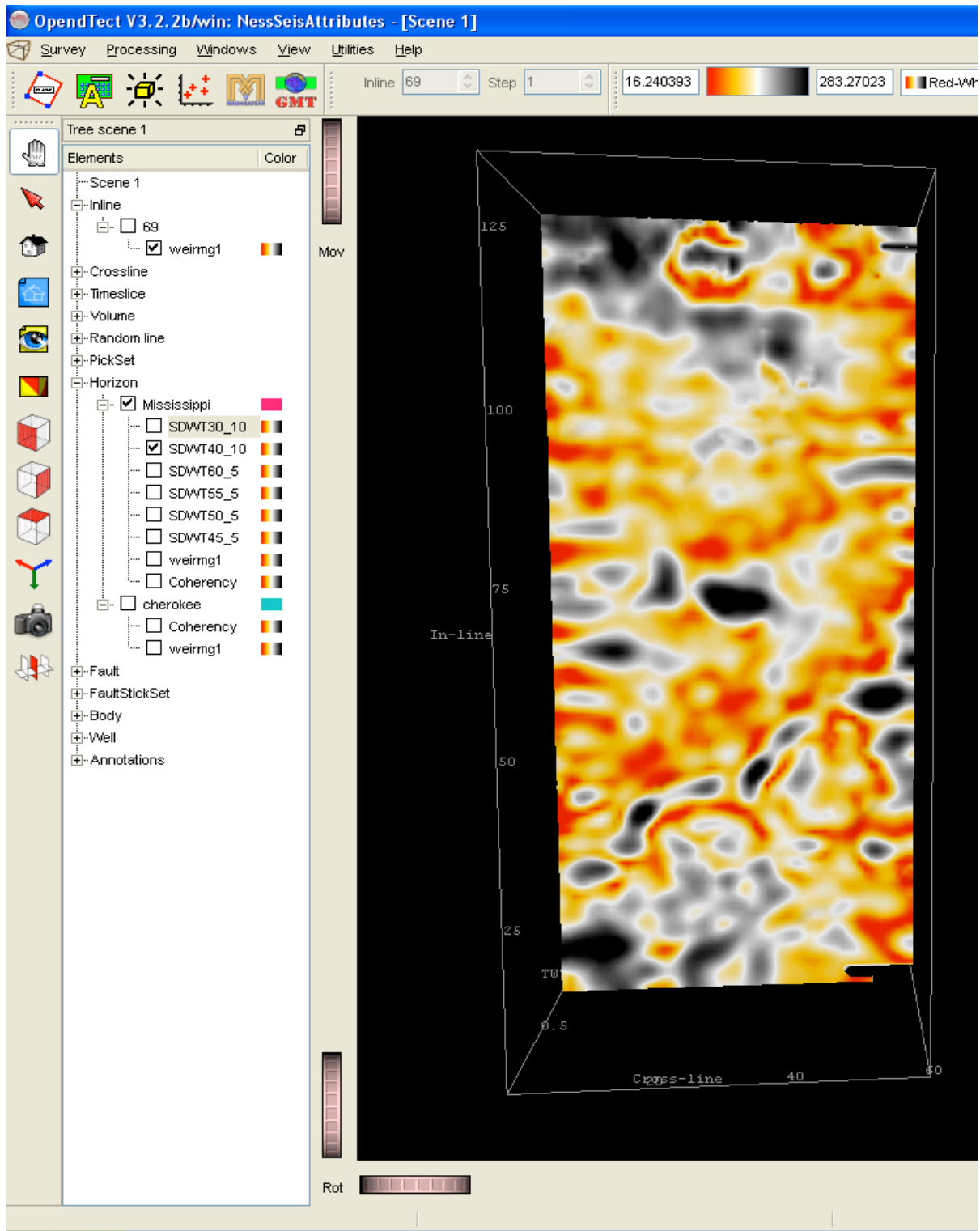


Figure 3-10 Spectral Decomposition 40 Hz Step 10 Hz: Mississippi Horizon

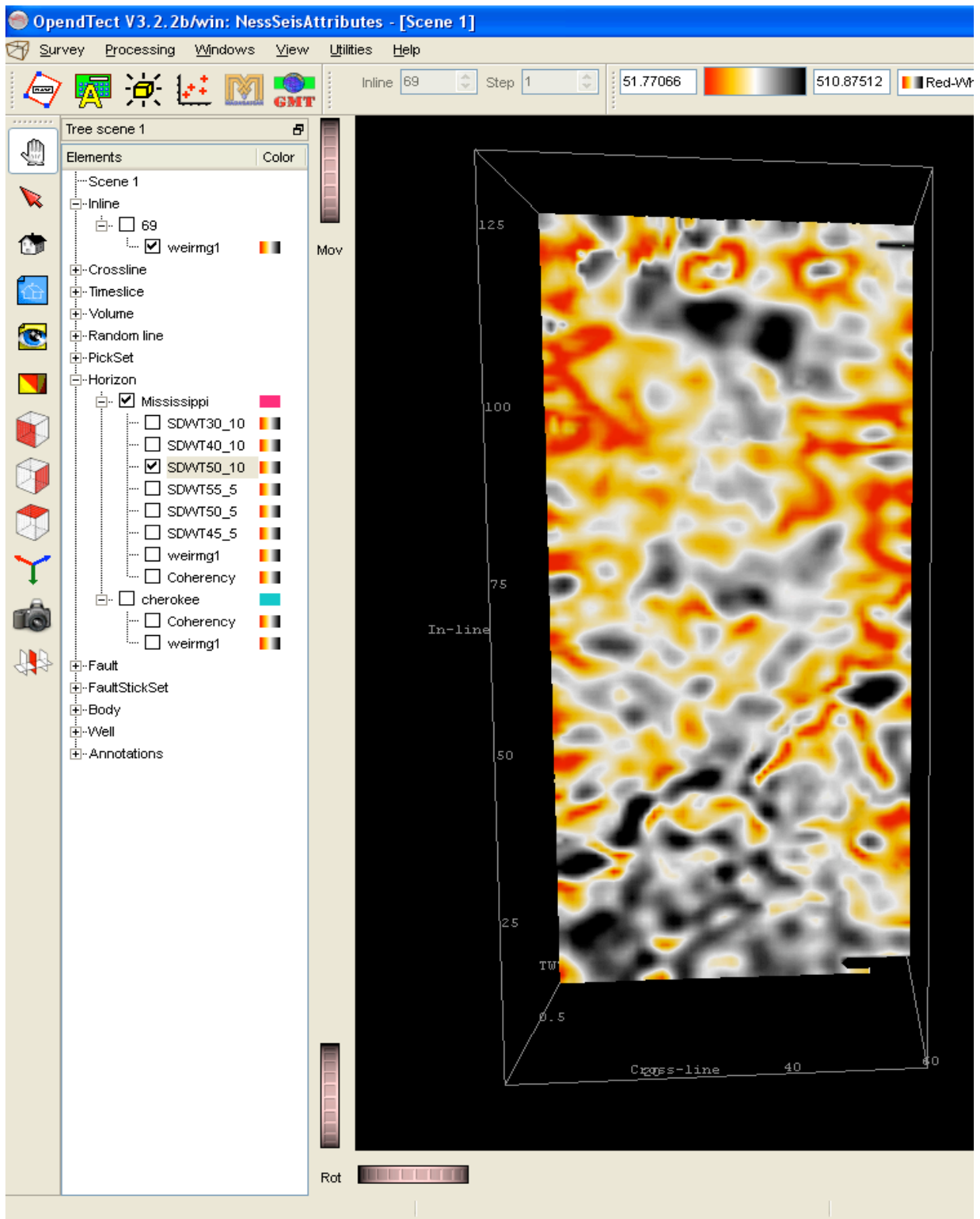


Figure 3-11 Spectral Decomposition 50 Hz Step 10 Hz: Mississippi Horizon

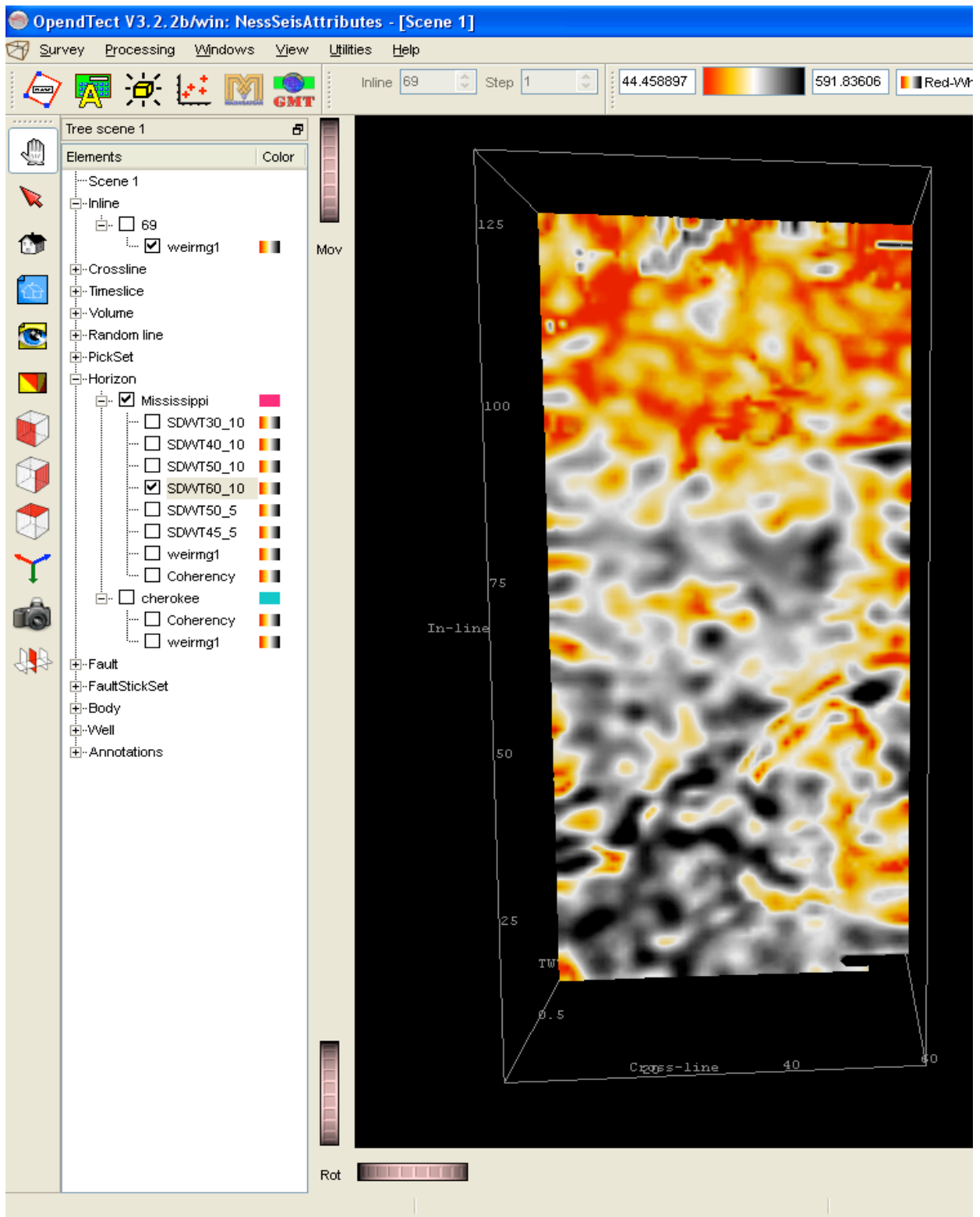


Figure 3-12 Spectral Decomposition 60 Hz Step 10 Hz: Mississippi Horizon

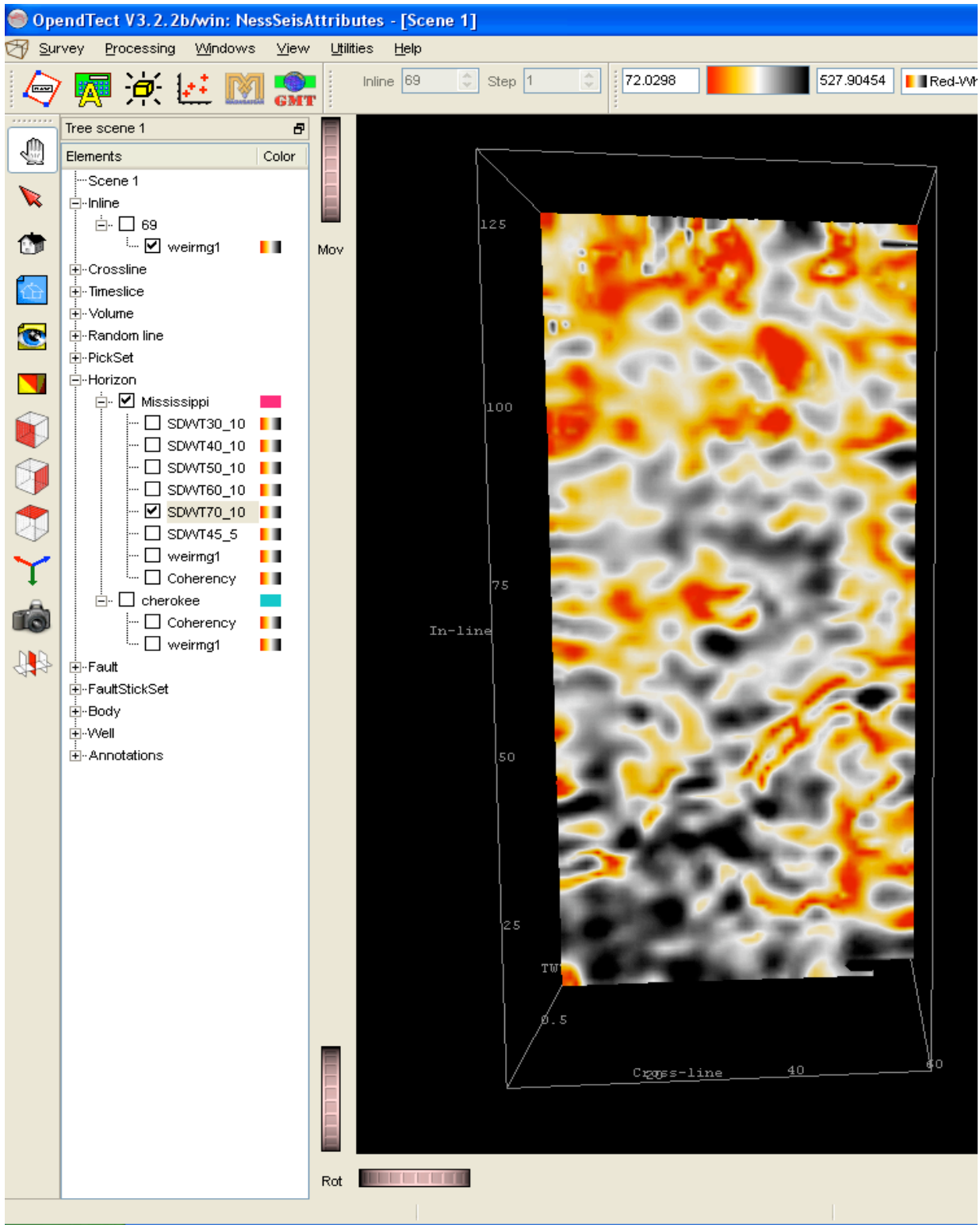


Figure 3-13 Spectral Decomposition 70 Hz Step 10 Hz: Mississippi Horizon

Qualitative Seismic Attributes

In this part of my study, I correlate the calculated set of seismic attributes maps with each other and compare with available well information to understand and map reservoir facies heterogeneities. This section ensures the understanding of each particular attribute and its contribution to reservoir characterization. The generation and analysis of seismic attributes has become a vital practice of seismic interpreters in order to gain knowledge about the subsurface structures and lithology of a particular area. Table 3 provides a guide to each seismic attribute completed in this study. All of these attributes may assist when characterizing the subsurface of the Weirman Field, located in Ness County, Kansas.

Amplitude Attenuation

Amplitude Attenuation can be defined as a gradual loss of amplitude intensity through the subsurface. In some areas of the subsurface, amplitude attenuates more or less depending on the medium it is travelling through. Amplitude attenuation $B(f,t)$ is expressed by:

$$B(f, t) = A(t)B(f) \exp\left(\sum_{i=1}^N \frac{\pi f \Delta t_i}{Q_i}\right)$$

where Q_i and Δt_i are quality factor and travel time in layer i . Signals will attenuate as a function of travel time and offset.

RMS Amplitude

Root-mean-square (RMS) Amplitude is a computed seismic attribute that is a measure of reflectivity within a time window. This attribute is used to map hydrocarbon indicators within a zone. It is defined as the square root of the sum of the squared amplitudes divided by the sample size of data within the time window desired. The RMS amplitude is calculated according to:

$$A_{rms} = \sqrt{\frac{\sum_{i=1}^N a_i^2}{N}}$$

where N is the number of samples in the calculation window.

Acoustic Impedance

Acoustic Impedance (AI) is the product of density and acoustic velocity. Well logs record measurements of both density and interval velocity therefore dividing the density log by the traveltime (sonic log) an acoustic impedance log may be generated (Chopra, 2007). This attribute emphasizes the velocity of rock formations rather than the distinctions between them, therefore accentuating rock properties (Sheriff, 1995). It was contributed during the middle of the 1970s, converting post-stack amplitudes into acoustic impedance, allow interpreters to study the physical property of rocks, including lateral changes in lithology and information about porosity of the subsurface (Chopra, 2007).

Coherency Map

A coherency map is used for 3D seismic interpretation of structural features or stratigraphy. Coherence is defined as a quantitative measure of the similarity or dissimilarity of nearby seismic traces (Bahorich and Farmer, 1994; 1995) and is typically calculated as a post-processing seismic attribute. Coherence is a measure of waveform similarity and integrates information from neighboring, adjacent traces in a nonlinear manor, which allows the extraction of information that may not have been seen on an individual time slice. Coherency maps allow the interpreter to see both structural and stratigraphic features and geometries of the desired window. Coherency can be given by:

$$\Phi(t,d) = \frac{\sum_{k=t-N/2}^{k=t+N/2} G_k H_{k+d}}{\sqrt{\sum_{k=t-N/2}^{k=t+N/2} G_k^2 \sum_{k=t-N/2}^{k=t+N/2} H_{k+d}^2}}$$

where Φ is the correlation coefficient at time t milliseconds and for a specified geologic dip d ms/trace, G and H are the correlated traces and N is the number of samples in the correlation time window. The continuity attribute is a very efficient means for illuminating geologic discontinuities that emerge as low-continuity zones.

Attribute	Definition	Implication	Figure
Amplitude Attenuation	Gradual loss of amplitude intensity due to frequencies above and below point of interest	Higher seismic P-wave attenuation would correlate with better reservoir properties	4-1 (Left)
RMS Amplitude	Measure of reflectivity within a time window. Calculated by square root of the sum of the squared amplitudes	Higher RMS amplitude in the extraction window indicates higher proportions of channel sands or better reservoir facies, especially when coupled with higher attenuation levels	4-1 (Middle)
Acoustic Impedance	Product of density and acoustic velocity	Higher average AI correlates with lower proportions of channel sands	4-1 (Right)
Coherency	Similarity or difference of nearby seismic traces	Show potential compartmentalization or structural features within study area	4-2

Table 3 3D Seismic Attribute descriptions

Chapter 4 - Discussion and Results

Discussion

The P-wave attenuation (Figure 4-1 (left)) shows the result of amplitude attenuation in the 3D seismic data. An outline area is characterized by higher level of attenuation. I have interpreted this area to be dominated by channel sands of thickness below seismic resolution and lies directly above the Mississippian limestone. In the interpreted channel outline (Figure 4-1 (left)), I have distinguished the attenuation patterns into four different sections labeled with roman numerals. The first section (I) shows a greater attenuation than the rest of the data. This section holds the highest reservoir potential, especially in areas with higher RMS amplitudes (greater acoustic impedance contrast with the underlying limestone) (Figure 4-1 (middle)) with and lower acoustic impedance (Figure 4-1 (right)). Section II is where the initially producing Keith No. 1 was drilled, and is shown in the Figure 4-1. As we travel from section I, to section IV, one will notice a decrease in attenuation response based on amplitude. I can conclude that this response is due to a change in facies of the formation or a decrease in the quality of the reservoir. This figure shows very strong compartmentalization and is not continuous. This could be a major factor as to why none of the other wells in the Weirman field were productive.

The RMS amplitude and acoustic impedance of the study area can be seen in Figure 4-1 (middle and right). The low areas are shown in greens and blues, while yellows and reds indicate the high areas. The initially productive Keith No. 1 well can be seen in areas of moderate attenuation, high amplitude, and moderate acoustic impedance. The location of Keith No. 1 is within the interpreted channel area. The well, Wanda Judeen 1 located in the proposed channel facies and producing section, was a dry hole. According to Figure 4-1, Wanda Judeen 1 was located in an area of high attenuation, high amplitude and high acoustic impedance. A reason that could explain the non-producing Wanda Judeen 1 is that it was located in an area of high impedance, which is a warning to any prospect in terms of reservoir properties.

The interpretation of 3D seismic surveys and integration with other geo-datasets has increased the success rate of many exploration and development programs around the world.

Among key elements contributing to this success is the high seismic 3D resolution of structural and stratigraphic characterization of reservoirs in a wide range of geological settings. There are occasions when seismic interpretation of subsurface geology does not conform to the actual geology encountered in the drilled well. This is such an occasion that occurred during the drilling of several test wells based upon a 3D seismic survey in Ness County, Kansas, where the predicted Cherokee sand did not meet the expectations set by the driller. The expectations were that the Cherokee sandstones were to be reservoir rocks to hydrocarbons. By better integrating the analysis of key seismic attributes in this study such as P-wave attenuation, Root-mean-squared (RMS) amplitude, and acoustic impedance, in addition to seismic coherency (Figure 4-2) interpretation, seismic facies heterogeneities and compound lithofacies/faulting compartmentalization were evidenced.

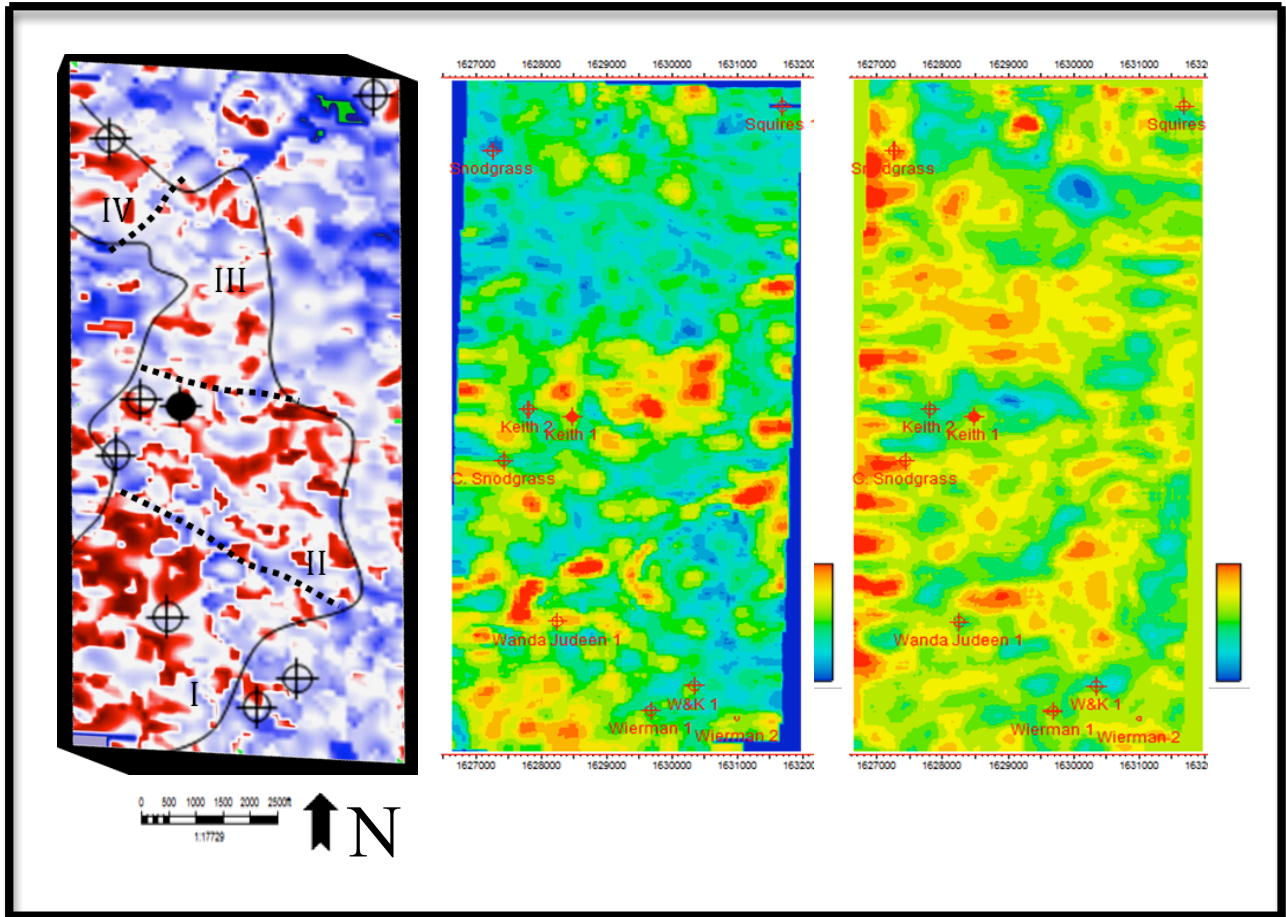


Figure 4-1 Amplitude Attenuation with four groups areas of different spatial distribution and attenuation level, RMS Amplitude, Acoustic Impedance time slices for average over 15 ms.

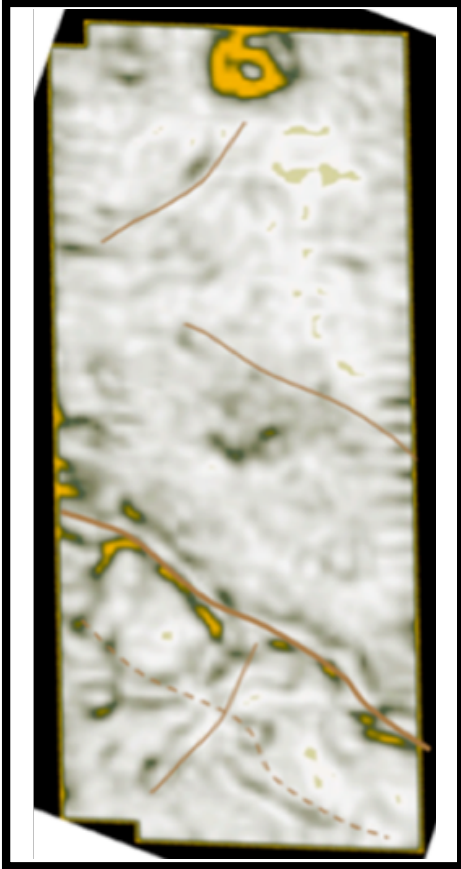


Figure 4-2 Coherency Map showing interpreted geologic discontinuities enhanced with golden color lines.

Results

As discussed in previous chapters, it is important to combine different seismic attributes to form a better understanding of subsurface facies, rather than looking at just one or two attributes. It was also imperative in this study to look at well cuttings and logs that were available for several of the wells in the area of study. Figure 4-3 shows the beginning of a series of attribute overlays, which can help visualize or form a better understanding of the study area

and may be helpful in indicating a zone of interest. This figure shows RMS amplitude overlaying amplitude attenuation, and with these particular attributes, higher values (reds and yellows) indicate possible zones that have greater potential fluid movement as well as hydrocarbon indicators or other geologic features when overlapping.

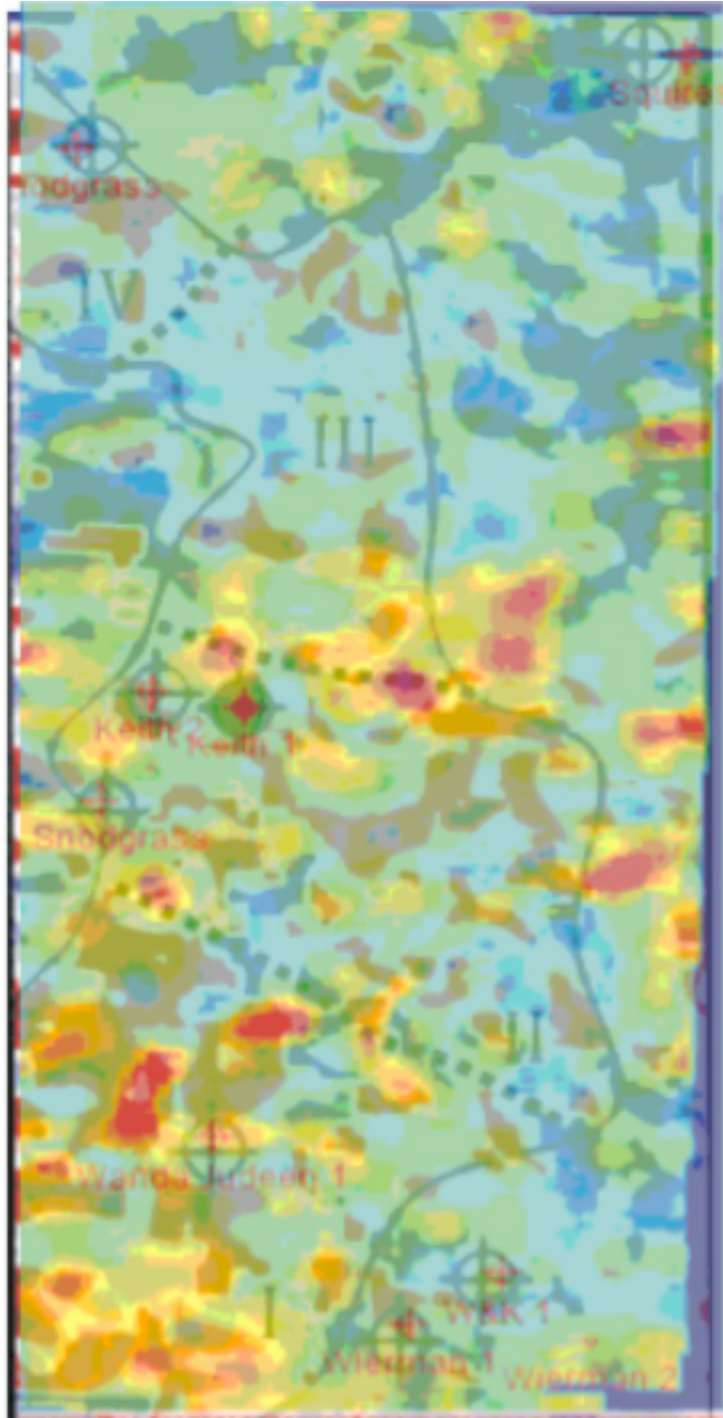


Figure 4-3 RMS amplitude transparency overlaid on amplitude attenuation

Figure 4-4 shows a coherency map on top of the same attenuation map. This figure may be able to correlate areas of greater fracture potential and fluid flow from the attenuation map with structural or lithologic features shown by the coherency map. Linear coherency anomalies indicate interpreted litho- or structural discontinuities; further analysis based on core samples and production well data is recommended. These anomalies may be interpreted as varying topography of the top of the Mississippian formation resulting from a discontinuous depositional surface. The compartmentalization caused by these discontinuities may be used to explain the lack of reservoir continuity.

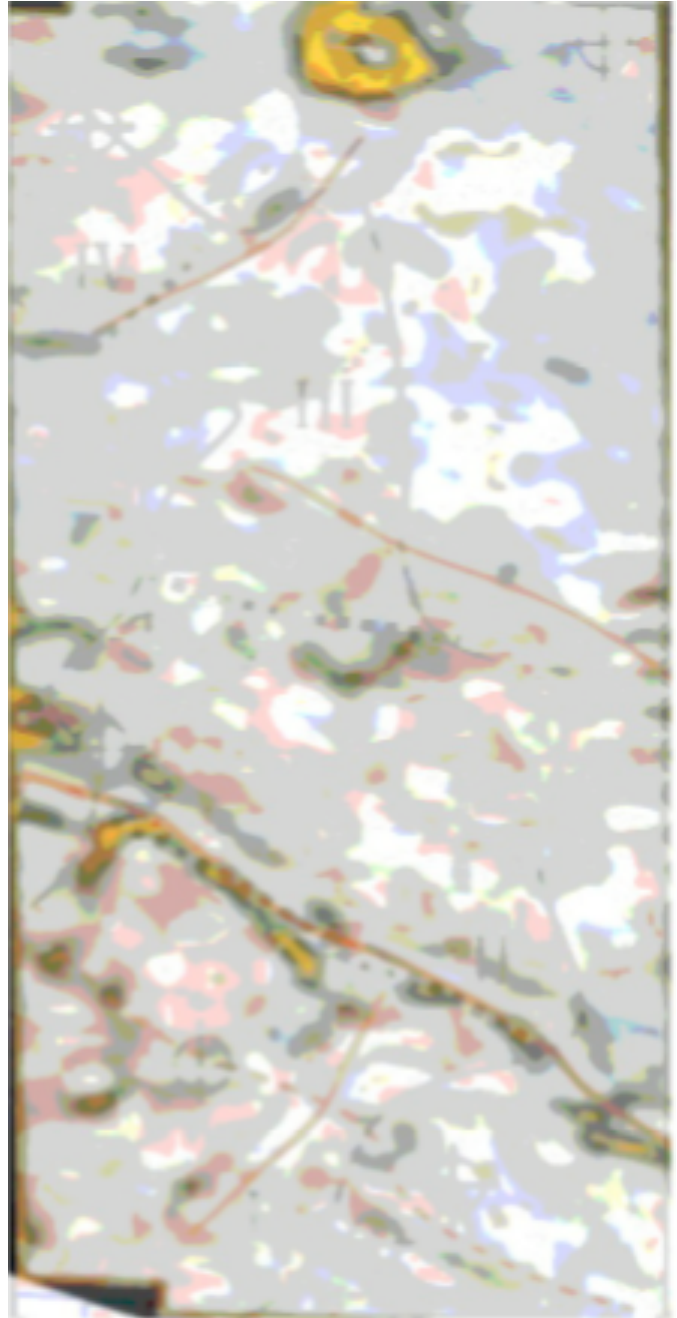


Figure 4-4 Coherency transparency overlaid on amplitude attenuation

Figure 4-5 shows the acoustic impedance attribute in grayscale overlaying the amplitude attenuation map. In this figure, one may observe the low values of acoustic impedance, (light gray and whites) which correlate to a better reservoir quality and potentially better porosity and/or fluid content. The amplitude attenuation map again has high values in red that indicate better porosity and permeability for a potential reservoir. All eight wells, which have been drilled in Weirman field, have been drilled in areas of high impedance (dark grays) that indicate a poor reservoir potential. This may contribute in part to the disappointing drilling results in the field.

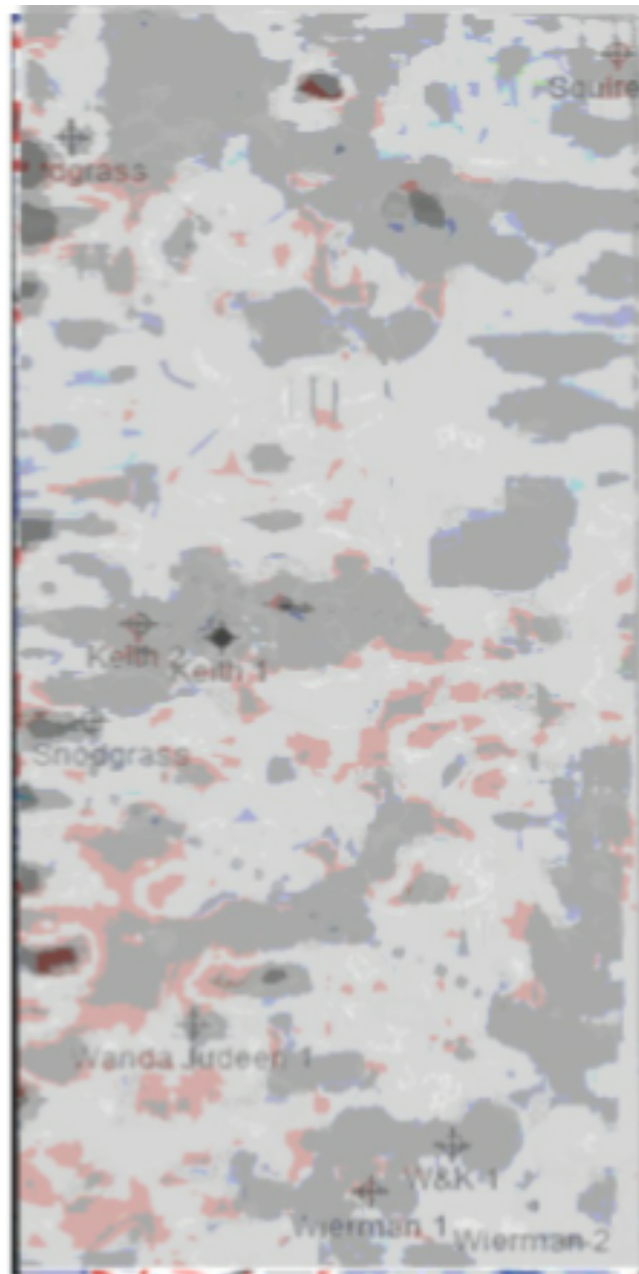


Figure 4-5 Acoustic impedance transparency in grayscale overlaid on amplitude attenuation

Figure 4-6 shows the RMS amplitude attribute in grayscale on top of the acoustic impedance map. Looking at the two maps, better reservoir potential is indicated by lower acoustic impedance values (blues and greens) and higher RMS amplitude values (dark grays and blacks).



Figure 4-6 RMS amplitude transparency in grayscale overlaid on acoustic impedance

Along with the seismic attribute analysis, well logs and cuttings were analyzed for a few of the wells located in the seismic survey area. Gamma ray logs showed characteristics of channel sandstones (Figure A-6). The sandstones from the Cherokee Group display an increase in radioactivity, which indicates that the lower portion of the sand is coarser, in reference to grain size, and gradually fines towards the surface. This observation may correspond to the different depositional environments sandstones may be involved in. According to Stoneburner (1982), shales and siltstones will correspond to floodplain facies, fine-grained sandstones will correspond to point-bar facies, and coarser grained sandstones, similar to those observed in this study, may indicate channel facies zones. Figure 4-7 shows a display of well cutting images at the Pennsylvanian aged Cherokee Group and to which well they correlate.

Areas of high attenuation and low impedance have a lower shale content within the well cuttings (well Keith #2) than areas of low attenuation and higher impedance (wells Keith #1 and W&K #1). Well W&K #1 had the most shale content of the three wells at the area of interest and well Keith #2 had the least amount of shale content of the three wells. Well Keith #1 had minor amounts of sand and a lesser amount of shale than well W&K #1. These well cuttings can possibly be an unreliable source for accurate information about reservoir stratigraphy due to the lack of isolated cuttings at certain depths. When well cuttings are collected per ten feet (which is standard) it is possible that fragments of rock from above formations may fall or be collected with the sample recorded at a different depth. The wells in Weirman field have limited resources in lieu of well cuttings and core samples, but a correlation was made from the well cuttings to the geologists report from the wells (Figure A-5). At well Keith #2, sandstone clusters were collected at the depth of the Cherokee sandstone, and these clustered sandstones mostly likely have a quartz cement, which could explain the lack of oil production of the well due to a decrease in permeability of the formation. Well Keith #1 cuttings at Cherokee depth contained loose sand, which could potentially explain why it produced oil, but stopped after only 162 barrels, due to the lack of continuity of the channel itself when compared to nearby Keith #2.

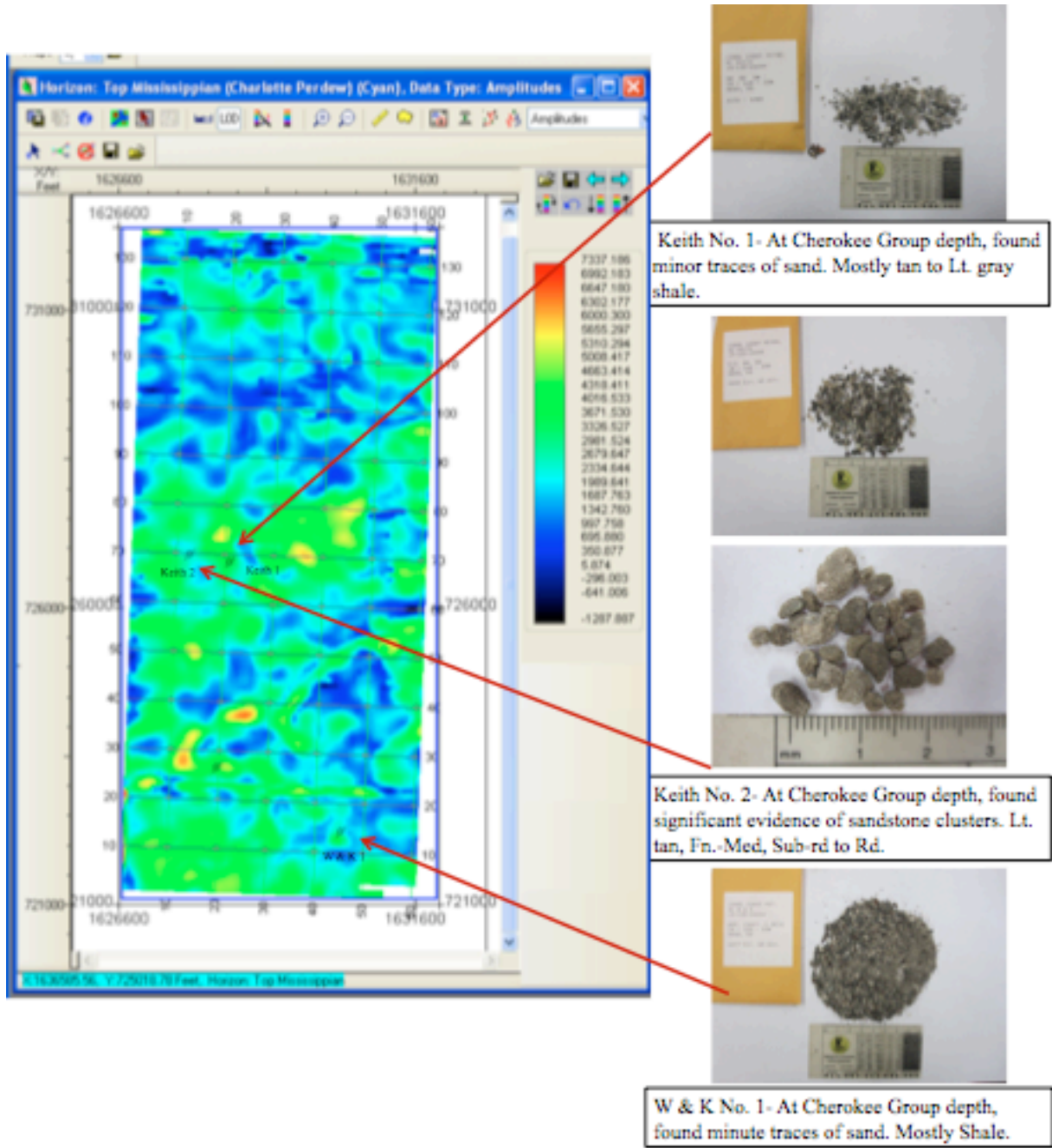


Figure 4-7 Well cuttings correlate to Mississippian horizon amplitude map

Chapter 5 - Conclusions

Conclusions

The identification of seismic lithofacies is based on seismic attributes and differential attenuation analyses, which add useful insight into the integration of seismic lithofacies in future development plans for Weirman Field; Ness County, Kansas. Seismic P-wave attenuation in addition to RMS amplitude and acoustic impedance attributes are key attributes in the process of understanding the subsurface lithofacies heterogeneities, prospect generation and evaluation in the subject area. The purpose of generating seismic attributes and completing spectral decomposition analysis was to potentially come up with observations based on qualitative results in order to identify a zone with potential hydrocarbon recovery. The channel facies is highly variable as referenced previously in the text as well as observed by the well cutting analysis. The lithofacies of a channel is very diverse and it is difficult to generalize the subsurface from a well log or well cuttings themselves. For future drilling plans of the Weirman field, the combined attribute and well cutting analyses need to be considered when prospecting new locations to drill. It is concluded that Weirman field is home to meandering channel sands, which are compartmentalized by lithographic or structural features causing a decrease of permeability within the reservoir. The analyses completed in this study are vital to its reservoir characterization and future production of the field.

References Cited

- Anstey, N.A. Simple Seismics. Boston: International Human Resources Corporation, 1982.
- Bahorich, M. S., and S. L. Farmer, 1994. 3-D seismic discontinuity: The coherence cube for faults and stratigraphic features. U.S. and Foreign Patents Pending.
- Bahorich, M. S., and S. L. Farmer, 1995. 3-D seismic discontinuity for faults and stratigraphic features: The coherence cube. Society of Exploration Geophysicists International Exposition and 65th Annual Meeting, Society of Exploration Geophysicists, Tulsa, Oklahoma, p. 93-96.
- Brenner, R. L., 1989. Stratigraphy, petrology, and paleogeography of the upper portion of the Cherokee Group (Middle Pennsylvanian), eastern Kansas and Northeastern Oklahoma. Kansas geological Survey, Geology Series 3.
- Chopra, S. & Marfurt, K.J. 2008, "Seismic attributes for stratigraphic feature characterization", 78th Annual International Meeting, *SEG Technical Program Expanded Abstracts*, vol. 27, no. 1, pp. 1590-1594.
- Chopra, S. & Marfurt, K.J. 2007, "Seismic Attributes for Prospect Identification and Reservoir Characterization." Society for Exploration Geophysicists. Tulsa, OK, USA.
- Chopra, S. & Marfurt, K.J. 2007, "Volumetric curvature attributes add value to 3D seismic data interpretation", *The Leading Edge*, **26**, no. 7, 856-867.
- Chopra, S. & Marfurt, K.J. 2006, "Seismic Attributes- a promising aid for geologic prediction," CSEG Recorder: special edition, 111-121.
- Cuzella, J. J., 1991, Depositional environments and facies analysis of the Cherokee Group in west-central Kansas. AAPG bulletin, **75**, no. 3, p. 560.
- Ewing Thomas E. "Synthetic Helps Spot the Target." AAPG Explorer. July: 1997. Exploration Inc., San Antonio, TX.
- Henley, C. David. More processing in the radial trace domain. 2004 CSEG National Convention. Expanded Abstract.
- Kearey, Philip. et al. An Introduction to Geophysical Exploration. Massachusetts: Blackwill Publishing Company, 2002
- Leblanc, R.J., 1971, Underground Waste Management and Environmental Implications, Proc of Symposium held at Houston, TEX, Dec. 6-9, 1971.

- Lozano, F.A. & Marfurt, K.J. 2008, "3D seismic visualization of shelf-margin to slope channels using curvature attributes", 78th Annual International Meeting, *SEG Technical Program Expanded Abstracts*, vol. 27, no. 1, pp. 914-918.
- Mazin, Y. Abbas, 2009. Incorporating Seismic Attribute Variation into the Pre-well Placement Workflow: A case study from Ness County, Kansas, USA. Master's Thesis. Kansas State University.
- Merriam, D. F., 1963, The geologic history of Kansas. Kansas Geological Survey Bulletin **162**.
- Miao, Xiao-Gui, & Moon, W. 1999, Application of Wavelet transform in reflection seismic data analysis, *Geosciences Journal*. Vol. 3, No. 3, p. 171-179.
- Ojo, C. and I. Sindiku, 2003, Interpretation and analysis of a channel using 3D seismic and well log data – a case study, 73rd Annual International Meeting, Society of Exploration Geophysicists Expanded Abstracts, 462-465.
- Russell, B.H., Hampson, D.P. & Lines, L.R. 2003, "Application of the radial basis function neural network to the prediction of log properties from seismic attributes --- A channel sand case study", 73rd Annual International Meeting, *SEG Technical Program Expanded Abstracts*, vol. 22, no. 1, pp. 454-457.
- Sheriff, R. E., and Geldart, L. P., 1995, *Exploration Seismology*, Second Edition, Cambridge University Press, pp. 3-6.
- Sinha, S. et al., 2005. Spectral Decomposition of Seismic Data with Continuous Wavelet Transform. *Geophysics*, November-December 2005; 70: p19-p25.
- Stoneburner, R. K., 1982, Subsurface study of the Cherokee Group on the western flank of the Central Kansas Uplift in portions of Trego, Ellis, Rush and Ness counties, Kansas.
- Suarez, Y., Marfurt, K. J., and Falk, M., 2008, Seismic attribute-assisted interpretation of channel geometries and infill lithology: A case study of Anadarko Basin Red Fork channels: 78th Annual International Meeting, SEG, 963-967.
- Van Dyke, R, 1976, Depositional environments of Cherokee reservoir sands, Kincaid Oil Field, Southeast Kansas. *AAPG Bulletin* v. 60, iss. 2, 322-323.
- Verma, A.K., Metilda Pereira, and B.R. Bharali, 2009, Use of Spectral Decomposition in Seismic Interpretation for finding out Fluvial Channel Sand Body: A Case study from Upper Assam Shelf Basin, India: 79th Annual International Meeting, SEG, 598-602.
- Walters et al., 1979, Channel Sandstone Oil Reservoirs of Pennsylvanian Age, Northwestern Ness County, Kansas: *AAPG Meeting Abstract*, 63, 2120.

Yilmaz Oz. Seismic Data Analysis. Oklahoma: Society of Exploration Geophysicists, 2001.

Zang, C. and Ulrych, T.J., 2002. Estimation of quality factors from CMP records. *Geophysics*, vol. 67, no. 5, 1542-1547.

Appendix A - Appendix

The first group of spectral decomposition figures are included to show testing was done to determine optimum testing parameters. The parameters chosen in the text are the continuous wavelet transform at 20-70 Hz with a step of 10. The parameters tested include continuous wavelet transform at 20-70 Hz step 5 and 20-70 Hz step 20. These parameters were tested for the top of the Mississippian horizon as well as time slice 902 milliseconds. Time gate tests were also introduced to test attribute evaluation at varying frequencies.

Geologist report of well Keith #2 and porosity log of well Keith #1 are also included to provide supplemental information for the reader regarding observations made within the text of this study. These figures were used in some of the analysis and discussion and are therefore included as supporting documentation.

Figure A-1 Spectral Decomposition 20Hz Step 20Hz: Mississippi Horizon

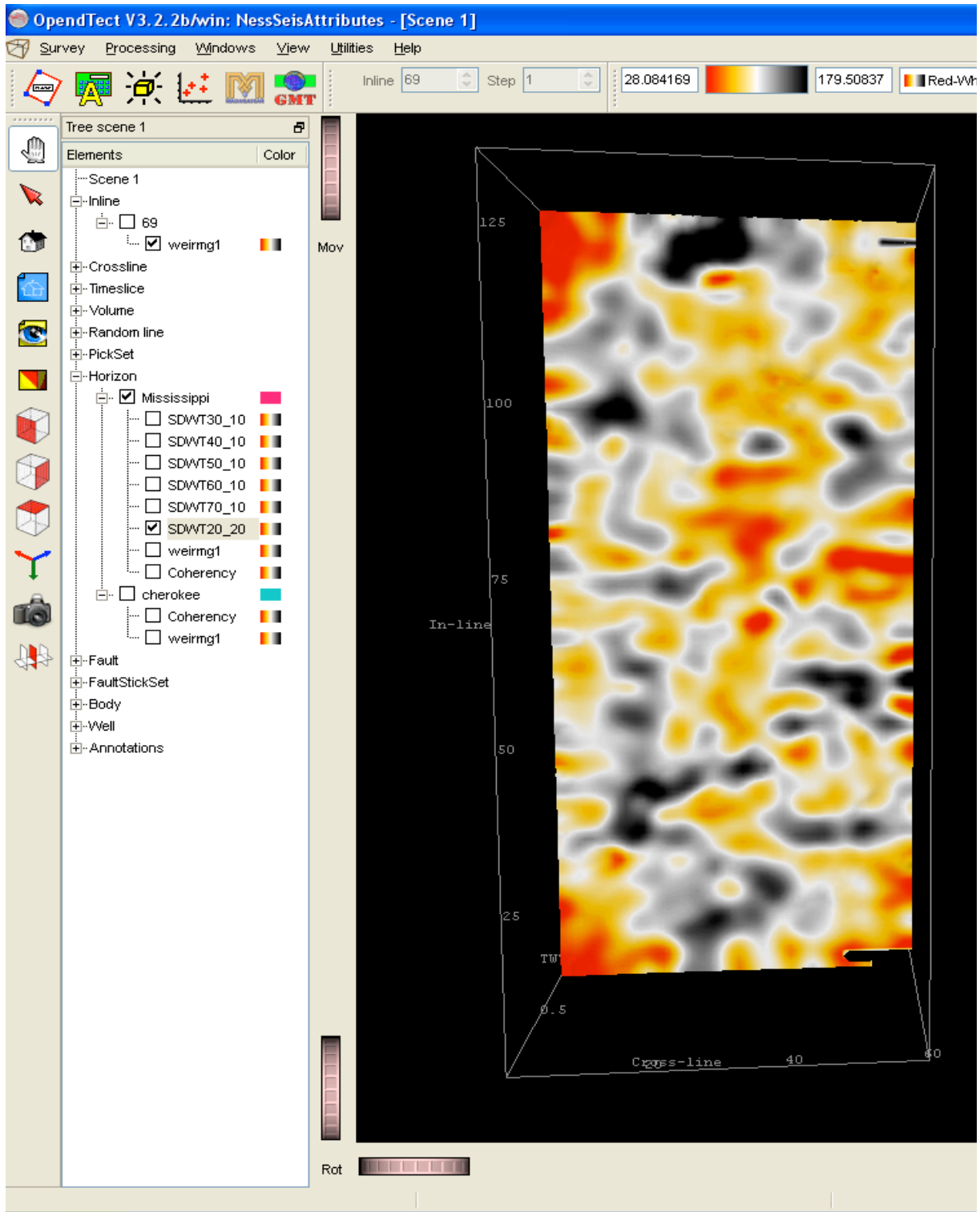


Figure A-2 Spectral Decomposition 40 Hz Step 20 Hz: Mississippi Horizon

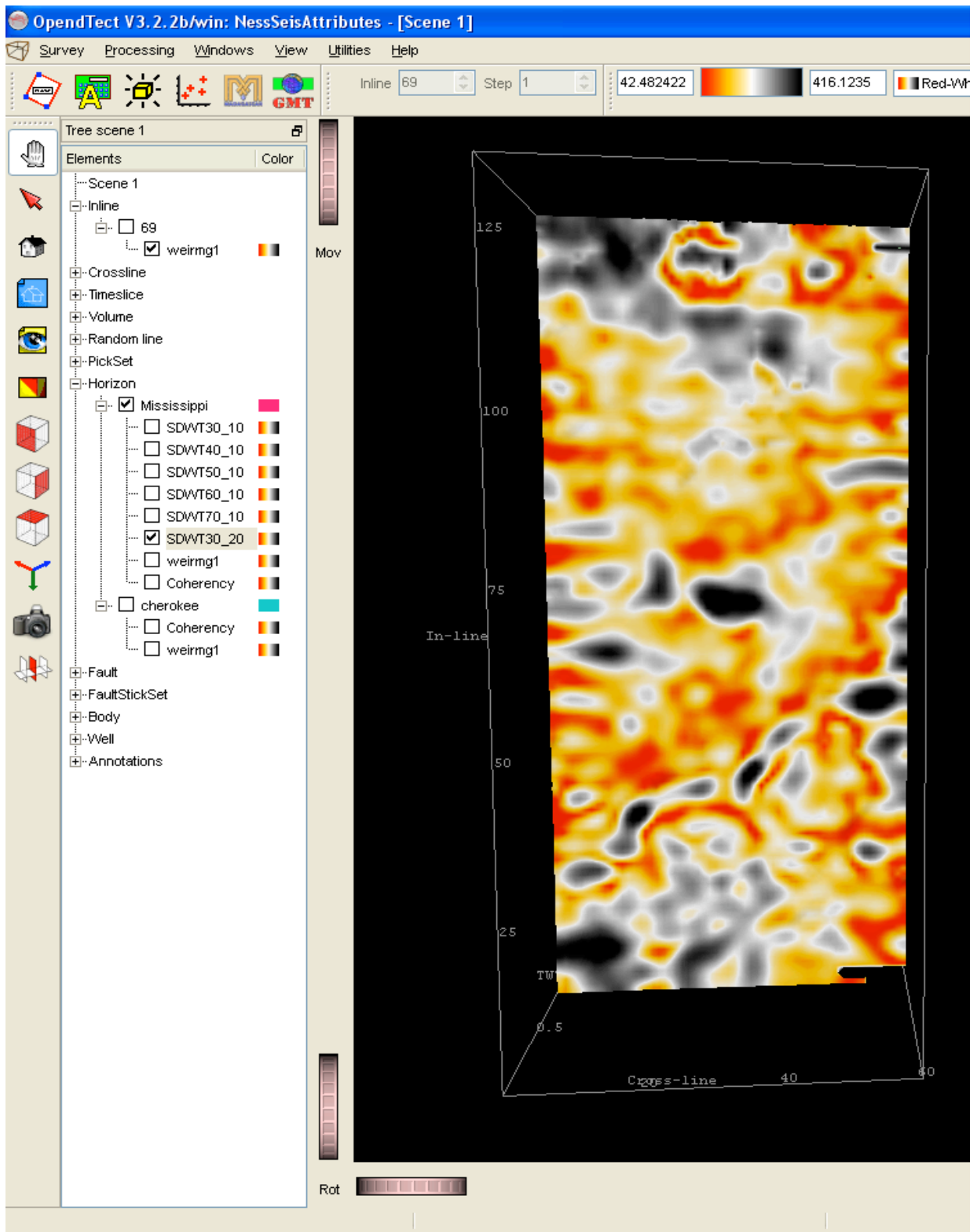


Figure A-3 Spectral Decomposition 60 Hz Step 20 Hz: Mississippi Horizon

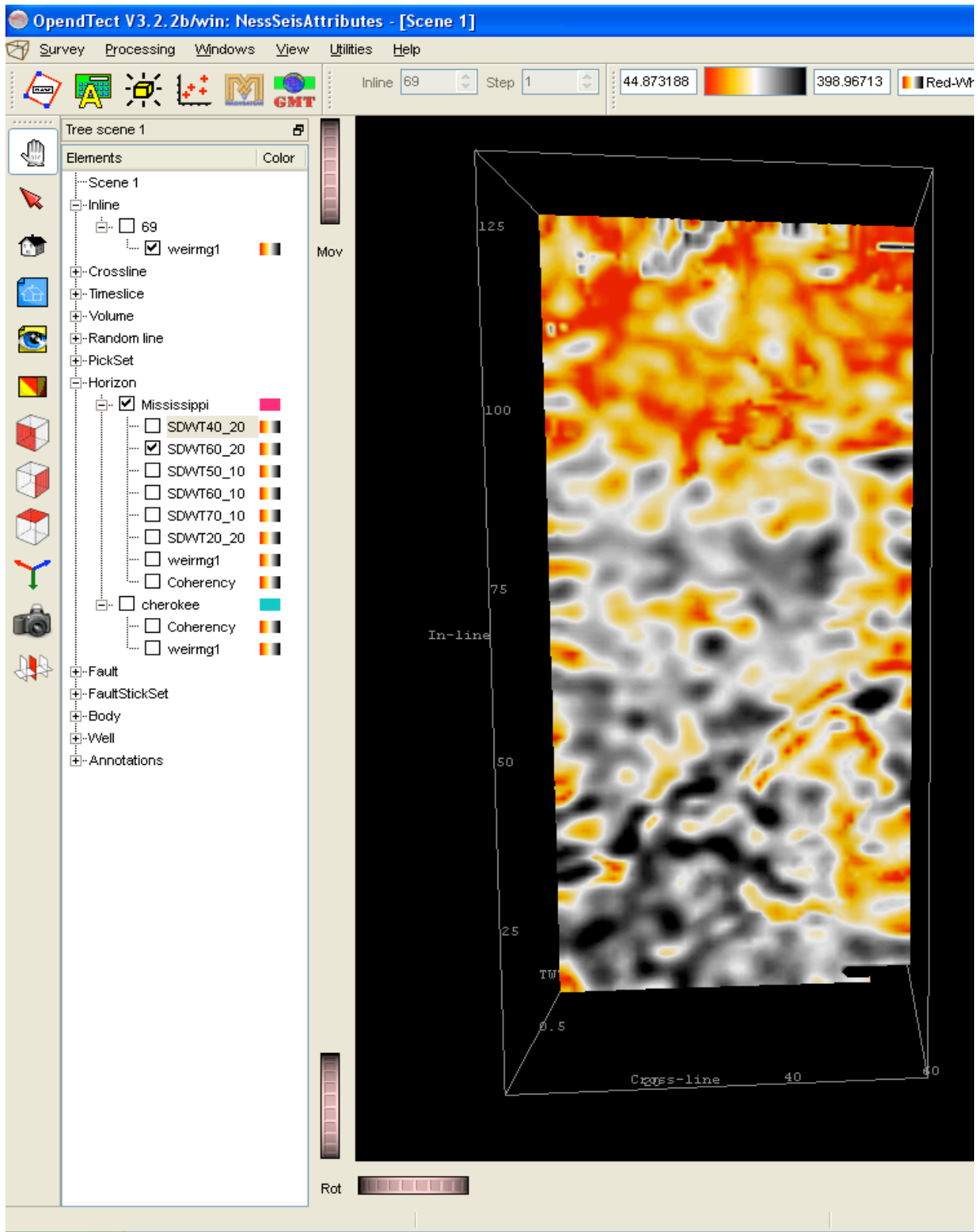


Figure A-5 Keith #2 Geologist's Report and Drilling time Log (Adjusted from Kansas Geological Survey, 2011).

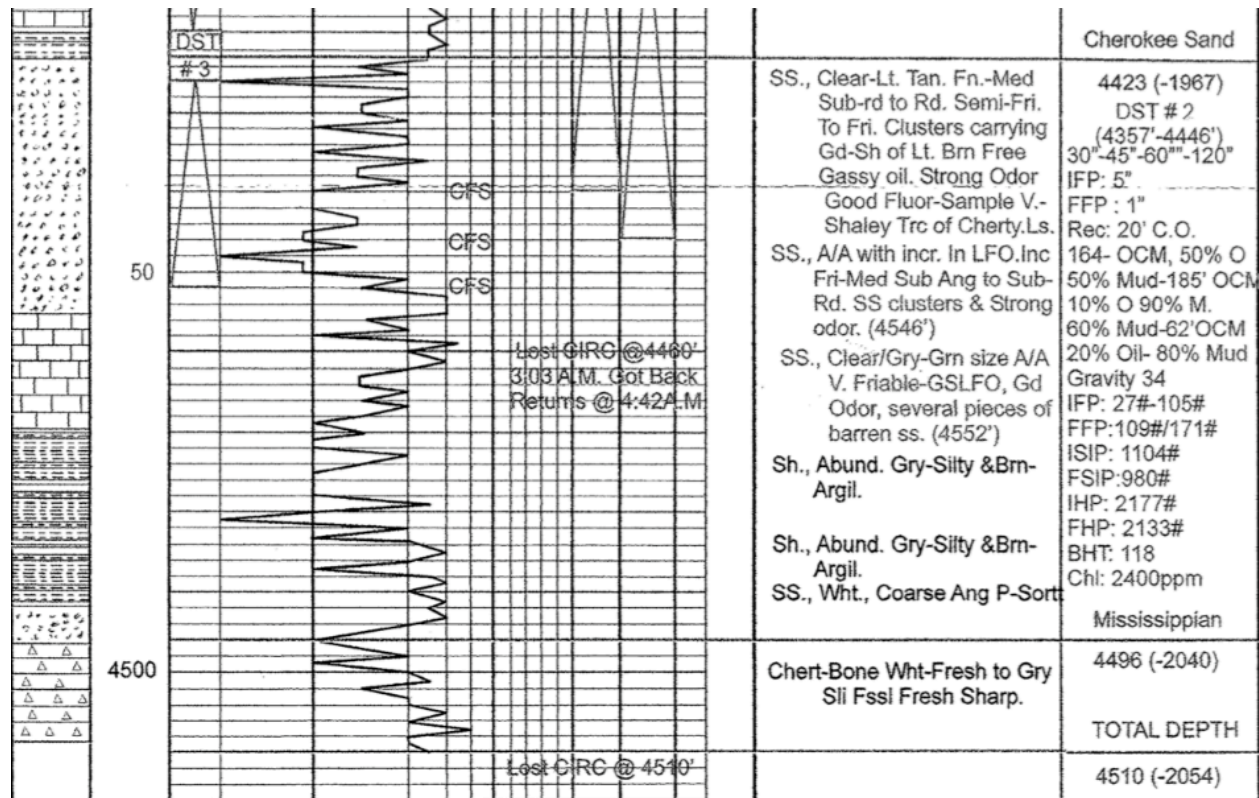


Figure A-6 Keith #1
Porosity Log (Adjusted
from Kansas Geological
Survey, 2011).

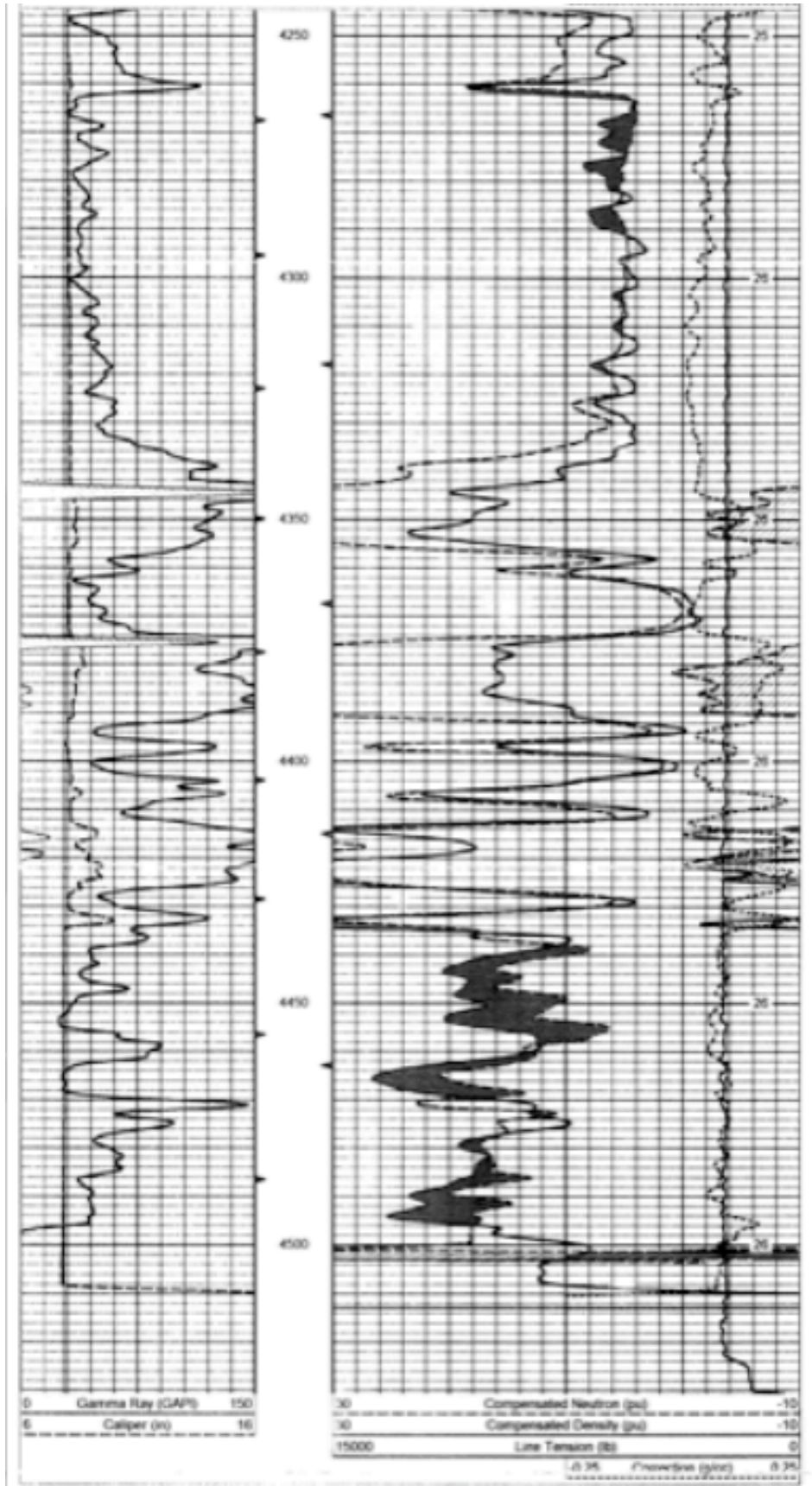


Figure A-7 Time slice with Mississippi Horizon at approximate inline # 902

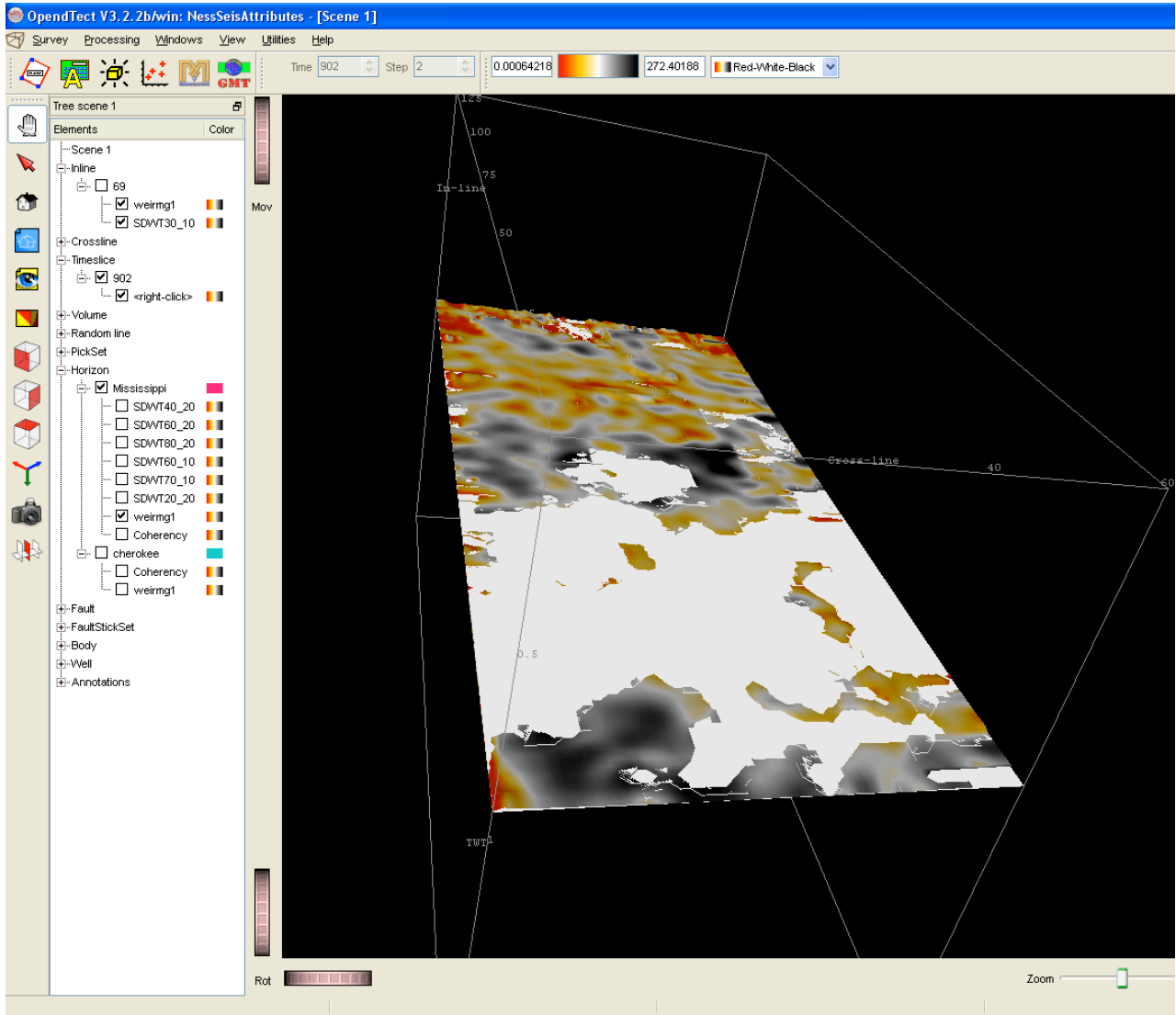


Figure A-8 Time slice overhead view of inline # 902

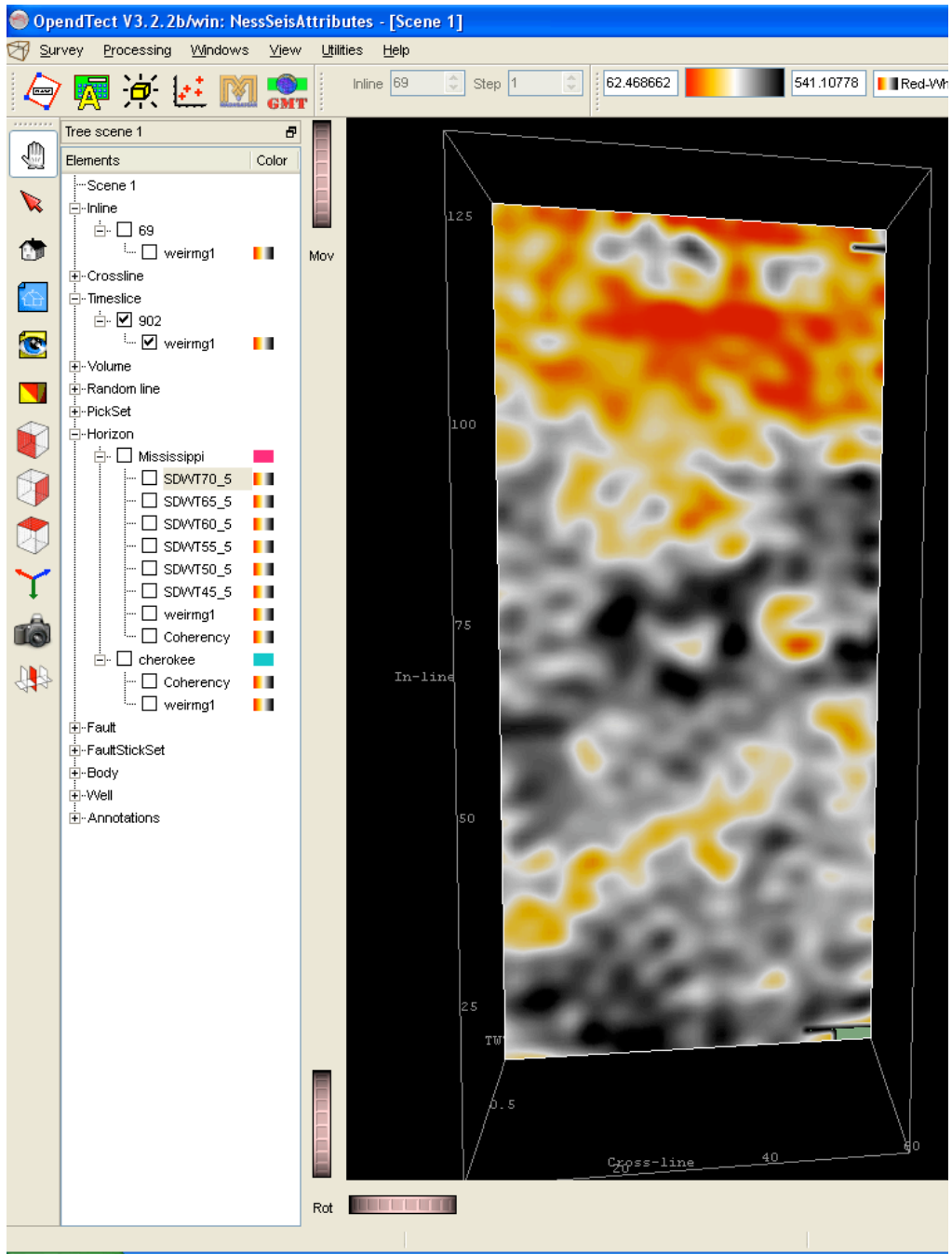


Figure A-9 Spectral Decomposition at Timeslice 30 Hz Step 10 Hz

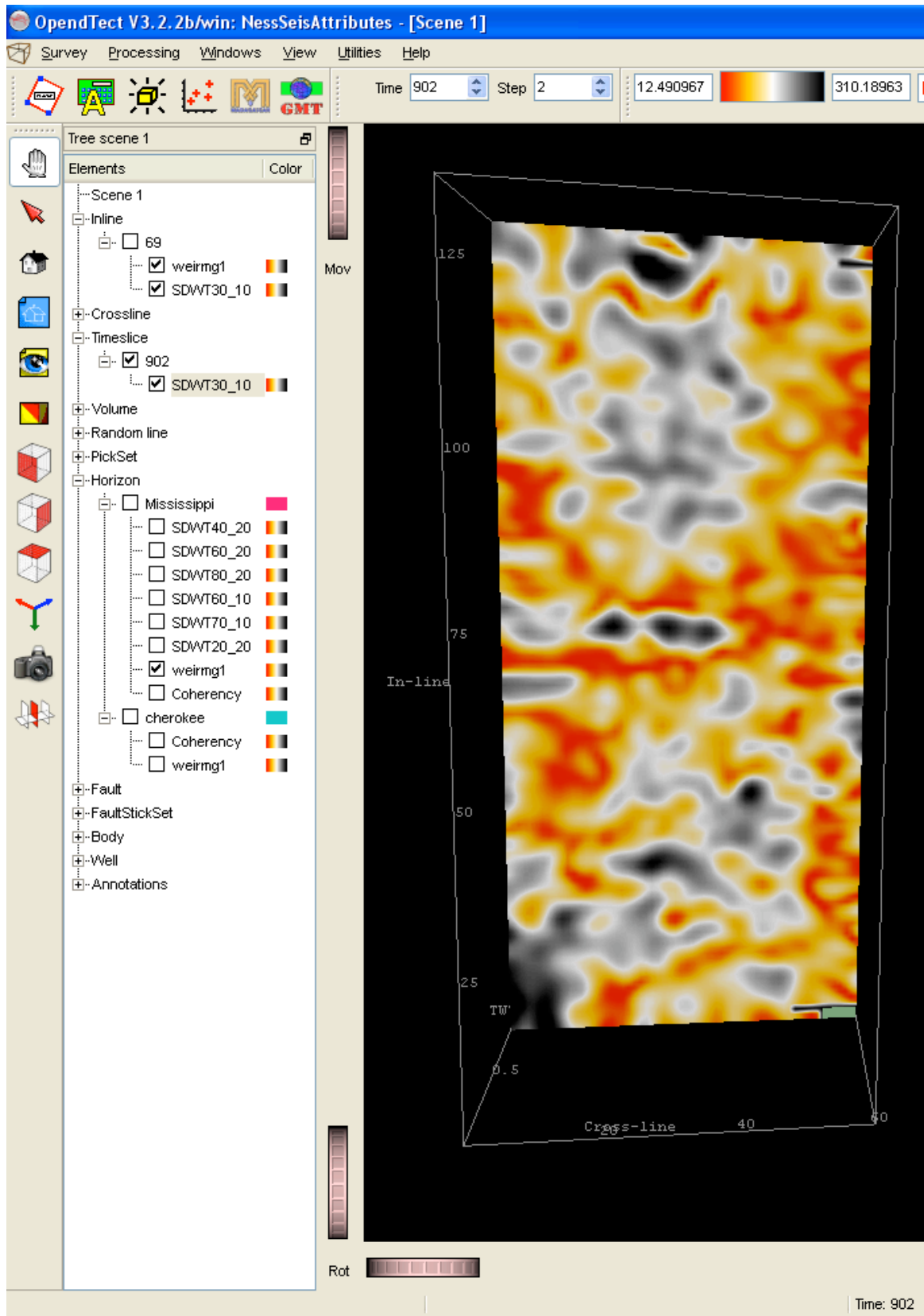


Figure A-11 Spectral Decomposition at Timeslice 50 Hz Step 10 Hz

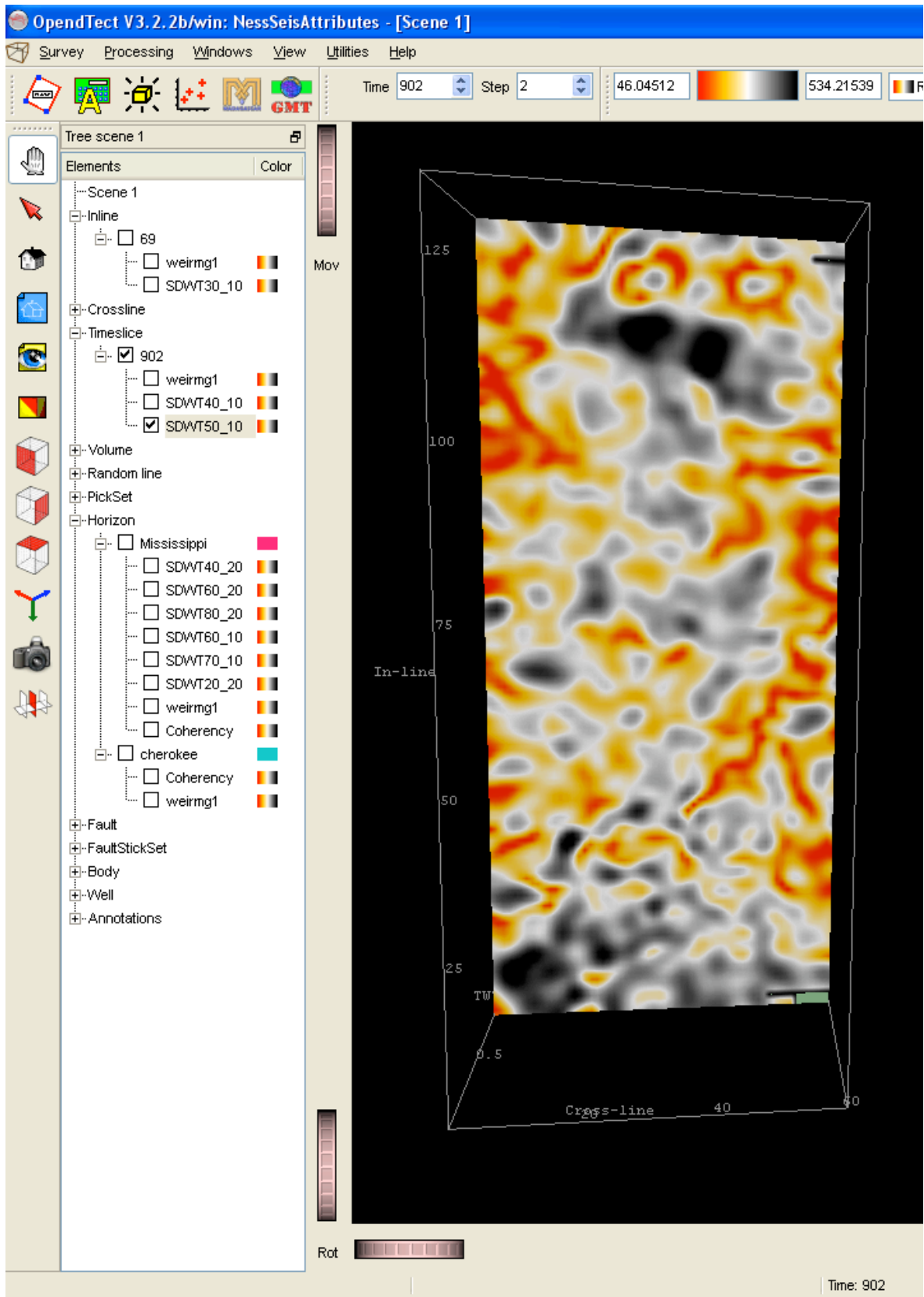


Figure A-12 Spectral Decomposition at Timeslice 60 Hz Step 10 Hz

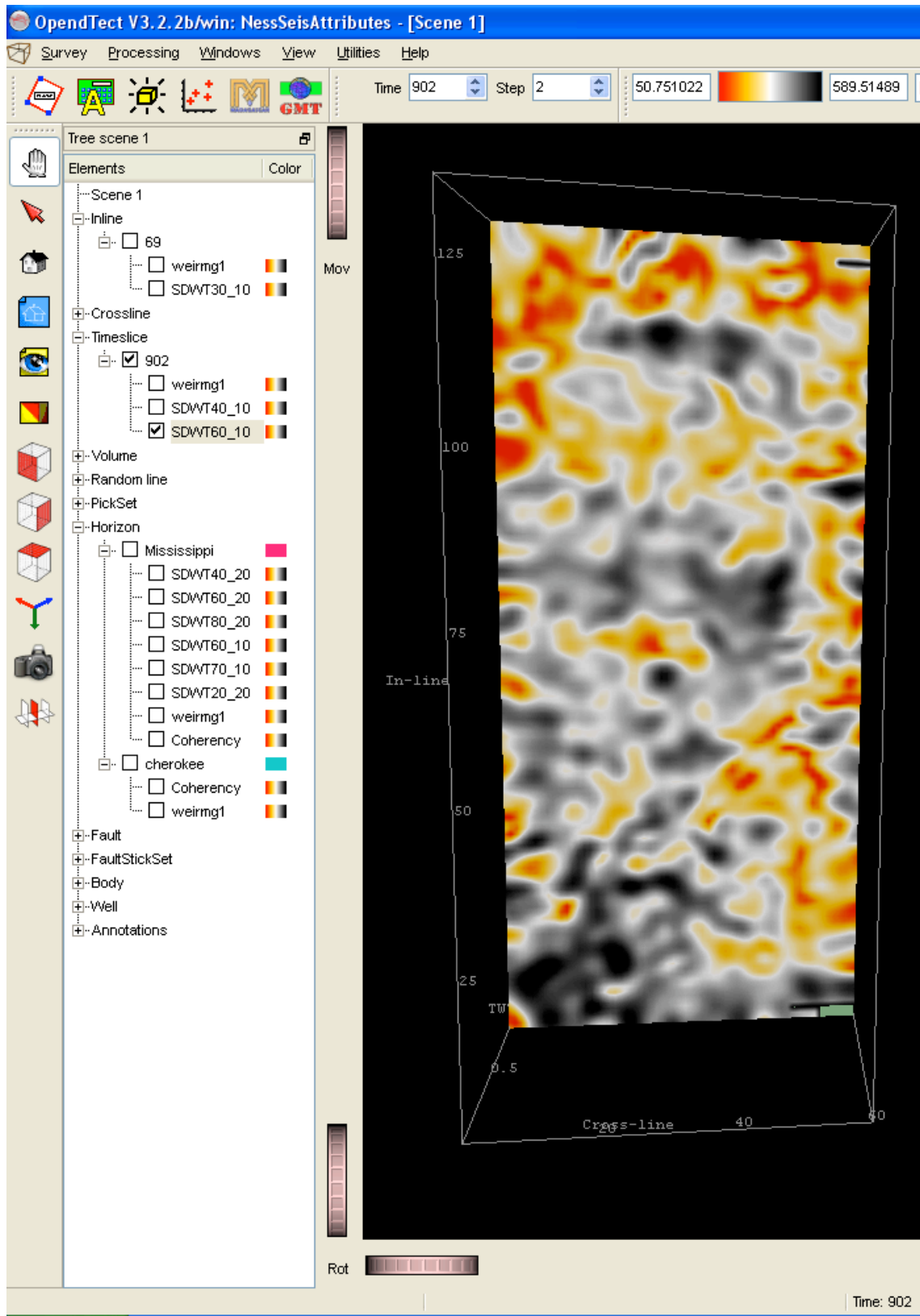


Figure A-13 Spectral Decomposition at Timeslice 70 Hz Step 10 Hz

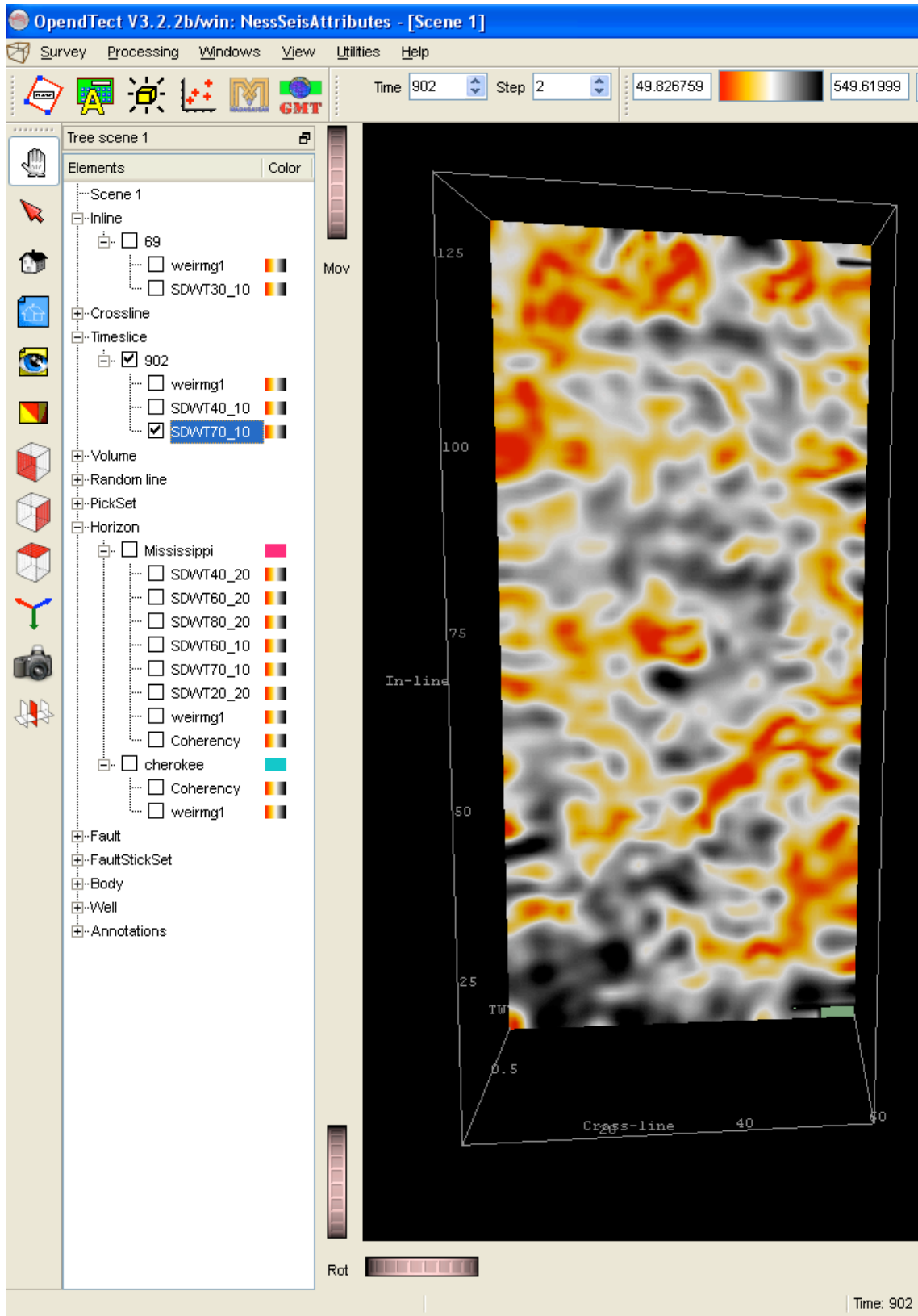


Figure A-14 OpenDtect Attribute generation homescreen

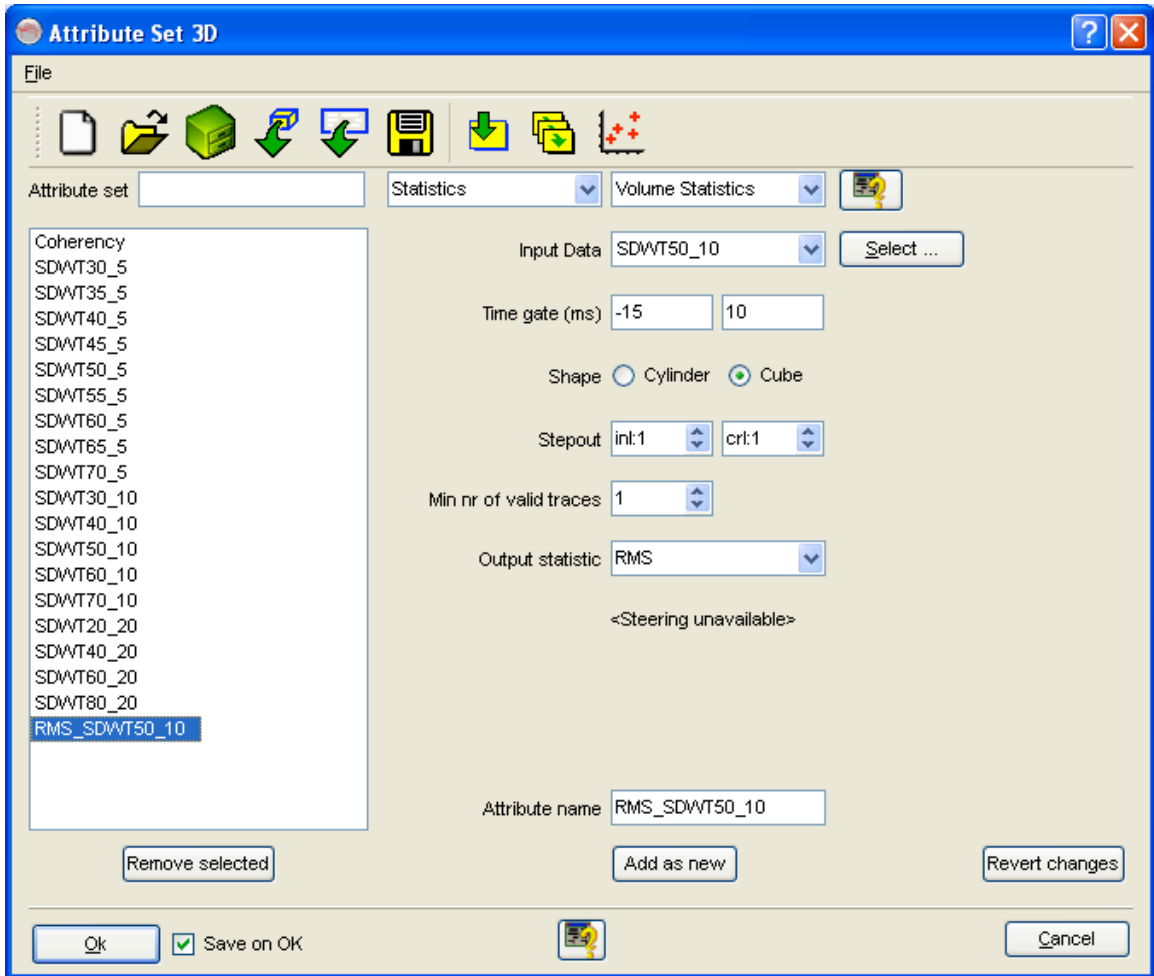


Figure A-15 RMS amplitude at Spectral Decomposition 50 Hz Step 10 Hz

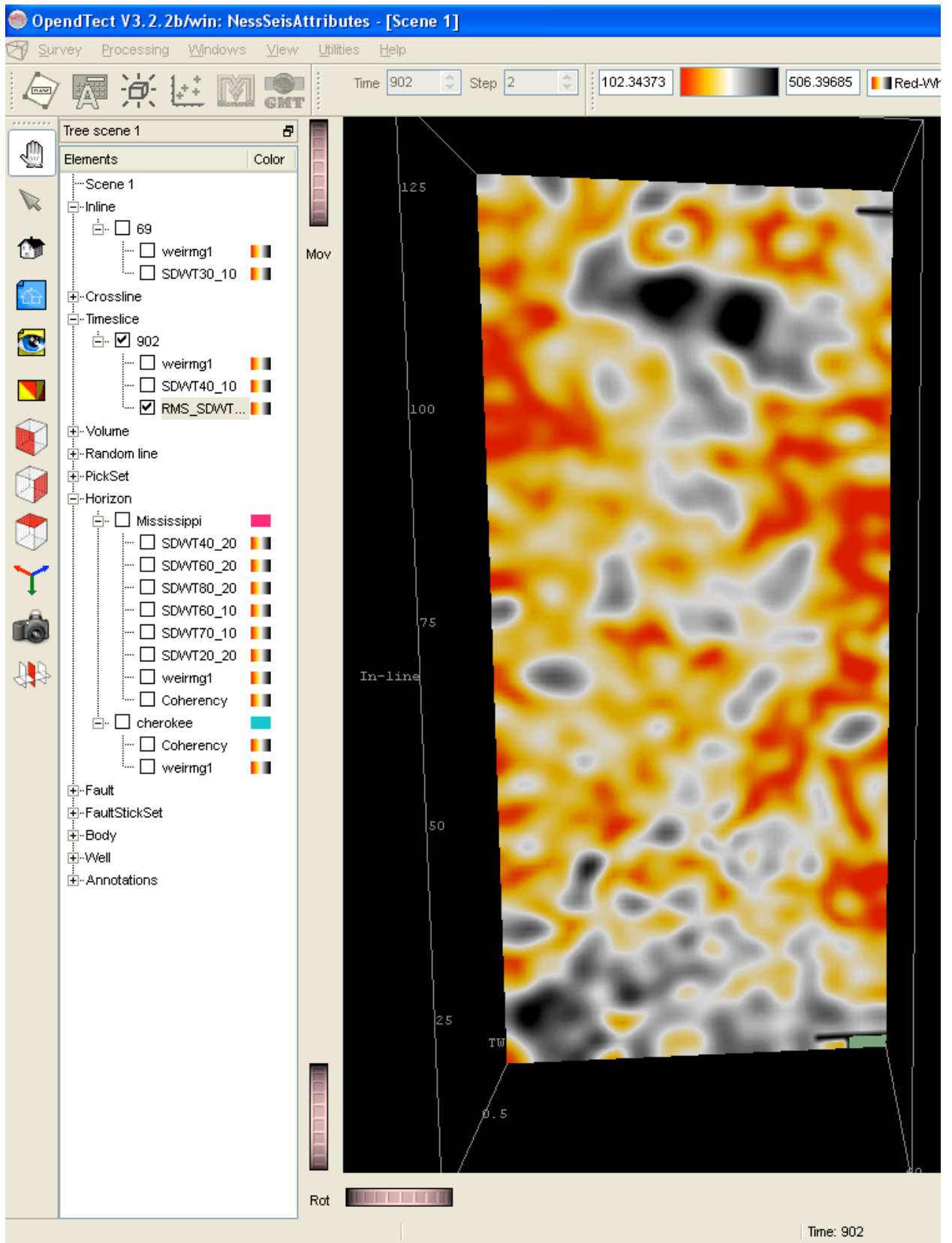


Figure A-16 Attribute Evaluation using varying time gates

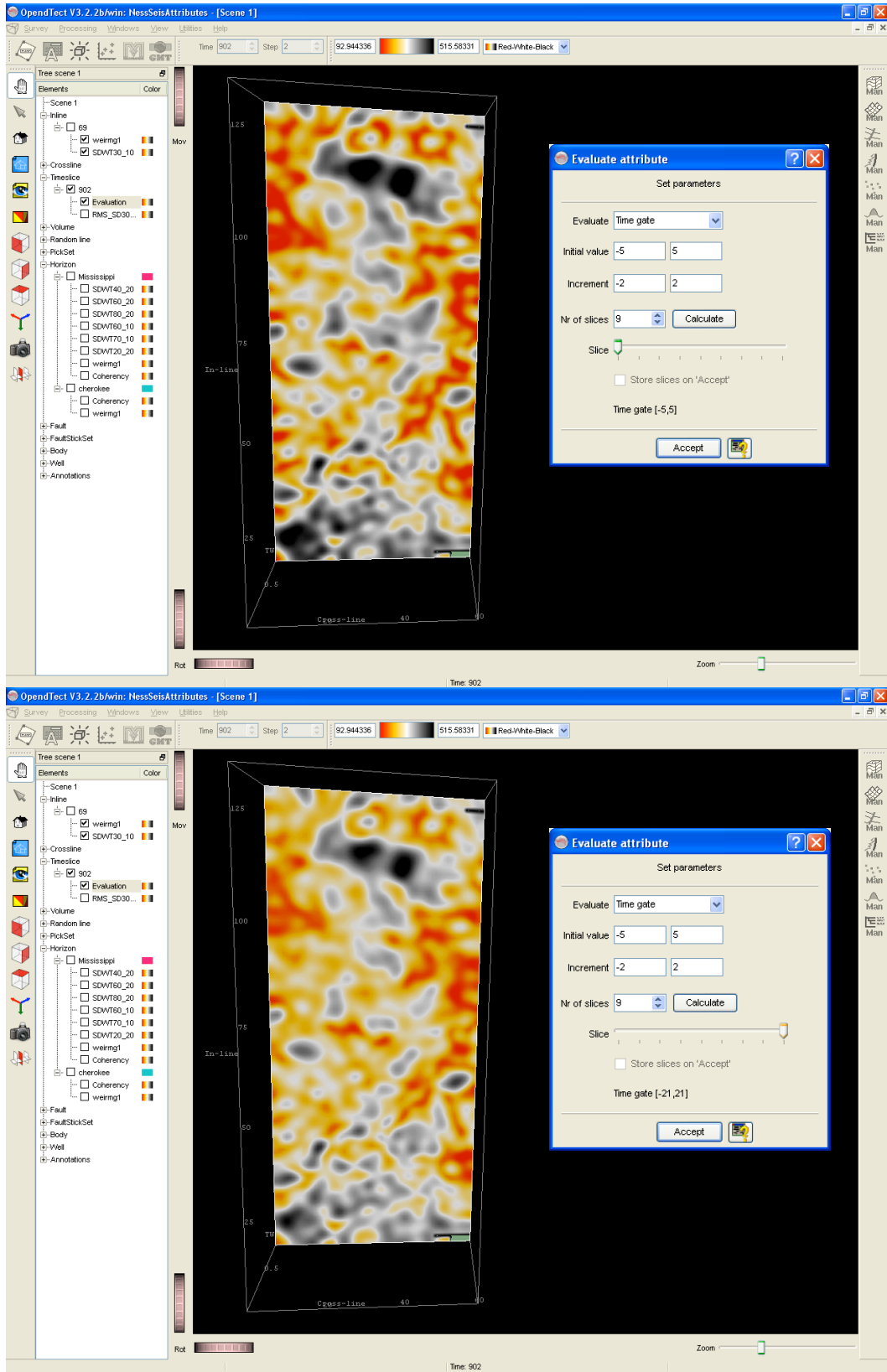


Figure A-17 RMS amplitude Spectral Decomposition 50 Hz Step 10 Hz and time gate (-9,9)

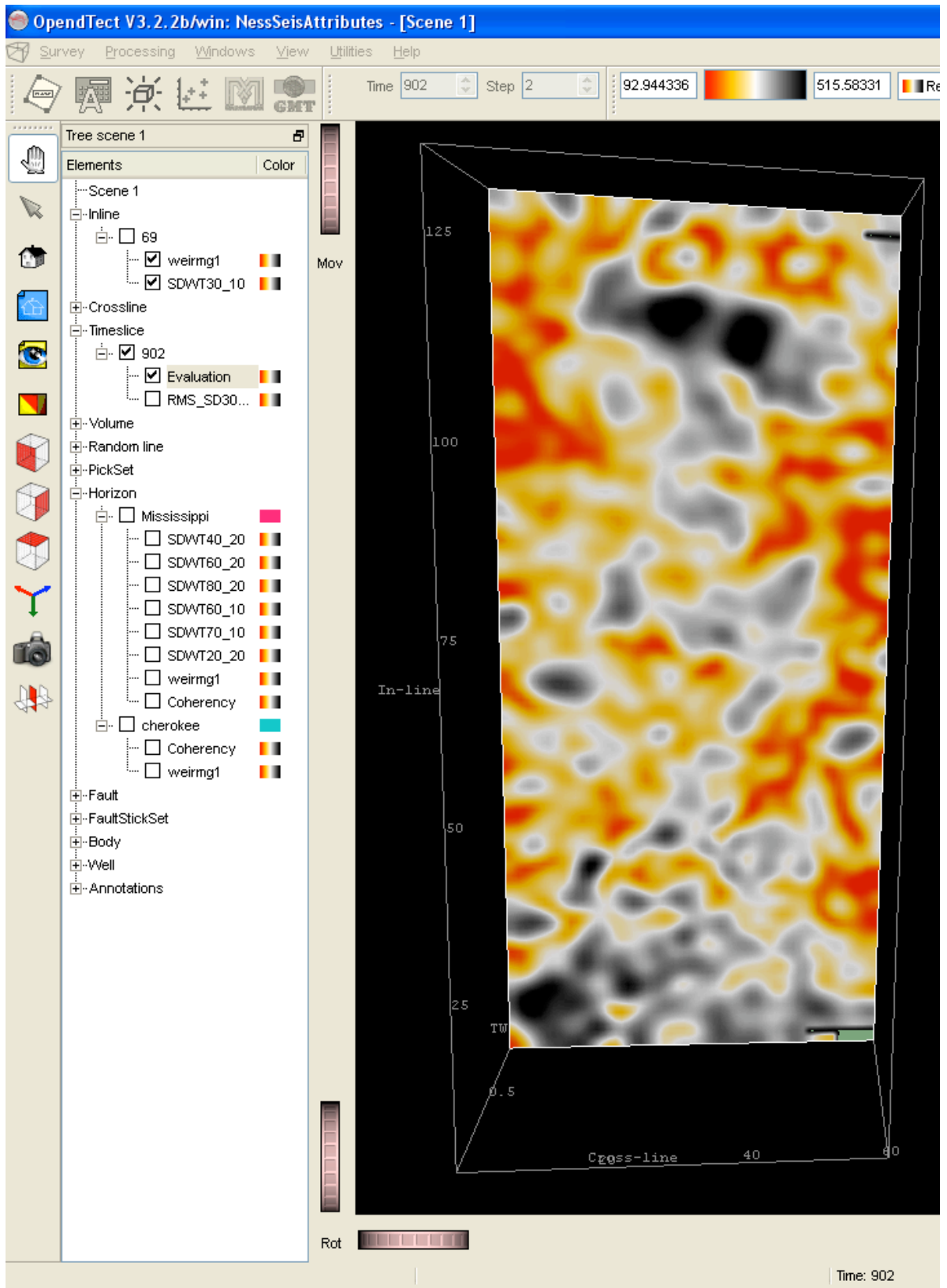


Figure A-18 RMS amplitude Spectral Decomposition 40 Hz Step 10 Hz

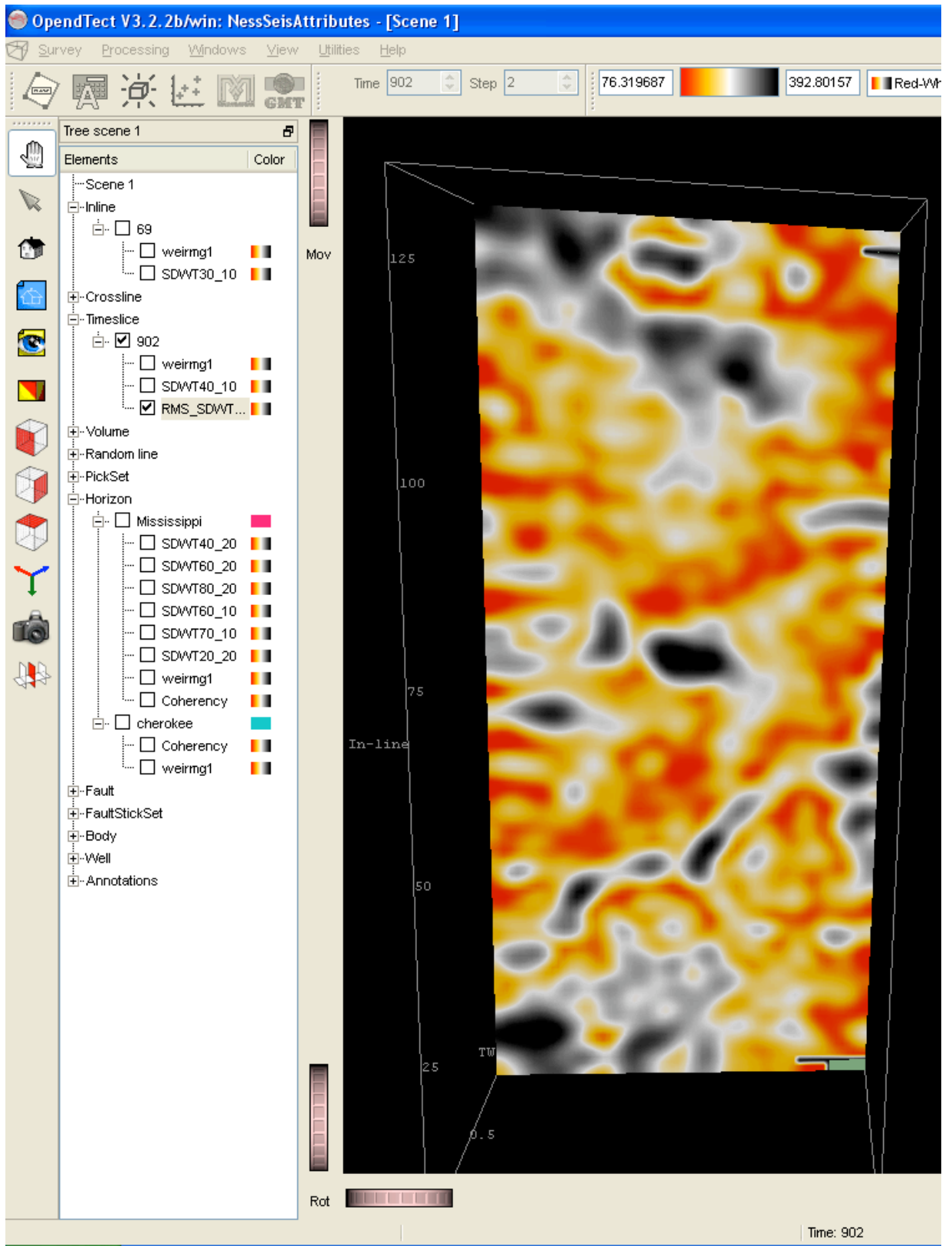


Figure A-19 Attribute Evaluation using varying time gates

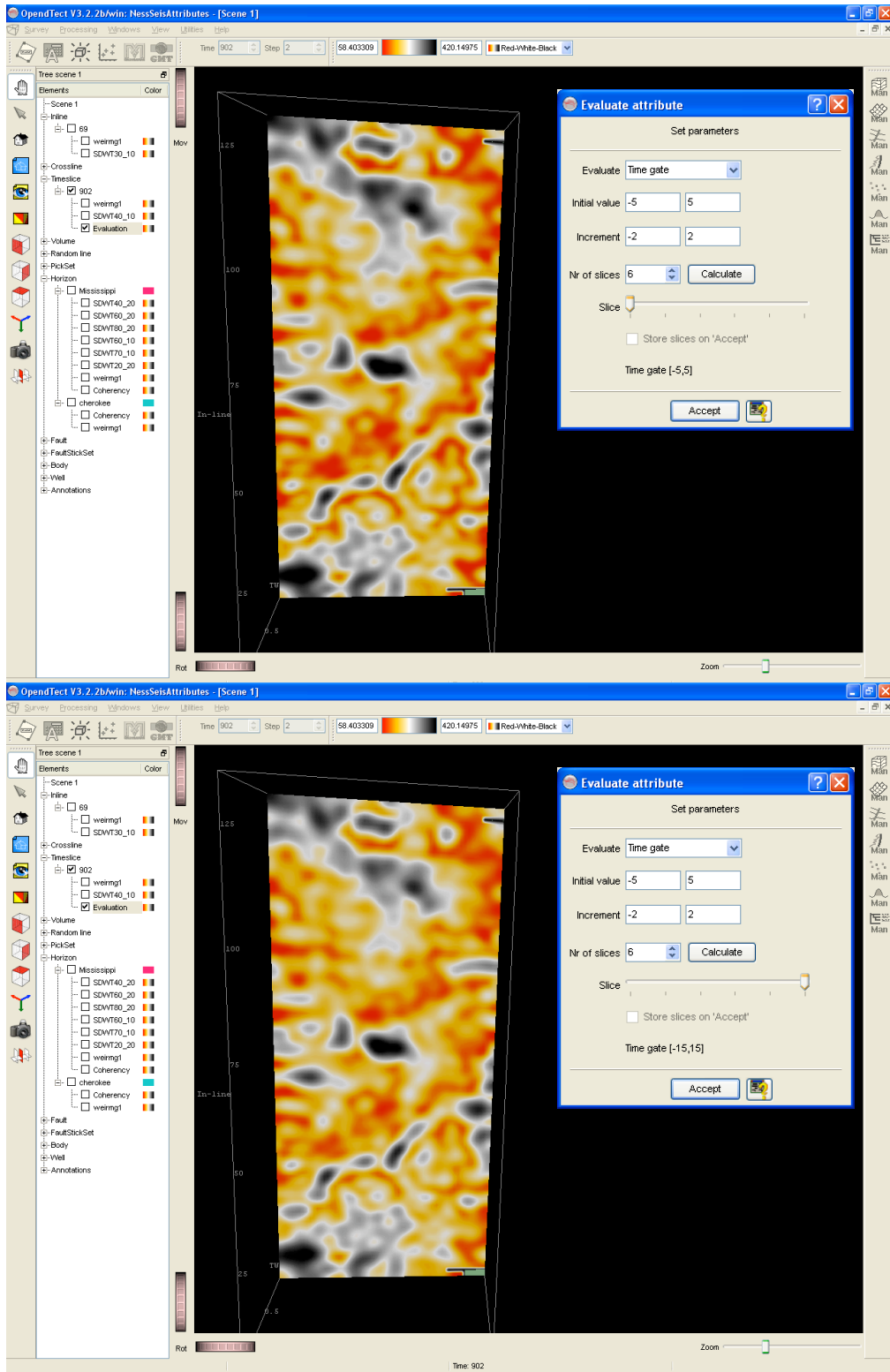


Figure A-20 RMS amplitude Spectral Decomposition 40 Hz Step 10 Hz time gate (-7,7)

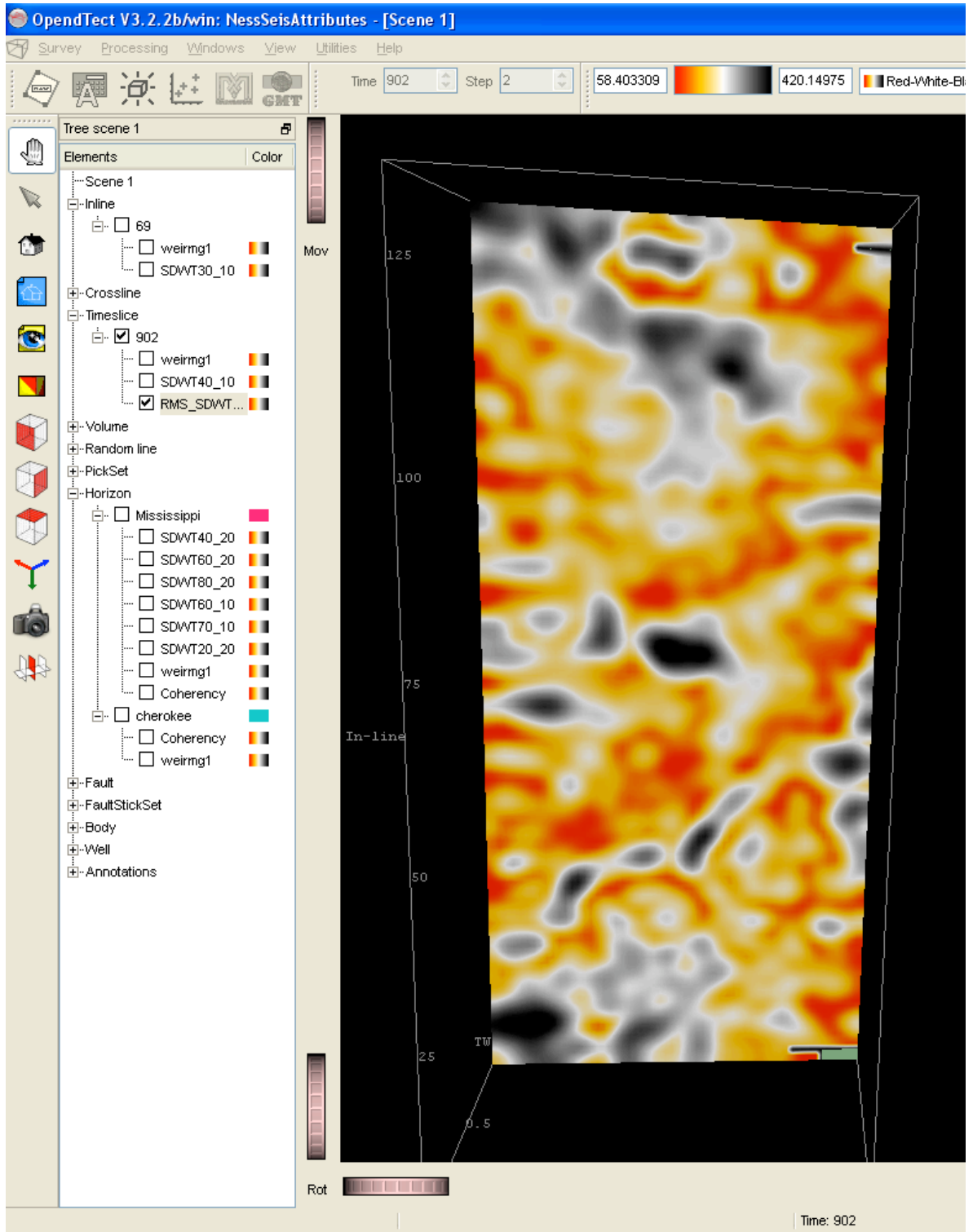


Figure A-21 RMS amplitude Spectral Decomposition 30 Hz Step 10 Hz

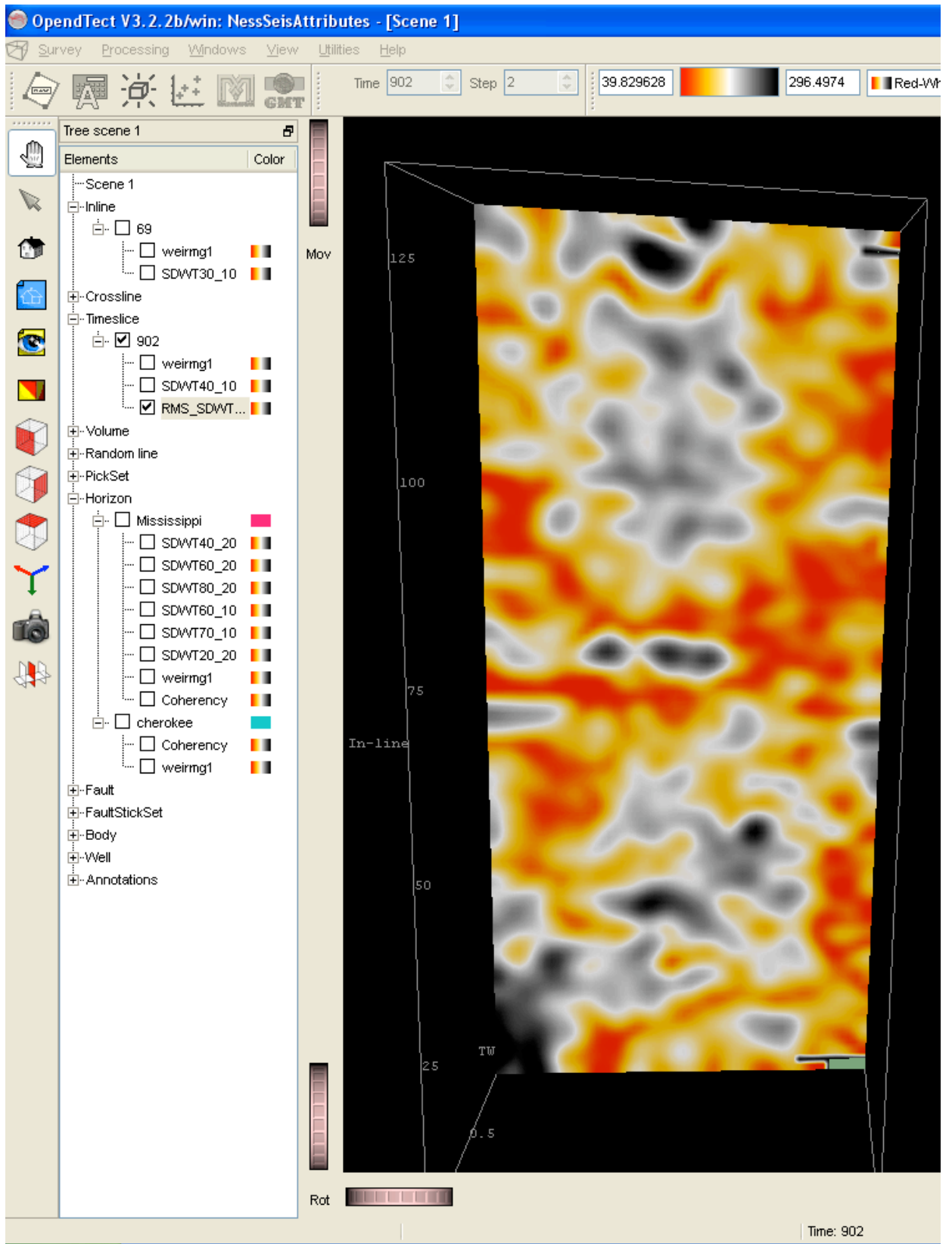


Figure A-22 Attribute Evaluation using varying time gates

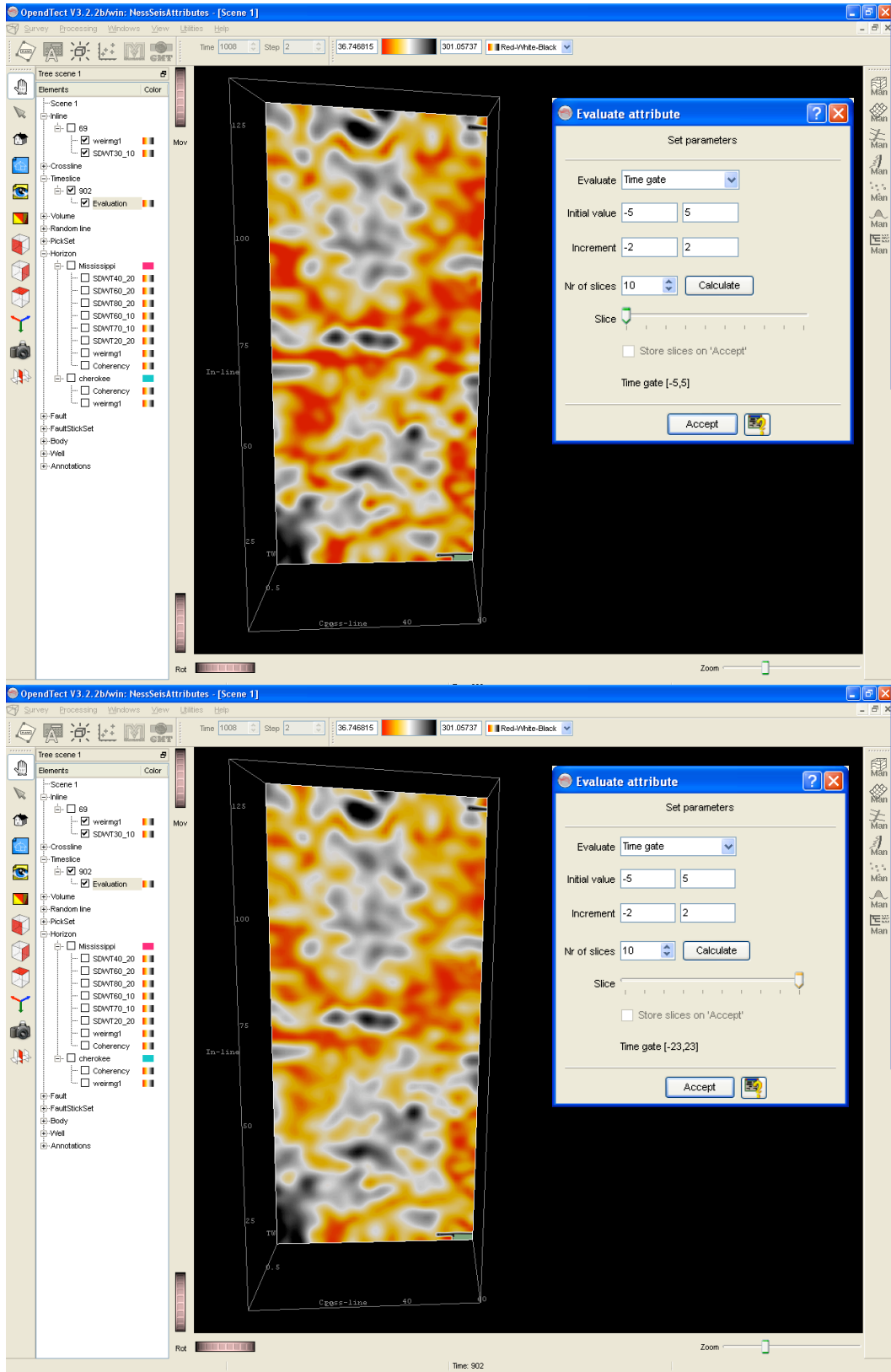


Figure A-23 RMS amplitude Spectral Decomposition 30 Hz Step 10 Hz time gate (-9,9)

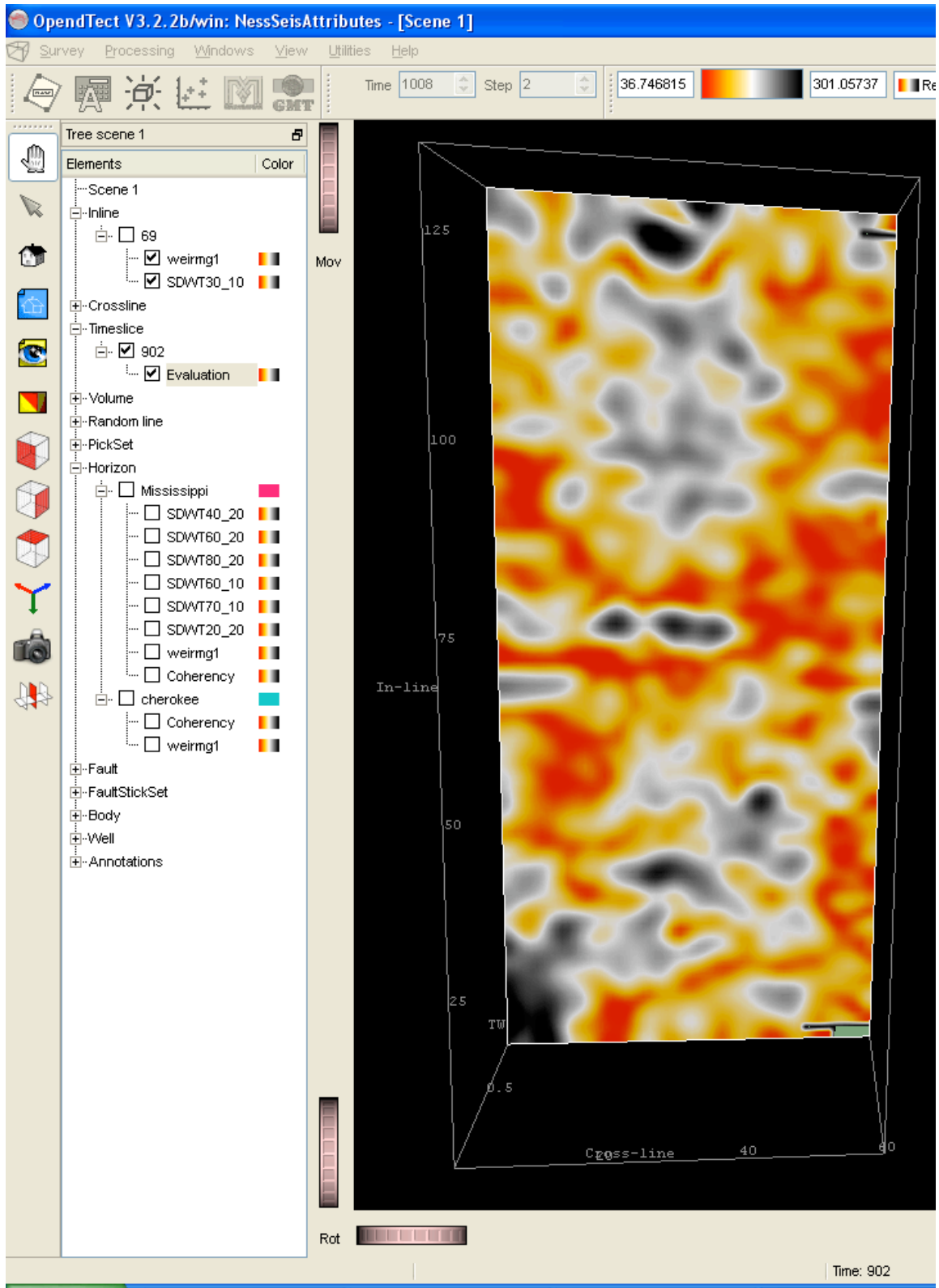


Figure A-24 RMS amplitude Spectral Decomposition 60 Hz Step 10 Hz, time window of (-15,10)

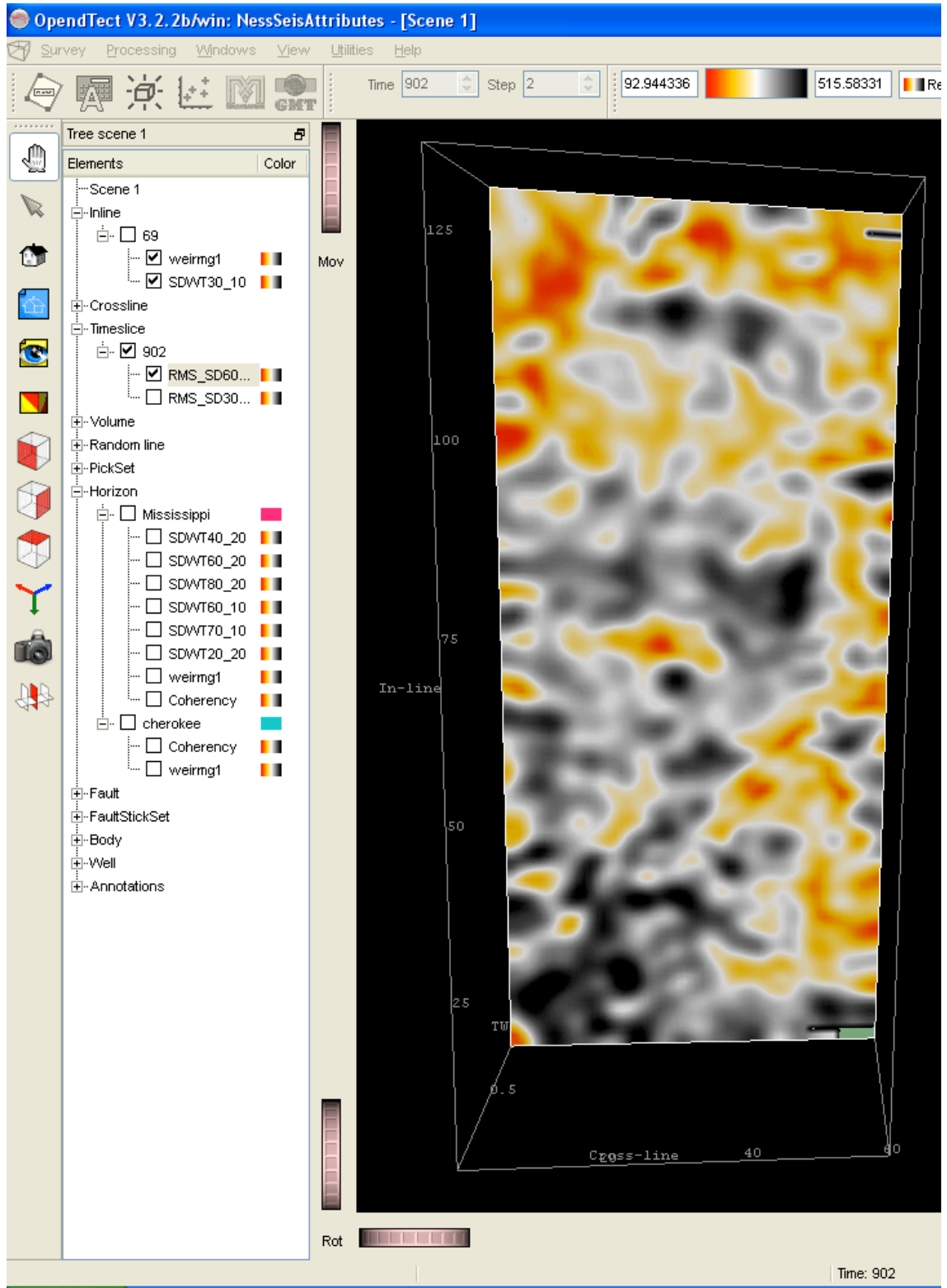


Figure A-25 Attribute evaluation using varying time gates

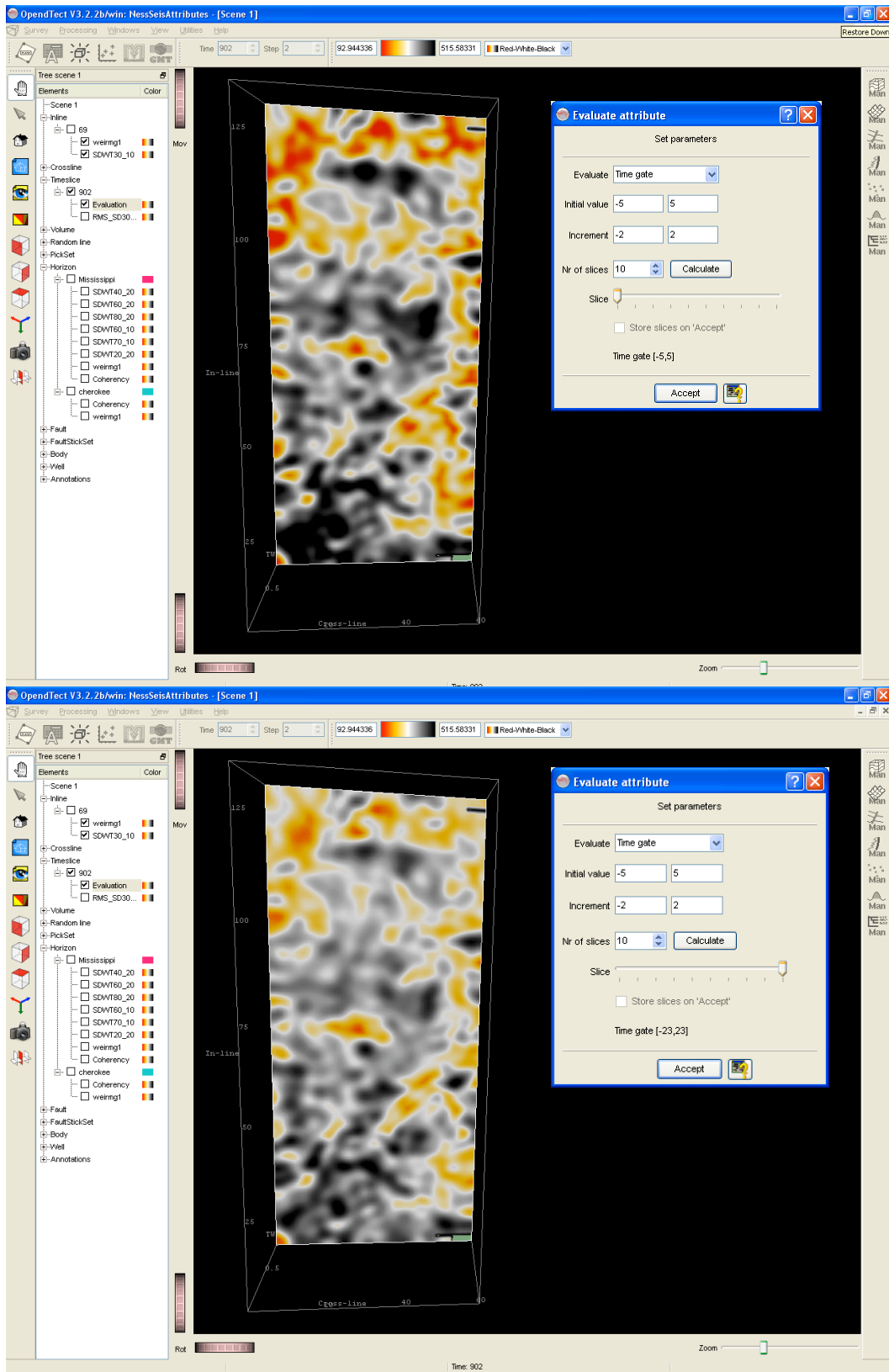


Figure A-26 RMS amplitude Spectral Decomposition 60 Hz Step 10 Hz time gate (-7,7)

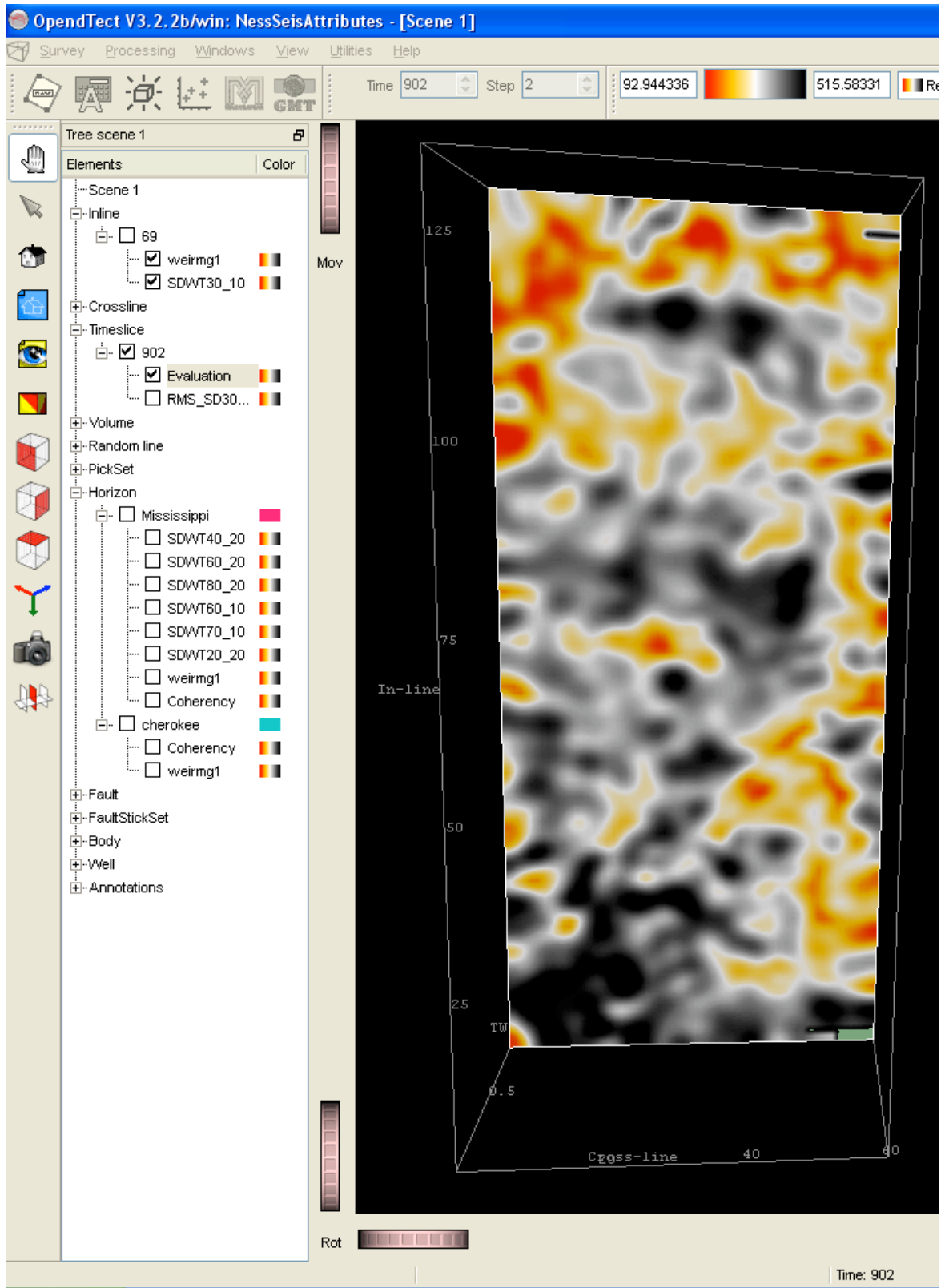


Figure A-27 RMS amplitude Spectral Decomposition 70 Hz Step 10 Hz, time window of (-15,10)

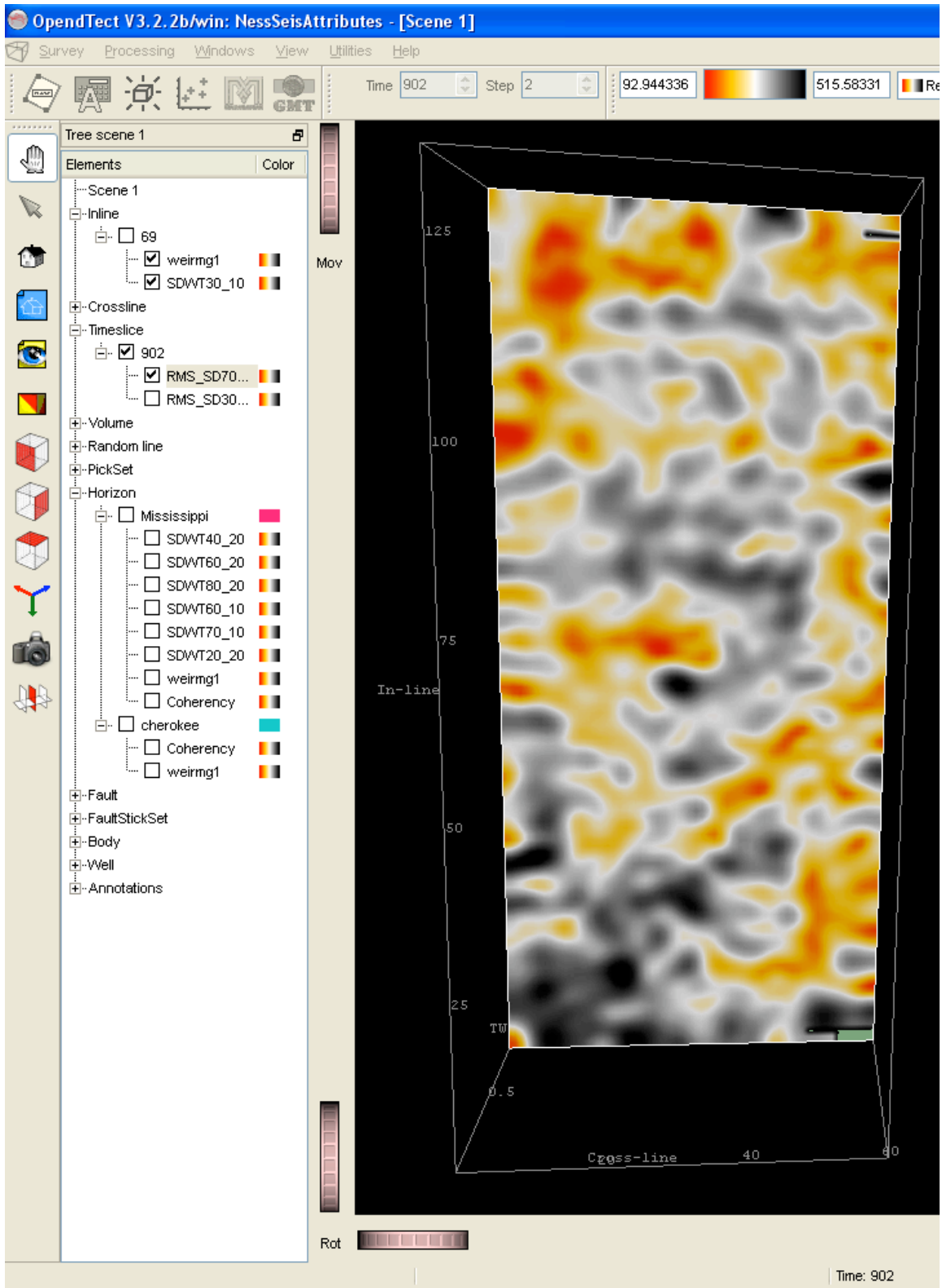


Figure A-28 Attribute evaluation of varying time gates

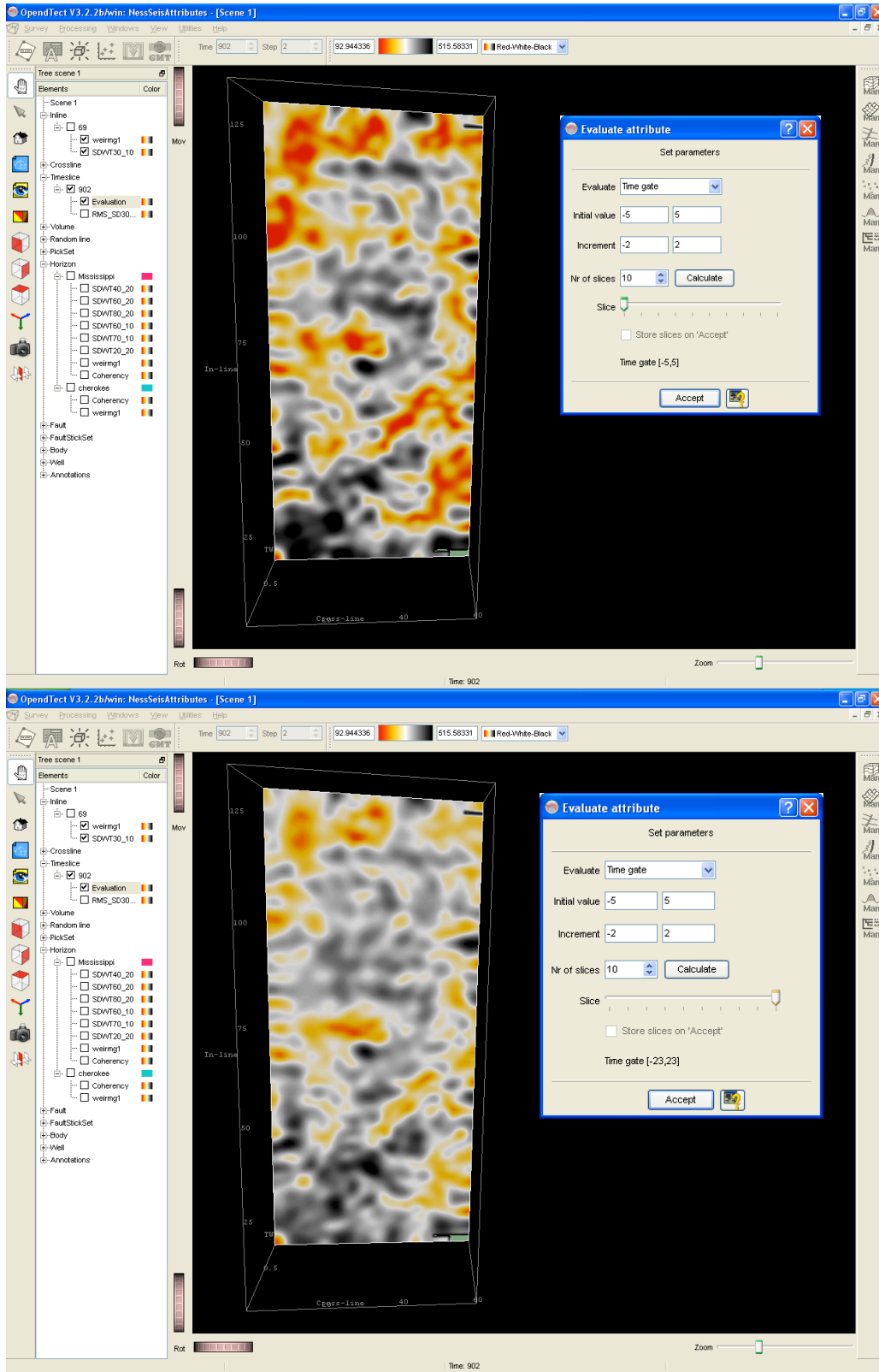


Figure A-29 RMS amplitude Spectral Decomposition 70 Hz Step 10 Hz time gate (-9,9)

